Sea-level change, carbon storage and greenhouse gas fluxes in a Northumberland (UK) salt marsh

Catrina Gore

MSc by research

University of York

Environment and Geography

September 2022

Abstract

Salt marshes are currently receiving increased attention because of their ability to act as climate change mitigators by sequestering carbon at high rates, while also providing multiple co-benefits. However, questions still exist concerning the precise functioning of these ecosystems which need to be addressed before any climate offsetting benefit is quantified. Using separate but linked elements, this study addresses two main questions aimed at providing more certainty about natural salt marsh functioning: first, the impact of sea-level rise on carbon accumulation rate and, second, the extent to which greenhouse gas fluxes – carbon dioxide, methane and nitrous oxide – detract from carbon sequestration. To this end, a proxy based sea-level reconstruction was developed for a salt marsh at Lindisfarne, Northumberland (UK). Complementary tide-gauge data were compared with high-resolution carbon and sediment accretion rates calculated for each centimetre down a core of sediment. Further, greenhouse gas fluxes were measured using static chambers across the marsh surface and converted to carbon dioxide equivalents from which estimates of net radiative balance were calculated. Rates of relative sea-level change over a ~60-year period were found to explain a significant proportion of variation in carbon accumulation rate, with high rates of sea-level rise associated with increased rates of carbon accumulation. The net radiative balance of the high marsh zone was -6.03 $\pm$ 2.20 SD t CO_2 eq ha^{-1} yr^{-1}, meaning that a beneficial net impact is still achieved when greenhouse gas fluxes are included in calculations. These findings support the assertion that salt marshes have a role to play as nature-based climate solutions. If the results of this study are reflected in other locations, it will be possible to state that where marshes keep pace with sea-level rise, increased carbon sequestration is likely and will not be significantly negated by greenhouse gas emissions from the marsh.

Table of Contents

Lists of Figure and Tables

List of Accompanying Material

Acknowledgements

First and foremost, I want to give big thanks to my supervisor Ed Garrett for giving me the opportunity to work on this project and for providing help and guidance throughout. Thanks also to my other supervisor, Roland Gehrels, for providing valuable feedback on my thesis.

I am grateful to Eloise Bryard for picking and counting the fossil foraminifera in core LI21/20, for assistance with field work during the first trip in September 2021 and for giving me a place to stay in her grandparents' house while in Northumberland. Subsequent field work trips would not have been possible without Luke Andrews and Lucy McMahon who drove to the site with me and provided help with gas flux measurements. Also, thanks and appreciation must go to Sylvia Toet for giving a great deal of time to guiding me through the greenhouse gas flux aspects of this project, and to Matt Pickering for a lot of help with gas chromatography.

I am grateful to the C-SIDE project for providing the lead, caesium, carbon, nitrogen, isotope and bulk density data used in this project, and for collecting the core focused on here, LI21/21. Thanks specifically to Craig Smeaton who provided this data and Bill Austin, PI of the project.

Finally, I want to thank Andrew Craggs and Natural England for allowing me to work on sites within Lindisfarne NNR, assistance with fieldwork and for always showing enthusiasm for the project.

Author’s Declaration

I declare that this thesis is a presentation of original work and I am the sole author. This work has not previously been presented for an award at this, or any other, University. All sources are acknowledged as References.

Chapter 1: Introduction

1.1 Introduction

Salt marshes are highly valuable ecosystems that provide a range of services important for humans, wildlife and the environment (Macreadie *et al.,* 2021). Most relevant to this study is their ability to sequester high levels of atmospheric carbon dioxide (CO_2), and, through this function, to aid in the mitigation of climate change. This is achieved through the input of organic matter from both the primary production of salt-marsh plants (autochthonous carbon) and from tidally delivered sediment (allochthonous carbon), coupled with the anaerobic conditions produced by frequent tidal inundation which lead to low decomposition rates of the accumulated carbon (Mcleod *et al.,* 2011). These features mean that salt marshes are classed among those blue carbon coastal ecosystems highlighted for their contribution to carbon sequestration similar to terrestrial forests (Macreadie *et al.,* 2019). In fact, the carbon sequestration capacities of these blue carbon ecosystems exceed that of latter. In one study, long term rates of carbon accumulation in three blue carbon ecosystems (salt marshes, mangrove forests and seagrass meadows) were found to range from 18 to 1713 g C m^{-2} yr^{-1} while long term rates for temperate, tropical and boreal forests ranged between 0.7 and 13.1 g C m^{-2} yr^{-1} (Mcleod *et al.,* 2011). These ecosystems are also hugely important when considered within the marine setting alone; despite occupying only 0.2 % of the ocean surface, blue carbon ecosystems enable 50 % of the carbon burial of marine sediments (Duarte *et al.,* 2013).

In addition to a high capacity for carbon sequestration, salt marshes provide a number of other ecosystem services. They, and blue carbon ecosystems more generally, are an important nursery habitat for a wide range of fish and crustacean species, making them beneficial in terms of both biodiversity and economically due to the fisheries value of these species (Boesch and Turner, 1984). Furthermore, salt marshes provide coastal protection by reducing wave energy, meaning that increased protection is provided to communities threatened by sea-level rise (Kiesel *et al.,* 2020).

It is clear, therefore, from the strength of salt marshes as carbon sinks and the numerous co-benefits they provide, that these are ecosystems of great importance. Despite this clear importance, many have become degraded due to human activity and climate change (Mariotti and Carr, 2014; Lopes *et al.,* 2021), and there are now initiatives under development to promote conservation. The carbon accumulation ability of salt marshes is of particular interest because one such initiative is the development of a United Kingdom (UK) Salt Marsh Blue Carbon Code, whereby organisations purchase carbon credits that allow them to offset their own unavoidable greenhouse gas emissions while providing funding for the management of blue carbon sites (Mason *et al.,* 2022). Therefore, carbon sequestration and storage and greenhouse gas emissions by salt marshes must be accurately quantified to ensure these carbon credits represent a genuine reduction in atmospheric CO_2 and this constitutes one of the main goals of this project.

Additionally, the role natural UK salt marshes play in climate change mitigation has recently received increasing attention due to the interest in using salt-marsh realignment to sequester increased quantities of atmospheric CO_2, and the potential for using these natural sites as analogues for the functioning of the newly restored areas. Realignment refers to the process by which coastal defences are deliberately

breached to allow the tide to inundate areas of land previously claimed by humans, usually for agricultural purposes (MacDonald et al., 2020). Analogues are necessary because salt-marsh realignment is a recent innovation, meaning there are few realigned sites old enough to allow for a detailed study of their climate impact throughout all stages of restoration (Burden *et al.,* 2019). The results of this study therefore have applicability to both natural and realigned sites.

The site chosen for conducting this study was Lindisfarne National Nature Reserve (NNR), on the coast of Northumberland in northeast England (Fig. 1). The importance of conducting investigations into the functioning of this site as a blue carbon ecosystem is highlighted by the recent announcement that Lindisfarne is to become one of five new highly protected marine areas (HPMAs) planned for English waters (Barkham and Horton, 2022). Given, therefore, the importance placed on the potential of this site to contribute toward rewilding, it is vital that its functioning as a carbon sink is understood. Accounting for the contribution of blue carbon to HPMAs could ultimately aid with the selection and management of such sites in the future. The perception of these ecosystems as highly effective carbon sinks (e.g., Macreadie et al., 2021) and their prevalence in carbon crediting schemes (e.g., Ullman *et al.,* 2013) could make them attractive choices for future HPMAs; therefore, the conclusions drawn from this study could have applicability to similar sites across the UK.

Sea-level change has been increasingly recognised as an important control on the carbon accumulation discussed above (e.g., Gonneea et al., 2019). Comparing the rate of sea-level change experienced by a marsh with the rate at which carbon is accumulated can be used to understand whether a rapid sea-level rise leads to higher carbon sequestration - as may be expected in a marsh accreting higher rates of sediment, and thus allochthonous carbon, to keep pace with this rise (Rogers *et al.,* 2019). This increased carbon sequestration could be driven by higher rates of sediment delivery and increased plant productivity (Kirwan and Guntenspergen, 2015). Alternatively, where sea-level rise is too rapid for the marsh to keep pace via sediment accretion, this could cause marsh loss by erosion and conversion to tidal flats, most likely leading to net export of carbon to the sea and to the atmosphere (Pendleton *et al.,* 2012). The study area focused on here does not have the advantage of tide gauges particularly close by, and besides this, tide gauges are limited in temporal extent. Therefore, in an attempt to understand the effect of sea-level rise on carbon accumulation, I turned to another useful function of salt marshes, that is, their ability to act as geological tide gauges for the Holocene (Barlow *et al.,* 2013). This arises from the way in which salt marshes accrete sediment to fill accommodation space and the presence of microfossils within this sediment which show a clear zonation, similarly to plants, to different elevations across the marsh (Gehrels *et al.,* 2001). Comparing those microfossils - in the case of this study, foraminifera were used - present within a core of salt marsh sediment to the assemblage of modern species found on the surface of the marsh during the present day, allows inferences to be made about the elevation at which the core assemblages were deposited and sea-level changes to be reconstructed (Gehrels, 1994). The other aspect of this project aims to utilise this functionality to generate a relative sea-level (RSL) reconstruction for the study site, Lindisfarne, which can then be compared with carbon accumulation rates for each centimetre of sediment down a core. Additionally, this will allow for increased understanding of late Holocene sea-

level change experienced by the area, especially important given recent rapid rates of sea-level rise (Gehrels and Woodworth, 2013) and the position occupied by the study site in Northumberland between Holocene emergence and submergence (Shennan *et al.,* 2000). Furthermore, producing a record of RSL can be useful for understanding whether the marsh in question is successfully keeping pace with sea-level rise, if that be the case, through sediment accretion (Horton *et al.,* 2018).

To the ends discussed above, therefore, this study focuses on three individual but connected elements: first, the development of a RSL record using sediment from a salt marsh to understand the impact of sea-level changes on carbon sequestration; second, an examination of the organic carbon (OC) content of a core of salt marsh sediment; and thirdly, quantification of the rates of greenhouse gas fluxes from the surface of the marsh. The overall aim is to calculate how the net carbon balance changes with sea-level rise.

Abundant work has been done considering each of these elements separately, and some studies endeavour to combine various elements, especially the connection between sea-level rise and increased rates of carbon sequestration (e.g., Rogers *et al.,* 2019). The conclusions drawn here suggest that rapid rates of sea-level rise can lead to higher levels of carbon sequestration by the salt marshes that succeed in keeping pace with this rise through sediment accretion (Kirwan *et al.,* 2016; Gonneea *et al.,* 2019). Various studies have also measured the rates of greenhouse gas fluxes from salt marshes and investigated the drivers behind these fluxes (e.g., Poffenbarger *et al.,* 2011; Murray *et al.,* 2015), a direction of study which receives increasing attention because the anaerobic conditions created by regular tidal inundation mean that methanogenesis and denitrification are favoured (Hirota *et al.,* 2007). Far fewer, however, have attempted to use these data to draw conclusions about the net radiative balance of salt marshes. Chmura *et al.* (2011) offers one of the few examples and concludes that the inclusion of methane (CH_4) and nitrous oxide (N_2O) emissions in the greenhouse gas budget of a salt marsh leads to only a minor reduction of 2 % in carbon sequestration rate. However, more data from a wide range of areas are needed before this is accepted as true of salt marshes generally.

By combining these different elements and disciplines, this project will contribute to increasing the understanding of salt-marsh functioning in terms of their overall contribution to climate change mitigation.

1.1 Aims and Objectives

The different elements involved in this project can be compared and combined to illustrate the overall climate impact of a natural salt marsh, the main goal of this work. This will be achieved through the following:

1. Develop local and regional modern training sets of salt-marsh foraminifera using new data from Lindisfarne and data from previously published sources.
2. Reconstruct RSL change at Lindisfarne using a foraminifera-based transfer function.
3. Compare the RSL record, and tide-gauge data, with OC accumulation rates.
4. Compare OC accumulation rates with rates of gas flux.

5. Calculate the net radiative balance of the study area.

Rates of carbon accumulation will be compared with the flux rates of the three major greenhouse gases: CO_2, CH_4, N_2O. The greenhouse gas budget of salt marshes will be quantified, a step beyond what is usually achieved by simply focusing on carbon storage. Net radiative balance will be calculated by converting rates of carbon accumulation and gas fluxes to CO_2 equivalents, allowing accurate comparisons to be made.

In addition to these objectives and hypotheses, the project also aims to establish a standard methodology for measuring gas flux rates from salt marshes using the static chamber technique. It is vital to establish a method that can be applied to different sites and therefore allow for comparison between studies. Ultimately, this could aid in addressing one of the major gaps recently identified in blue carbon science, namely, understanding the drivers behind carbon and greenhouse gas fluxes in natural and restored salt marshes (Mason *et al.,* 2022).

Chapter 2: Study Site

Lindisfarne National Nature Reserve (NNR) is situated approximately 16 km to the south of Berwick-upon-Tweed in Northumberland (Fig. 1). The site comprises 3500 hectares of sand dunes, salt marshes and mudflats (Natural England, 2014). The Holy Island of Lindisfarne has a rocky headland and is separated from the mainland by a tidal causeway. Sand dunes dominate the area surrounding the Snook on one side of the causeway while on the opposite side there is a salt marsh and mudflat (Fig. 1). The underlying geology of Lindisfarne NNR has been described by previous studies conducted in the area. Parrack (1986) described the sand dunes adjacent to the Snook salt marsh (Fig. 1) as being developed on clay, hard pan and underlying sandstone; the impermeable nature of these layers mean that the sand dune slacks often contain standing freshwater for long periods of time. Those slacks on the south side (i.e., facing the Snook salt marsh) were described by Parrack (1986) as receiving variable levels of saltwater seepage, likely from the regular tidal inundation of the marsh. Furthermore, the majority of the dunes are mature, but a new system was found to be forming on the north-facing shore while wind erosion was a force affecting the southside (Parrack, 1986).

Figure 1. Map showing the location of Lindisfarne NNR and the two salt marsh study sites that were the focus of the project.

In 1954 Lindisfarne was first designated a Site of Special Interest, when fifty-three features were listed in support of this status (Pullan *et al.,* 2013). These features included the high levels of biodiversity supported by the site which provides a habitat for a range of organisms. For example, it is an important winter site for Pale Bellied Brent Geese and Widgeon, with 60 % of the World population of the latter using the site to over winter (Evans, 1986; Pullan *et al.,* 2013). The site also supports breeding colonies of seals (Barkham and Horton, 2022). Following this, Lindisfarne became an NNR in 1964, a RAMSAR site in 1990 and a Special Protection Area in 1992 (Pullan *et al.,* 2013). Therefore, it is clear Lindisfarne NNR is highly valuable in terms of the biodiversity the site supports; this is often the case with blue carbon sites and highlights the co-benefits of these ecosystems (Hagger *et al.,* 2022).

As previously mentioned, Northumberland lies at the transition between Holocene submergence and emergence and, as such, the sea-level histories of areas to the north and to the south show marked differences (Shennan *et al.,* 2000). Lindisfarne NNR is situated to the north of the county (Fig. 1) and has experienced a mid-Holocene sea-level maximum approximately 2.5 m above the present-day level (Shennan *et al.,* 2000). As a result, Plater and Shennan (1992) found the coast of Northumberland to be characterised by responses to low rates of sea-level change and local variations in sediment supply.

The tidal range of the site is 2.74 m and the mean tide level (MTL) 0.33 m; from this, the highest astronomical tide (HAT) was calculated as 3.07 m (Ed Garrett, personal correspondence; see Materials and Methods 4.1.4 for methodology). Therefore, Lindisfarne can be classified as a mesotidal site given that the tidal range is between 2 and 4 m (Davies, 1964). The average rainfall experienced by Lindisfarne NNR, based on data gathered over a thirty-year period, is 246.8 mm (http://lindisfarnennr.blogspot.com/). The farmland surrounding the NNR has historically been comprised of arable and grassland, with a recent switch to winter cropping reported (Pullan *et al.,* 2011; Pullan *et al.,* 2013).

Two salt marshes within Lindisfarne NNR were studied. The first, the Snook salt marsh, is the area of greatest focus within this study. This site is located adjacent to the causeway leading from the mainland to Holy Island (Fig. 1). The salt marsh displays clear zonation of plant species in high, mid and low marsh zones; the high marsh has a preponderance of *Armeria maritima* and *Puccinellia maritima*, both of which continue in high proportions into the mid marsh but with increasing levels of *Atriplex portulacoides*. The low marsh zone plant community is dominated by *S. anglica* and *Salicornia europaea* (Fig. 2). Snook salt marsh is located in close proximity to a busy road used throughout the year by visitors to Holy Island (Fig. 2) and the site is not used for livestock grazing. Both marshes are actively accreting as no erosional features, such as cliffs, were present at their seaward edges. The majority of the work in this study was undertaken on or used material from the Snook salt marsh, including the cores of sediment used to reconstruct RSL and investigate soil OC accumulation and stocks, and the measurement of gas flux with the static chamber techniques (see Chapter 3).

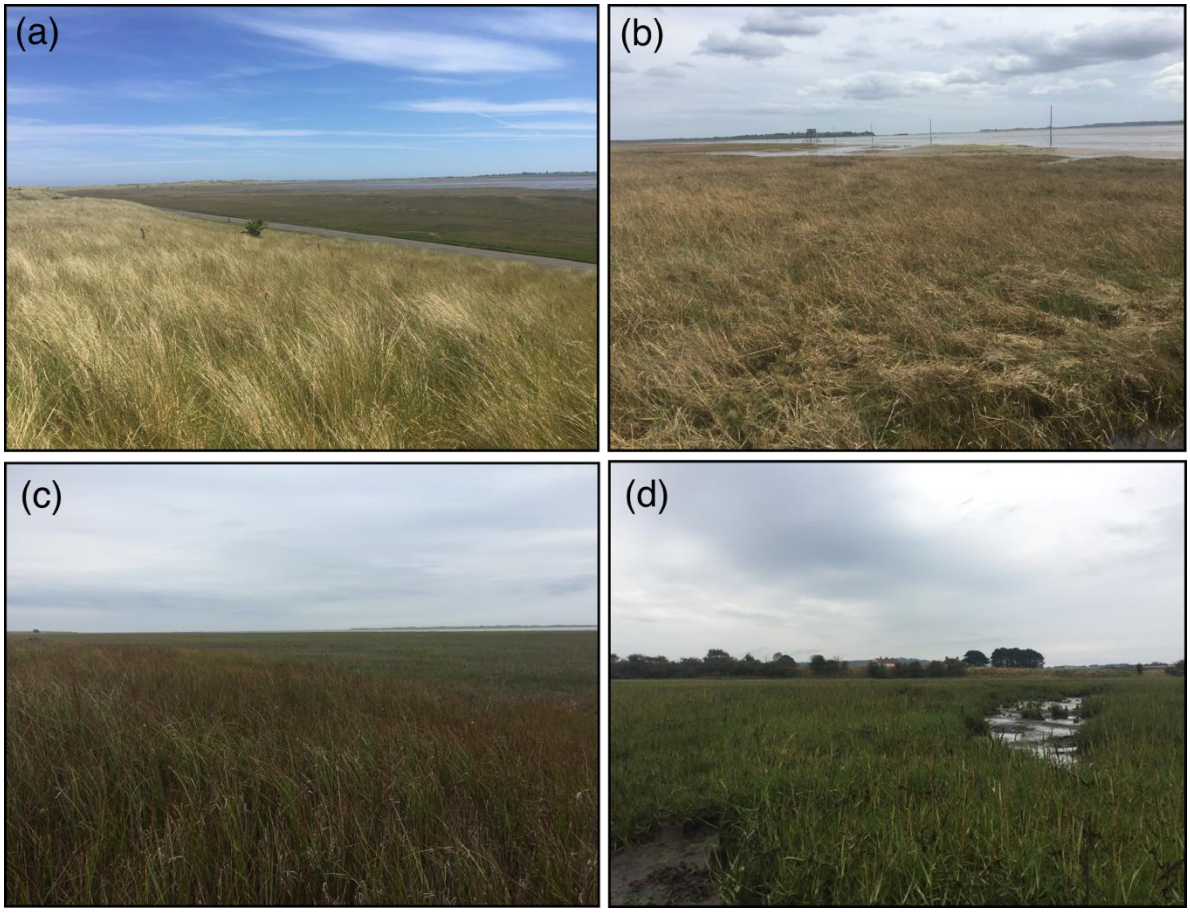

Figure 2. Photographs of Lindisfarne NRR with the (a) the Snook salt marsh and road, (b) the low marsh Snook *S. anglica* community and (c and d) Fenham salt marsh with *S. anglica* dominating the high marsh and low marsh zones. Photograph (a) was taken in June 2022 and (b) in May 2022; both (c) and (d) were taken in September 2021.

The second site, Fenham marsh, is located south of Holy Island – on the opposite side of the Holy Island Sands (Fig. 1). Sediment from this site was used to reconstruct RSL through the development of a modern foraminiferal training set and so this area was less of a focus than the Snook. The lower part of Fenham marsh was, until relatively recently, a mudflat and was anthropogenically altered through the planting of *Spartina anglica*, which was first introduced in 1929 (Frid *et al.,* 1999), and is by far the dominant species across the low marsh (Fig. 2). The upper marsh and adjacent supratidal areas are also used for the grazing of cattle. Efforts have been made in the past to control the *S. anglica* community in this area because of concerns regarding its ability to outcompete and replace the *Zostera marina* stands important for over-wintering birds (Percival *et al.,* 1998). Evans (1986) reported that *S. anglica* covered 36 ha of the intertidal zone in 1963, 40 ha in 1969 and 400 ha in the early 1980s. Control of the species depended on the use of the herbicide Dalapon in the 1980s (Evans, 1986); later, physical disruption through burial in sediment became the favoured means of control (Frid *et al.,* 1999).

Chapter 3: Literature Review

3.1 Blue Carbon

3.1.1 Blue Carbon Ecosystems and Carbon Credits

Blue carbon ecosystems include a range of different coastal and ocean environments that occur throughout the world and are similar in their ability to sequester and store large quantities of organic carbon (Macreadie *et al*., 2019). Most notable amongst these ecosystems are salt marshes, mangrove forests and sea grass meadows, with recent attention also being given to the potential of widespread macroalgae in carbon sequestration (Krause-Jensen and Duarte 2016). The focus of this study, however, is on salt marshes and their effectiveness as climate change mitigators in the UK. Salt marshes are numerous in the UK and realignment initiatives have been undertaken to return land previously claimed for agricultural purposes to its natural state through the breaching of sea walls and the reintroduction of the tide, which leads to the gradual return of these areas to their natural state (Masselink *et al*., 2017), with the aim of enabling these ecosystems to sequester more carbon than otherwise would have been possible if they remained as agricultural fields used for growing crops or supporting livestock (Wollenberg *et al.,* 2018; Mossman *et al.,* 2021). Additionally, there is increasing interest in creating so-called carbon credits from the gains in carbon sequestration made in blue carbon ecosystems which can be purchased with the aim of allowing unavoidable greenhouse gas emission to be offset (Emmer *et al.*, 2015). Therefore, blue carbon ecosystems are already being used in attempts to mitigate climate change through the reduction of excess greenhouse gases to the atmosphere and because of this it is vitally important that their efficacy is studied and understood.

3.1.2 Salt-Marsh Blue Carbon

Salt marshes possess a range of qualities that make them useful and important ecosystems; one of these qualities – and the one that is focused on here – is their ability to act as powerful carbon sinks able to sequester large quantities of carbon and keep it buried for millennia (Macreadie *et al.,* 2013). Further to the figures discussed above (see Introduction 1.1) there is range of other information in the literature to illustrate the carbon sequestration capabilities of salt marshes. In 2003, Chmura *et al.* compiled data from studies of 21,988 km^2 of salt marsh ecosystems around the globe and estimated that they sequester 210 g m^{-2} yr^{-1} of carbon, meaning that approximately 4.60 Tg of carbon is sequestered each year in these marshes. Similar work in an undisturbed area of tropical rain forest resulted in an estimate of 102 g m^{-2} yr^{-1} of carbon, a considerably lower figure (Grace *et al.,* 1995). More recently, Macreadie *et al.* (2021) have estimated that the global carbon stock of salt marshes could range from ~862 to 1,350 Tg. The range in this estimate is so great because there is a paucity of data available to accurately account for the full global distribution of salt marshes (Macreadie *et al.,* 2021). In the UK specifically, surficial soil organic carbon stock was recorded as 2.32 $\pm$ 0.47 Mt by a recent study (Smeaton *et al.,* 2022) and this represents a first step towards including salt marsh blue carbon stocks in the national inventory.

Carbon sequestration in salt marshes is achieved through two primary mechanisms (Saintilan *et al.,* 2013). Firstly, the regular tidal inundation that characterises salt marshes transports allochthonous sediments; carbon accumulation is a function of

the sedimentation rate of this tidally delivered material (Saintilan *et al.,* 2013). Secondly, autochthonous carbon is contributed by the plants growing on the marsh; carbon dioxide (CO_2) taken from the atmosphere during plant growth is ultimately added to the supply of recalcitrant carbon stored in the marsh, as opposed to being released back into the atmosphere upon decomposition of the plant material (Sasmito *et al.,* 2020).

3.1.3 Salt-Marsh Co-Benefits

The focus of this study is on the contribution of salt marshes to climate change mitigation through their accumulation and storage of carbon; however, they also provide numerous other co-benefits (Barbier et al., 2011). Coastal protection is provided by the ability of salt marshes to substantially decrease the energy of incoming waves (Morgan and Burdick, 2009), which is important for the protection of coastal communities and in reducing the cost of damage caused by extreme weather events (Costanza *et al.,* 2008). Additionally, salt marshes provide a refuge and vital resources for many species of fish and crustacean, meaning they are important for the protection of both biodiversity and economically important fishery species (Boesch and Turner, 1984). Therefore, the significance of salt marshes goes beyond their ability to act as carbon sinks and further highlights the need to investigate the functioning of these key ecosystems.

3.1.4 Impact of Sea-Level Rise

Recent rapid rates of sea-level rise and the impact of human activities on tidal regimes and sediment supplies mean there has been concern about the survival of salt marshes (Reed, 1995; van der Spek, 1997; Craft *et al.,* 2009; Yang *et al.,* 2011). The factors crucial to determining whether a marsh survives a rising sea level include accommodation space, sediment supply and sediment accumulation rate (Allen, 1990). When the rate at which a marsh accumulates sediment is greater than the rate of local RSL, accommodation space is filled, and the surface emerges further from the tidal frame (Gehrels and Kemp 2021). On the other hand, if the sediment rate is insufficient to keep pace with sea-level rise, accommodation space is created and the marsh surface moves downward in the tidal frame, resulting in submergence (Gehrels and Kemp, 2021). More recently, however, Kirwan *et al.* (2016) have suggested that salt marshes are able to rapidly adapt to sea-level rise and that other mechanisms of marsh adaption – beyond accommodation space and sediment supply – must be considered. In certain conditions, marsh plants also respond to sea-level rise and can increase marsh stability through enhanced root growth and increased organic matter accumulation (Kirwan and Guntenspergen, 2012; Kirwan and Megonigal, 2013). Furthermore, there is evidence to suggest that salt marshes will sequester carbon at higher rates in response to sea-level rise due to increased biomass productivity and sediment accumulation (Gonneea *et al.,* 2019), which, as previously discussed, are the main mechanisms by which salt marshes accumulate and store carbon. This effect is seen most prominently in areas with particularly rapid RSL rise (Rogers *et al.,* 2019). The ability of salt marshes to adapt rapidly to a rising sea level and simultaneously remove greater quantities of greenhouses gases from the atmosphere further enhances their importance as climate change mitigators both now and in the future.

Sea-level rise also has the potential to affect the fluxes of other greenhouse gases in salt marshes. Yang and Silver (2016) have discussed the way in which redox dynamics are altered through sea-level rise which in turn affects N_2O emission. Furthermore, Mueller *et al.* (2020) showed that the changing salt marsh plant community that arises from sea-level rise affects methane fluxes. These greenhouse gases are the focus of one aspect of this project.

3.2 Relative Sea-Level Reconstruction

3.2.1 Records of RSL

Relative sea-level (RSL) reconstructions enable local sea levels to be followed back through time into the pre-industrial and pre tide-gauge era, and for the timing of the transition to recent rates of rapid sea-level rise to be better understood (Church and White, 2011). Consequently, investigations of changing RSL are an important part of understanding global climate change and their vitality can only increase in the years to come. Late Holocene sea-level reconstructions often rely on the vertical zonation of foraminifera found in salt marsh ecosystems (Edwards and Wright, 2015); this approach entails a standard methodology with some room for tailoring sample collection and analysis to the aims of the study and the features of the area of interest.

The importance of developing these RSL reconstructions is manifold. Several factors contribute to global sea-level rise but this rise is not globally uniform and thus the relative sea level differs between locations. Large contributions are made by the melting of land ice and the thermal expansion of water caused by rising global temperatures (Mitrovica *et al.,* 2001; Palmer *et al.,* 2020). Specifically, melt water distribution in the oceans, and thus RSL, is not uniform and is affected by the Earth's rotation and gravity field, known as gravity-rotation-deformation (GRD; Palmer *et al.,* 2020). Another contributor is sterodynamics, which includes sea-level changes caused by variability in ocean circulation such as the El Niño-Southern Oscillation (Harvey *et al.,* 2021). Yet another variable that must be considered is change in the land-level caused by differing rates of subsidence which subsequently affects the amount of sea-level rise experienced in a particular area (Nicholls *et al.,* 2021). Therefore, generating microfossil based RSL reconstructions, to be compared with instrumental records such as tide gauges, for a variety of locations around the world helps to quantify the regional differences in sea-level rise caused by the differing contributions of these factors. Records of past sea-level change then become important for generating and improving models of glacial isostatic adjustment (GIA; Bradley *et al.,* 2011; Peltier *et al.,* 2015) which simulate vertical land movements along the coast and are therefore an important tool for predicting future sea-level rise. In addition, understanding the responses of salt-marsh environments to past changes in RSL helps to elucidate the impact of future changes on these important ecosystems (Gehrels *et al.,* 1994).

3.2.2 Salt Marshes and Foraminifera

Salt marshes have been used in the study of RSL for over eighty years owing to the effectiveness of their sediments as geological tide gauges (Barlow *et al.,* 2013). These methods were pioneered by Godwin (1940) using pollen, and the work of

Scott and Medioli (1978) began to show that foraminifera are accurate indicators of sea-level change. The vertical zonation found in salt marshes is caused by the decreasing elevation of land from the high marsh to the tidal flat which leads to differing durations of tidal inundation across the marsh, ultimately resulting in varying degrees of salinity and differences in such factors as particle size and organic matter content, meaning there are habitats suitable for different plant and animal species in different zones (Scott and Medioli 1980). Therefore, foraminifera assemblages – and those of other microfossils such as diatoms (Gehrels *et al.,* 2001) – and plant fragments found in a core of salt-marsh sediment can be used to determine the elevation at which they were originally deposited and from this past sea level is determined (Gehrels *et al.,* 1994). Plants, however, can have a large vertical range within the salt marsh – introducing uncertainty – while foraminiferal assemblages have been shown to be more precise as sea-level indicators (Gehrels *et al*., 1994). Owing to this, RSL reconstructions based on foraminifera and investigations of their ecology have been established around the globe (e.g., Gehrels 1999; Murray 2001; Berkeley *et al.,* 2007; Avnaim-Katav *et al.,* 2017; Rush *et al.,* 2021).

Elevation does not directly impact the distribution of foraminifera but is used as a proxy for inundation frequency which in turn affects several other environmental variables (de Rijk 1995). As previously discussed, different zones within salt marshes show variability in a range of characteristics such as salinity, pH, organic matter content, particle size and biomass; all of these factors have an impact on foraminifera distribution (Edwards *et al.,* 2004b). However, elevation and inundation frequency have been shown in several studies to be the main factors determining foraminifera distribution across saltmarshes (e.g., Horton *et al.,* 1999a; Avnaim-Katav *et al.,* 2017). Therefore, despite other environmental factors having some influence on distribution, elevation shows the strong correlation with assemblage composition necessary for foraminifera to be considered useful proxies in sea-level research (Murray 2001). Having said this, de Rijk and Troelstra (1997) demonstrated the vitality of conducting a thorough surface study of any marsh to be used for RSL reconstruction. Their investigation of the Great Marshes, Massachusetts showed that the microtopography of this area results in the salinity gradient being independent of the elevation gradient and thus the foraminifera did not display a vertical zonation. Consequently, any salt marshes used for RSL studies must be considered on a case-by-case basis to ensure the implicit assumptions of the RSL reconstruction methodology are met.

3.2.3 Transfer Functions

Foraminifera-based reconstructions of sea-level change are performed through relating the changes in species abundances in modern surface samples, across an elevation gradient, to the species found at different depths within a core of salt marsh sediment. Foraminifera of the same species identified in both the modern marsh and the core samples being assumed to respond similarly to environmental changes. This is generally achieved using transfer functions; these are numerical techniques used to produce quantitative reconstructions of RSL from the relationship between tidal elevation and microfossil assemblages (Kemp and Telford, 2015). Utilising transfer functions is a two-step process; first, the transfer function must be developed through relating the distribution of modern species to the environment (Telford and Birks, 2009). This first stage requires a modern training set, samples

collected from the surface of the modern marsh with assemblage distributions controlled primarily by the variable of interest (Avnaim-Katav *et al.,* 2017). Second, the transfer function is applied to the microfossil assemblages in the core and the correlations detected here are used to determine the indicative meaning of different sections of salt marsh sediment within the core; this is the relationship between the sediment and the tidal setting in which it originally formed (Shennan, 1986; van de Plassche, 1986). For instance, a given assemblage might provide an indicative meaning of within 20 cm of mean higher high water (MHHW). Following this, a palaeo-marsh curve can be generated which displays the position of a sample based on its distance from a particular tidal datum at the time of its deposition (e.g., Edwards *et al.,* 2004a; Long *et al.,* 2010). The palaeo-marsh surface elevation prediction of each sample is ultimately subtracted from the field elevation of each sample to generate an RSL reconstruction.

To ensure RSL reconstructions achieve high precision, the transfer function technique has been developed extensively and is frequently applied. Guilbault *et al.* (1995) first applied the term transfer function in their study to test the results of qualitative analysis and the use of these techniques in the field has continued from then (Barlow *et al.,* 2013).

Several different methods for developing transfer functions exist, including both linear and unimodal approaches (Birks, 1995). The former assumes a linear distribution of foraminifera and an example is the maximum likelihood method (Telford and Birks, 2009). However, the unimodal approach is usually more suitable for RSL studies due to the high rate of species turnover along the elevation gradient (Birks, 1995). Some of the most common unimodal approaches include weighted averaging (WA) and weighted averaging partial least squares (WA-PLS; Kemp and Telford 2015). WA-PLS differs from WA in being able to incorporate the correlation displayed in the residuals into the model, thus improving its fit, meaning it is generally perceived as a superior approach (ter Braak and Juggins 1993). When applying the WA-PLS method, selecting the number of components to be used is an important step which influences the reconstructed elevations and their reliability (Wright *et al.,* 2011). It is generally held that a 5% or more increase in the Root Mean Squared Error of Prediction (RMSEP) is sufficient justification (Birks, 1998), although some argue that exceeding the second component adds needless complexity and that the decision to increase the number of components included should be based on further evidence (Wright *et al.,* 2011). Recently, Bayesian modelling has been used as a new approach to transfer function development (Salonen *et al*., 2012); this method does not assume a unimodal distribution and so could lead to improved transfer function calibration but is not widely used at present due to the computational expense it requires (Cahill *et al.*, 2016).

3.2.4 Age Modelling

One vital aspect of RSL reconstruction is the establishment of chronology for the cores of salt-marsh sediment used in the reconstruction. Radiocarbon dating, which involves the determination of the quantity of carbon-14 (^{14}C) isotope in biological material (Walker, 2005), is used to establish the precise ages of fragments of plant material found within cores and thus to determine the calendar date at which the sediment was deposited (Gehrels 1994; Nydick *et al.,* 1995). This, combined with the

palaeo-marsh elevation, can be used to follow sea-level change through time. Radiocarbon dating alone, however, has its limitations; fluctuations in atmospheric ^{14}C over the past 500 years have led to plateaus in the calibration curve used to convert radiocarbon years into calendar dates, which means several calibration options may exist for a single date (Stuiver and Quay 1980). The issues related to radiocarbon dating have necessitated the development of other chronological methods. The use of ^{210}Pb allows the calculation of the age and accumulation rates of sediments by measuring the residual radioactivity of the unsupported isotope, which is originally deposited from 'rain-out' onto the surface of the marsh (Appleby and Oldfield 1978; Appleby and Oldfield 1983). ^{210}Pb possess a half-life of 22.23 years (Aquino-López *et al.,* 2018) and so is useful for constraining the chronology of sediments deposited over the past 100-150 years (Krishnaswamy *et al.,* 1971; Aquino-López *et al.,* 2020). The activity of ^{137}Cs, which possess a half-life of 30 years, can also be used to date salt marsh sediments (Appleby 1997); the levels of this isotope in different parts of a core can be related to various events such as nuclear weapons testing, starting in 1954 and reaching a peak in 1963, and the Chernobyl reactor fire in 1986, thus allowing the date at which the sediment was deposited to be constrained (Walker, 2005). Other useful chronological markers include pollution horizons introduced by human activity, such as trace metals, and pollen markers known to appear in relation to certain events, such the arrival European settlers in New Zealand (Cundy and Croudace 1995; Gehrels *et al.,* 2008).

3.2.5 Regional Training Sets

Reconstructing RSL based on microfossil assemblages assumes that the species composition of these assemblages closely approximates the species found in the core (Birks, 2003). If past environmental conditions differ significantly from those of the present, this close approximation is unlikely to be the case and necessitates the use of modern training sets from different locations to generate a regional training set (Gehrels *et al.,* 2001; Watcham *et al.,* 2013; Hocking *et al.,* 2017; Rush et al., 2021). However, when the local training set provides sufficient analogues to the fossil assemblage it is preferable to continue with this approach due to the increased precision of the reconstruction generated (Woodroffe and Long, 2010). When a regional training set is used it is necessary to convert elevation values into a standardised water level index (SWLI) so that comparisons between sites with differing tidal ranges can be made accurately (Horton *et al.,* 1999b). The tidal range of the environment used as the basis for an RSL reconstruction can also impact the error associated with the reconstruction; microtidal environments – defined as having a tidal range of 2 m or less (Davies, 1964) – will generate more precise reconstructions because the indicative ranges are smaller (Edwards and Horton 2006). Another approach to transfer function development, namely, locally weighted models, aims to strike a balance between the conflicting advantages of local and regional training sets (Kemp and Telford 2015). This is achieved by developing a unique model for each fossil sample which includes a particular number of analogues (usually 30 or 50) selected by the modern analogue technique (MAT); this means large training sets can be used to ensure there are analogues for each fossil sample but without the need to weaken the model by including every modern sample each time (Kemp and Telford, 2015).

3.2.6 Count Size

The low diversity of foraminifera in salt marshes means that studies aiming to produce RSL reconstructions have usually aimed to count high numbers of individuals in both modern and core samples to ensure comparisons are statistically meaningful (Kemp *et al.*, 2020). For example, at the higher end of the scale, Southall *et al*. (2006) aimed to count 300 individuals from each sample where possible. Recently however, Kemp *et al*. (2020) have demonstrated that counting beyond approximately 50 individuals returns little in terms of improved transfer function performance; the time saved counting fewer individuals per sample can then be invested in processing a greater number of samples.

3.2.7 UK Relative Sea-Level Change

Past efforts to quantify RSL for Britain have been numerous (e.g., Edwards and Horton, 2000; Horton and Edwards, 2005; Long *et al.,* 2014), with Shennan *et al.* (2018) providing the current database of UK RSL data. Relevant to this study, there have been several previous investigations of sea-level change along the Northumberland coast using paleoenvironmental records. Plater and Shennan (1992) found that RSL had changed by only approximately 2.6 m over the past 8000 years, which was determined using sediment from Elwick, Alnmouth and Warkworth. They also found that the regional sea-level signal becomes increasingly suppressed towards the present date as site specific factors have an increasing impact (Plater and Shennan, 1992). This highlights the importance of a regional approach to RSL reconstruction. As mentioned in chapter 2, Shennan *et al.* (2000) found that mid-Holocene sea level recorded by the northern sites, including Beal Cast and Bridgehouse Farm and Bridge Mill situated on the mainland adjacent to Holy Island, used in their study, to be approximately 2.5 m above the present level. These existing reconstructions make it possible to understand the likely sea-level trends experienced by the study area further back through time than was possible within the scope of this study and before tide gauge records begin. It can be concluded that this area experienced low rates, generally less than 1 mm yr^{-1}, of sea-level change through the Holocene (Plater and Shennan, 1992).

The overall sea-level trend has fallen since the middle Holocene, which has been reversed in recent centuries by rapid rates of sea-level rise (Church *et al.,* 2001; Gehrels *et al.,* 2005). This sea-level rise provided the accommodation space for marshes to develop and, due to the relatively recent onset of these rates, UK marsh sediment is expected to be thin in most area (Gehrels and Kemp, 2021).

3.3 Gas Flux

3.3.1 Net Radiative Balance

The need to achieve carbon neutrality by ensuring that the system in question takes up as much carbon as it releases and so does not contribute to the overall levels of CO_2 in the atmosphere has been investigated in a variety of settings from commercial building developments (Zuo *et al*., 2012) and aviation (Krammer *et al.,* 2013) to salt marshes (e.g., Smith *et al.,* 1983). The emissions of other greenhouse

gases, methane (CH_4) and nitrous oxide (N_2O) for example, have also been measured and studied extensively (e.g., Kirschke *et al.,* 2013; Thompson *et al.,* 2014). Perhaps not as well studied or understood is the overall picture, that of climate neutrality. This term has become increasingly prevalent in recent years and, despite there being some debate around its true definition (Ziegler, 2016), is generally used when discussing the mitigation of several greenhouse gases, as opposed to simply focusing on CO_2 flux. Looking more broadly at climate neutrality, by calculating the net radiative balance of a particular ecosystem, is likely to produce a better understanding of the overall effect a particular system is having on climate change and, because of this, should lead to more effective mitigation techniques being employed (Worth, 2005).

As discussed above, salt marshes are powerful carbon sinks; however, focusing on carbon sequestration alone does not give an accurate picture of the overall effect an ecosystem has on climate change. There exists a plethora of competing processes that can lead to increases, as well as decreases, in greenhouse gas emissions. The respiration of salt marsh inhabiting plants and microbes results in CO_2 emissions that can start to negate the benefits of carbon sequestration; more significantly, CH_4 and N_2O can be emitted from salt marshes via a range of mechanisms (Fig. 3; Hirota *et al.,* 2007). Discovering the environmental drivers behind fluxes of these gases has been identified as a key question to be investigated as a part of blue carbon science into the future (Mason *et al.,* 2022). Both gases have a considerably greater radiative forcing (RF; meaning the contribution made by these gases to the balance of energy entering or leaving the atmosphere) effect than CO_2; the RF efficiency of CH_4 being 26 times greater than that of CO_2, and that of N_2O being 219 times greater (Myhre *et al.,* 2013; Ramaswamy *et al.,* 2019). Therefore, even emissions of these gases that seem relatively minor when compared with the high carbon sequestration rates of a particular salt marsh can in fact detract from climate change mitigation due to their high RF potency.

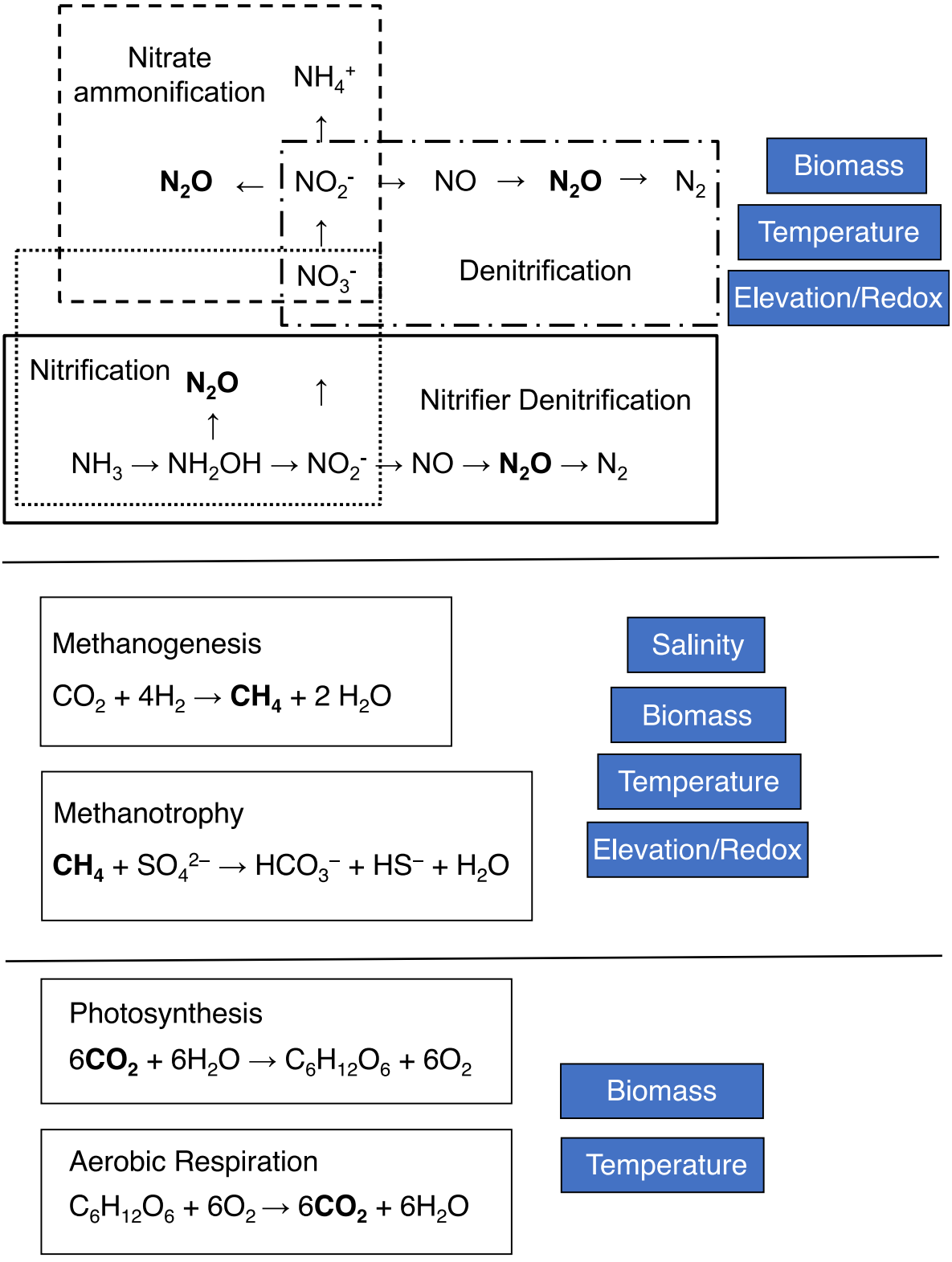

Figure 3. Reactions leading to the production or consumption of the greenhouse gases focused on in this study and the environmental variables expected to impact each. The nitrous oxide diagram is taken from Baggs (2008).

3.3.2 Methane Flux

The fact that salt marshes alternate between periods of time when they are submerged by sea water and periods when the tide withdraws means that they switch regularly between aerobic and anaerobic conditions (Blackwell *et al*., 2010). The regular anaerobic conditions produced by tidal inundation mean that salt marshes provide the perfect conditions for methanogenesis to occur (Fig. 3; Moore *et al.,* 1994). Given this, these ecosystems have the potential to be net sources of CH_4 (Magenheimer *et al.,* 1996). Conversely, regular tidal inundation means that salt marshes are well supplied with sulphate, allowing sulphate-reducing microbes to outcompete methanogens and so inhibiting CH_4 emission (DeLaune *et al.,* 1983; Poffenbarger *et al.,* 2011). Several studies using salinity as a proxy for sulphate concentration have concluded that CH_4 emissions from salt marshes are relatively minor (e.g., Poffenbarger *et al.,* 2011). However, more recently, emphasis has been placed on the importance of other environmental drivers in determining the net CH_4 emissions of salt marshes and other blue carbon ecosystems (Al-Haj and Fulweiler, 2020). One important factor - given the ability of plants to transport greenhouse gases from the soil to the atmosphere via their aerenchyma - is plant biomass and species composition (Magenheimer *et al.,* 1996). Specific plant species have been shown to produce this effect more than others; for example, Ford *et al.* (2012) found the presence of *Juncus gerardii*, an aerenchymatous species, led to increased emission rates.

Further to this, Whiting and Chanton (1993) found a positive correlation between primary productivity and methane emission, which they suggest may be explained by an increased supply of organic matter to the soil, as well as a greater number of plants acting as organs for gas exchange. Temperature too is a factor that impacts CH_4 emission; during warmer seasons, microbial activity is increased which results in higher emission rates (Emery and Fulweiler 2014). Furthermore, the warmer temperatures of the growing season also mean higher rates of primary productivity which results in higher inputs of organic matter via such mechanisms as root exudation. Noyce and Megonigal (2021) demonstrated that an increase in temperature of 5°C can lead to a doubling in CH_4 emission, meaning that climate warming could detract from the benefit salt marshes provide as carbon sinks. Global change also has the potential to impact CH_4 emissions via other mechanisms; as discussed above, Mueller *et al.* (2020) showed that the changing plant species composition of salt marshes caused by a rising sea level can have a significant impact on rates of CH_4 emission. Therefore, there are a multitude of factors influencing the rate of CH_4 emission, all of which are variable with marsh zone and at different times of year; notably, there is substantial uncertainty surrounding whole ecosystem CH_4 emission on an annual time scale (Chamberlain *et al.,* 2018). These considerations combine to make CH_4 flux a highly complex variable to assess and, potentially, minimise.

3.3.3 Nitrous Oxide Flux

The frequent cycling between aerobic and anaerobic conditions discussed above also means that salt marshes are favourable for both denitrification and nitrification (Roughan *et al.,* 2018). Both of these processes produce N_2O, an important gas to consider when assessing the net radiative balance of an ecosystem (Myhre *et al.,*

2013). Denitrification is an anaerobic process that involves soil microorganisms reducing nitrate (NO_3^-) to nitrogen gas and N_2O which can then diffuse from the soil and into the atmosphere (Fig. 3; Kaplan *et al.,* 1979). On the other hand, nitrification is an aerobic process that leads to the production of NO_3^- from nitrite (NO_2^-) with N_2O released as a part of the process (Fig. 3; Dollhopf *et al.,* 2005). Emissions of N_2O from long-established salt marshes have been investigated previously and found to be relatively low (e.g., Blackwell *et al.,* 2010). However, Moseman-Valtierra *et al.,* (2011) have demonstrated the potential of anthropogenic nitrogen inputs to cause certain salt marshes to change from sinks to sources. Anaerobic conditions favour denitrification, but this process is often limited in salt marshes by low NO_3^- concentrations in saline waters (Koch et al., 1992). Furthermore, low NO_3^- is likely to result in microbes reducing the less energetically favourable N_2O, which would result in more anaerobic areas being N_2O sinks and releasing N_2 (Koop-Jakobsen and Giblin 2010; Yang and Silver 2016). Rates of nitrification are likely low under anaerobic conditions, but low oxygen levels could stimulate increased N_2O emission from this process even in the limited capacity in which it does occur (Goreau *et al.,* 1980; Yang and Silver 2016). Furthermore, during the growing season, plant competition with microbes for soil nitrogen suggests that rates of N_2O emission will be lower (Chmura et al., 2011); contrastingly, the higher temperatures expected during the growing season will lead to greater microbe activity and thus N_2O production (Koch et al., 1992). Therefore, as with CH_4, there are several conflicting processes that, when combined, could result in a marsh acting as an overall source or a sink of N_2O. The contributions of these processes again differ with location within the marsh because of varying levels of tidal inundation and, therefore, time spent under anaerobic conditions, and with temperature at different times of year.

3.3.4 Carbon Dioxide Flux

Despite CH_4 and N_2O having a considerably greater radiative forcing effect than CO_2, fluxes of this gas are also worth considering to ensure a truly comprehensive picture of the net radiative balance is developed. CO_2 emission is more straightforward to consider; Magenheimer *et al*., (1996) concluded that plant respiration is a major contributor to CO_2 emission due to the positive correlation seen in their study between plant biomass and the rate of emission. Additionally, CO_2 is produced from microbial respiration during decomposition using the reduction of sulphate (Howarth 1984; Magenheimer *et al.,* 1996). In some cases, the emission of CO_2 from plant and microbe respiration is sufficient to offset carbon accumulation, as was the case in a study by Murray *et al.* (2015). The marshes they investigated were found to be carbon sources and they suggest that a warming climate may lead to even greater carbon loses due to higher respiration rates. CO_2 emission is, therefore, clearly an important factor to include in any assessment of net radiative balance, especially given the potential warming effect of future climate change.

3.3.5 Salt-Marsh Greenhouse Gas Flux

When attempting to assess the efficacy of salt marshes as climate change mitigators, it is vital to consider whether the emissions of greenhouse gases which occur as a result of the characteristic tidal inundation, offset the benefits provided by the ability of salt marshes to sequester carbon by way of that same mechanism. The importance of this is made evident by the fact that, over recent decades, as the potential of salt marshes as carbon sinks has been increasing realised and appreciated, significant efforts have been made to realign areas previously converted from salt marshes into agricultural land (Boorman and Hazelden, 2017; Macreadie *et al.,* 2021). Ensuring these realigned sites are fulfilling their purpose by acting as net greenhouse gas sinks can be made easier by a clearer understanding of the factors that contribute to the fluxes of different gases. Furthermore, it is important that the functioning of natural sites is also understood so that the contributions of these areas is neither under nor over estimated. The impact of realigned and natural sites can differ, with Mason *et al.* (2022) showing that N_2O flux was significantly different between the sites included in their literature review. Therefore, it is important to consider a range of different sites before making generalisations about greenhouse gas flux from salt marsh sites. Ultimately, realignment and existing sites could be managed in such a way that these factors are, as far as possible, maximised or minimised to produce the desired effect.

3.4 Synopsis

To conclude, salt marshes have been used extensively as geological tide gauges for the purpose of reconstructing sea-level change and the functioning of these ecosystems as carbon sinks is focused on a great deal within the literature (Barlow *et al.,* 2013; Macreadie *et al.,* 2021). The first knowledge gap this study aimed to address is the link between sea-level rise and carbon accumulation rate on a multiannual scale and at a much high resolution than was attempted by Rogers *et al.* (2019) in their large scale review. Secondly, the effect of greenhouse gas fluxes on the net radiative balance of a UK salt marsh was assessed by this project as there is a paucity of studies attempting similar assessments of these ecosystems. Ultimately, addressing these questions should illuminate the functioning of salt marsh ecosystems further so they can be effectively managed and accounted for accurately in any carbon crediting schemes.

Chapter 4: Materials and Methods

4.1 Relative Sea-Level Reconstruction

4.1.1 Sample Collection and Preparation

Modern surface samples were collected at two different locations within the Lindisfarne National Nature Reserve (NNR), Northumberland. In April 2021, 18 surface samples were taken from the Snook area (Fig. 4a). Subsequently, in September 2021, a further 41 modern surface samples were taken from Fenham marsh (Fig. 4b). The Fenham marsh samples were taken along a 690 m transect at elevations ranging from 3.02 m OD to 0.9 m OD. The Snook samples were taken along three transects (Fig. 4a); two of which, labelled 1 to 7 and 13 to 18 on Figure 4a, are vertical lines from the high to low marsh and measure 345 m and 288 m respectively. The third transect, comprising samples 12 through to 8 on Figure 4a, traces a diagonal line across the marsh surface and is 385 m in length. The elevations of the Snook surface samples range from 5.57 m OD to 1.98 m OD. Elevations in the Snook were determined using a dGPS while those in Fenham were measured with a Dumpy Level and staff; these elevations were expressed relative to a temporary benchmark, due to the lack of a geodetic benchmark. Subsequently, elevation of the temporary benchmark was measured with a dGPS which allowed all elevations to be converted to heights with respect to Ordinance Datum (OD). Collecting modern samples from two separate locations within the same area and from multiple different transects should help to ensure that a greater range of modern analogues are available within the training set for application to the fossil data. Furthermore, overlapping samples allow for the exploration of variability between samples that is not related simply to elevation and the potential effect of this small-scale variability on the accuracy of RSL reconstructions (Milker *et al.,* 2015)

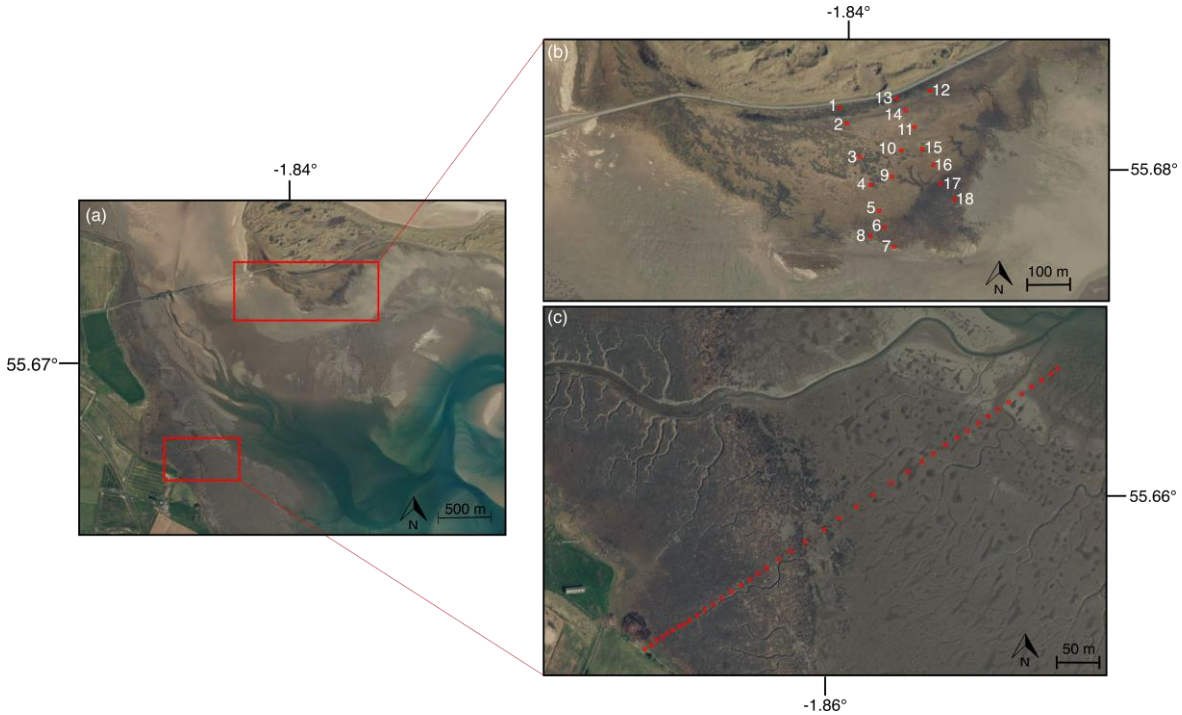

Figure 4. Locations of modern surface samples taken (a) Lindisfarne NNR and, specifically, from the (b) Snook and (c) from Fenham marsh. All images are from Bing (https://www.bing.com/maps, image copyright DigitalGlobe, 2020).

Each surface sample comprised approximately a 10x10 cm section of sediment of 1 cm thickness, cut from the marsh surface with a knife. Samples were refrigerated before being returned to the laboratory where they were combined with a rose Bengal-ethanol solution to allow differentiation between living and dead foraminifera (Walton 1952). Following this, all samples were sieved and the fraction between 63 and 500 µm retained. Samples were refrigerated in 5 % ethanol before analysis.

To analyse the samples, first, a wet splitter was used to divide each sample into eight equal aliquots. The aim was to count a minimum of 50 dead individuals for each sample; where this figure was not obtained in the first aliquot, further splits were processed until this benchmark was reached or the entire sample was counted. Following Kemp *et al.* (2020), samples with dead counts as low as 30 individuals were included in the final training set used for analysis. Individuals were only counted as living if rose Bengal staining was visible in the final few chambers of the test; this ensured that the staining seen was in fact protoplasm and not, for example, bacteria accumulating on the outermost chamber (Murray and Bowser, 2000). Counts of dead foraminifera alone were used for statistical analysis and transfer function development to avoid seasonal bias and significant differences between surface and subsurface samples (Horton and Edwards, 2003; Berkeley *et al.,* 2007).

The core of salt-marsh sediment used to reconstruct RSL was collected during the April 2021 visit from the location marked number 1 on Figure 4a. This Russian core, LI21-20, was sampled at a 1 cm resolution and the resulting samples stained, sieved and stored in the same manner as the modern surface samples discussed above. Again, a wet splitter was used to divide the samples into eight aliquots; the aim here was to count 100 dead individuals or the entire sample when this figure was not

reached. In the core samples, a high count was aimed for because of the possibly higher species diversity of these samples which increases the effect of count size on the resulting reconstruction (Kemp *et al.,* 2020).

4.1.2 Statistical Analysis and Transfer Function Development

The modern data was subject to a variety of statistical tests and analyses to assess the applicability of the assemblages seen to RSL reconstruction. To begin, the Partitioning Around Medoids (PAM) algorithm (Rousseeuw *et al.,* 1987; Kemp *et al.,* 2012) was applied using the R packages *cluster* (Maechler *et al.,* 2021) and *factoextra* (Kassambara and Mundt, 2020) to investigate clustering in the modern dead assemblage data. The silhouette widths generated by PAM quantify how well each sample is classified; these widths range from -1 (incorrect classification) to 1 (perfect classification). The average silhouette widths for 1 to 10 clusters were calculated and the optimum number of clusters was selected based on the highest average silhouette width generated. In addition to PAM analysis, non-metric multidimensional scaling (NMDS) was used to visualise the relationship between the samples in the R package *vegan* (Oksanen *et al.,* 2020). Bray-Curtis dissimilarity was chosen, and modern sample elevation was passively projected.

Detrended Canonical Correspondence Analysis (DCCA; ter Braak, 1986) using the CANOCO software package v.4.54 (ter Braak and Šmilauer, 2002) was applied to determine whether the modern assemblages display a linear or unimodal distribution across the elevation range covered. The threshold generally accepted to indicate that a unimodal distribution is present in the data is a DCCA axis possessing a gradient length greater than two standard deviations (ter Braak and Prentice, 1988; Birks, 1995). This is often found to be the case in studies of foraminifera distribution (e.g., Horton and Edwards, 2005; Rush *et al.,* 2021) and means that unimodal statistical models are commonly used to analyse data of this kind. DCCA also indicates the percentage of variation in the dead modern assemblages explained by the elevation gradient.

Due to the determination that the assemblages display a unimodal distribution, weighted averaging (WA; ter Braak 1988) and weighted averaging partial least squares (WAPLS; ter Braak and Juggins 1993) regression models were developed using the R package *rioja* (Juggins 2020). The performance of these transfer functions was assessed by considering the cross-validated (bootstrapped, 1000 cycles) correlation between observed and predicted elevation (r^2_{boot}) and the root mean square of error (RMSE). The bootstrapped residuals of all samples were reviewed and those with values 2.5 standard deviations from the mean were investigated further and if, after examining the assemblage more closely, evidence suggested the sample was an outlier differing substantially from the species-environment relationship, the sample was removed from the training set (Juggins and Birks, 2012).

In addition to developing local transfer functions, the Lindisfarne modern data was incorporated into the regional North Sea training set, a dataset comprising foraminiferal assemblages from sites in England, Scotland, Denmark and Germany (Rush *et al.,* 2021). Using a regional training set is advantageous because of the greater likelihood that the assemblages will contain a wide range of modern

analogues truly representative of the different environmental conditions represented by the core over time (Hocking *et al.,* 2017; Rush *et al.,* 2021). Conversely, sample-specific errors tend to be higher when using regional training sets and so the relative benefits must be considered carefully. To allow for differences in tidal ranges between the various sites included in the regional training set, the elevation of each modern sample was converted into standardised water level index (SWLI) values (Horton and Edwards, 2005). The following equation was used for this standardisation:

$$SWLI_n = \frac{100(h_n - MTL_s)}{HAT_s - MTL_s} + 100$$

Where h_n is the elevation of the sample in the local datum, MTL_s is mean tide level of the site (s) and HAT_s is the highest astronomical tide of the site (s). Following this, various transfer functions were developed using the resulting regional training set, including WA, WAPLS, locally-weighted weighted averaging (LW-WA; Juggins, 2001) and locally-weighted weighted averaging partial least squares (LW-WAPLS; Zhao et al., 2021). The latter two transfer function types were developed in addition to those also applied to the local training set because of the greater number of samples available in the North Sea training set. The performances of these transfer functions were assessed by the same parameters used when considering the local transfer functions; additionally, performance was compared with the values reported by Rush *et al.,* (2021) to determine if the addition of the Lindisfarne site led to an improvement. The RMSEP values obtained from the regional transfer functions were converted from SWLI to meters, in order to compare with the performance of the local training set, by working out the value of one SWLI unit and multiplying the RMSEP values by this figure.

To assess whether the training set provided a range of analogues representative of the assemblages found in the core, the modern analogue technique (MAT) was used to calculate the minimum dissimilarity coefficients (MinDC) between each fossil sample and the modern training set using the squared cord distance dissimilarity measure (Birks, 1995). Generally, the 20th percentile of dissimilarity values is used as the cut-off between “poor” and “fair” modern analogues for a fossil sample while the 5th percentile of values represents the cut-off between “fair” and “good” modern analogues, and this was the convention followed here (Watcham *et al.,* 2013).

Finally, the significance of the predictions produced by the transfer function were assessed. Reconstructed results were considered significant if they explained more of the variance in the fossil data than reconstructions generated by transfer functions trained on random environmental data (Telford and Birks, 2011). If this test does not lead to a significant result, doubt is cast on the likelihood of the resulting reconstruction being better than a random one and so the results should be interpreted with caution given its reduced credibility (Telford and Birks, 2011). Furthermore, this test can be used to test the credibility of transfer functions trained on both the local and regional training sets to assist with selecting the one most likely to produce a reliable reconstruction. The function *randomTF* in the R package *PalaeoSig* was used to perform this analysis (Telford, 2019).

4.1.3 Relative Sea-Level Reconstructions

Based upon the performance statistics, r^2_{boot} and RMSEP, the most appropriate transfer function for reconstructing RSL was selected and applied to the assemblages of dead fossil foraminifera found in a core of salt-marsh sediment from the Snook marsh. This provided estimates of palaeo-marsh surface elevation (PMSE). The PMSE value of each sample was then subtracted from the field elevation of the sample in question to generate estimates of RSL relative to OD.

4.1.4 Tidal Data

Tidal information, such as the HAT and MTL values used in the SWLI calculations, were obtained using a BaroTROLL 500 and Rugged TROLL 100 water-level logger. These devices were deployed near the landward side of the Lindisfarne NNR causeway (at 55.677°, -1.871°) between 10/03/22 and 20/04/22. The resulting time series were analysed in MATLAB (2018). First, the TPXO global tidal model (Egbert *et al.,* 2010) was scaled to fit the data obtained from the water-level logger; however, this failed to result in a suitable fit between the model and the data recorded by the logger. Instead, the logger data were compared with tide-gauge data from North Shields (77 km from the study site). The tide-gauge data were scaled to fit the logger data and the scaling factor then applied to the published North Shields tidal datums to derive datums for Lindisfarne. MTL was assumed to be the same at Lindisfarne and at North Shields.

4.1.5 Chronology

The layers of sediment in core LI21/20 were dated using a combination of methods: ^{210}Pb and ^{137}Cs were gathered as part of the C-Side project and are used for Bayesian age-depth modelling here. These three approaches each provide different information which cumulatively result in a reliable age-depth model. ^{210}Pb can be used to date sediment records within the last 100-150 years and relies on deposition of this isotope on the surface of the study site and its decay over time (Appleby and Oldfield, 1978). The radioactive isotope, ^{137}Cs, is prevalent in the atmosphere following 1950-60s nuclear weapons testing and the Chernobyl fallout of 1986, form a distinctive marker horizon in cores of sediment which can be attributed to these events and used to constrain age models generated from ^{210}Pb data (Walker, 2005).

Levels of unsupported ^{210}Pb were determined at each cm down the core until a depth of 20 cm, after which two more measurements were made at 25 cm and 30 cm depths. Activity of ^{137}Cs was measured at the same resolution and depths to determine the depth at which the peak activity of this radionuclide occurred, which would indicate the likely depth of sediment deposited in the year 1986. The chronological data was gathered as a part of the NERC funded C-Side project, with radionuclide samples run at the Consolidated Radio-isotope Facility (CoRIF), University of Plymouth.

The age-depth model generated using this data was developed in the R package *rplum* (Blaauw *et al.,* 2021). This approach was chosen over more traditional techniques, such as the Constant Flux model and OxCal program (Appleby and Oldfield, 1978; Ramsey, 1995), because of the multiple advantages it provides.

Namely, using *rplum* negates the need to select an equilibrium depth, which is a decision that carries important consequences for the age-depth model produced, because this package infers ^{210}Pb flux (Aquino-López *et al.,* 2020). Additionally, while other approaches use the ^{137}Cs time marker to correct the chronology, *rplum* can use this additional data to improve the chronology and reduce uncertainty (Aquino-López *et al.,* 2020). Furthermore, *rplum* does not require that the whole core be sampled and missing data, as in this case, does not become problematic (Aquino-López *et al.,* 2018). The code used for running the age model is available in the data repository figshare (10.6084/m9.figshare.21151522; Table S7).

4.2. Salt-Marsh Carbon Stocks

Organic carbon content was measured at high resolution in core LI21/20 as a part of the C-Side project. To obtain measures of carbon density – following the practices recommended in the Blue Carbon Manual (Howard *et al.,* 2014) – for each centimetre of sediment in the core, dry bulk density and organic carbon content (OC %) were determined. The latter was quantified using Thermo Flash EA 1112 NC elemental analyser. I then used this data to calculate carbon density (g cm^{-3}; the product of OC and bulk density) which allowed an estimate of blue carbon stock to be developed for the location.

In addition to the two variables discussed above, the C-SIDE project also gathered a range of elemental and isotope data useful for determining the sources of OC present in the core and the impact of sea-level change (Ruiz-Fernández *et al.,* 2018); these data include nitrogen content (N %), the carbon to nitrogen ration (C/N), $\delta^{13}C$ and $\delta^{15}N$ levels. I then considered C/N and $\delta^{13}C$ in relation to one another and data from Khan *et al.* (2015) was used to interpret the various signals of organic matter sources seen here.

It was possible to obtain sediment accretion rates (SAR) for each centimetre of core LI21/20 from the age-depth model generated by the *rplum* package discussed above. These values were multiplied by the carbon density from the corresponding core depth to obtain carbon accumulate rates (CAR). Both SAR and CAR values were compared with rates of sea-level change calculated from the tide gauge record to determine whether the marsh is succeeding in keeping pace with sea-level rise and the effect of a changing RSL on the carbon accumulation achieved by the marsh through time. Sea-level change was calculated by smoothing the data in R with the lowess function from the *stats* package (R Core Team, 2022); these data was then averaged over the age range given by the r*plum* age model for each centimetre of sediment in the core for which sea-level data was available. In order to investigate the impact of sea-level rise on CAR, regression analysis was performed and the normality of the data was assessed using the Shapiro-Wilk test ($p.<0.05$). To allow carbon accumulation rates to be compared with rates of gas flux, they were converted to gCO_2 equivalents m^{-2} yr^{-1}; this was done by multiplying the carbon values by 44 g CO_2 / mol Ceq (Wieser, 2006).

4.3 Salt-Marsh Gas Flux

4.3.1 Sites

Gas flux rates were measured at the Snook site shown in Figure 4a. The locations numbered 1, 4 and 7 were selected for placing the static chambers to ensure measurements were taken from the high, mid and low marsh zones. In station one, the thickness of the peat layer is 16 cm, in station 4 it is 10 cm and in station 7 the top layer is silt, which is 30 cm deep. At each station, two replicate measurements were taken during the March visit, with this figure increasing to three replicates for every subsequent visit (Fig. 5a).

The first measurements were taken on the 10th of March 2022, this visit aimed at capturing flux rates before the beginning of the growing season. Subsequent measurements were taken throughout the growing season, the first on the 20th of April 2022. Following this, monthly measurements were taken on the 19th of May, 20th of June and 20th of July 2022.

4.3.2 Gas Flux Measurements

First, collars made of brown PVC drainpipe - 20 cm in diameter, 10 cm tall and 0.9 cm thick - were sunk ~5cm into the marsh surface at each location where a chamber was to be placed (Fig. 5b). The chambers - 25 cm tall and 20 cm in diameter and made with 0.6 cm thick Perspex - were placed on these collars and the join between chamber and collar sealed with electrical tape (Fig. 5a). Gas samples were taken with a 20 ml syringe at set time intervals: 0, 1, 2, 3, 4, 5, 10, 20, 30 and 40 minutes after the chamber was placed in March, June and July and 0, 1, 2, 3, 4, 5 and 10 minutes in April and May. These samples were stored in evacuated Exetainers® (Labco Limited, High Wycombe, UK) for transport and storage before analysis was performed. Fans were not placed inside the chambers as it was determined that real-world conditions could not be appropriately replicated; therefore, the fluxes measured predominantly represent those produced by diffusion of gases (Redeker *et al.,* 2015).

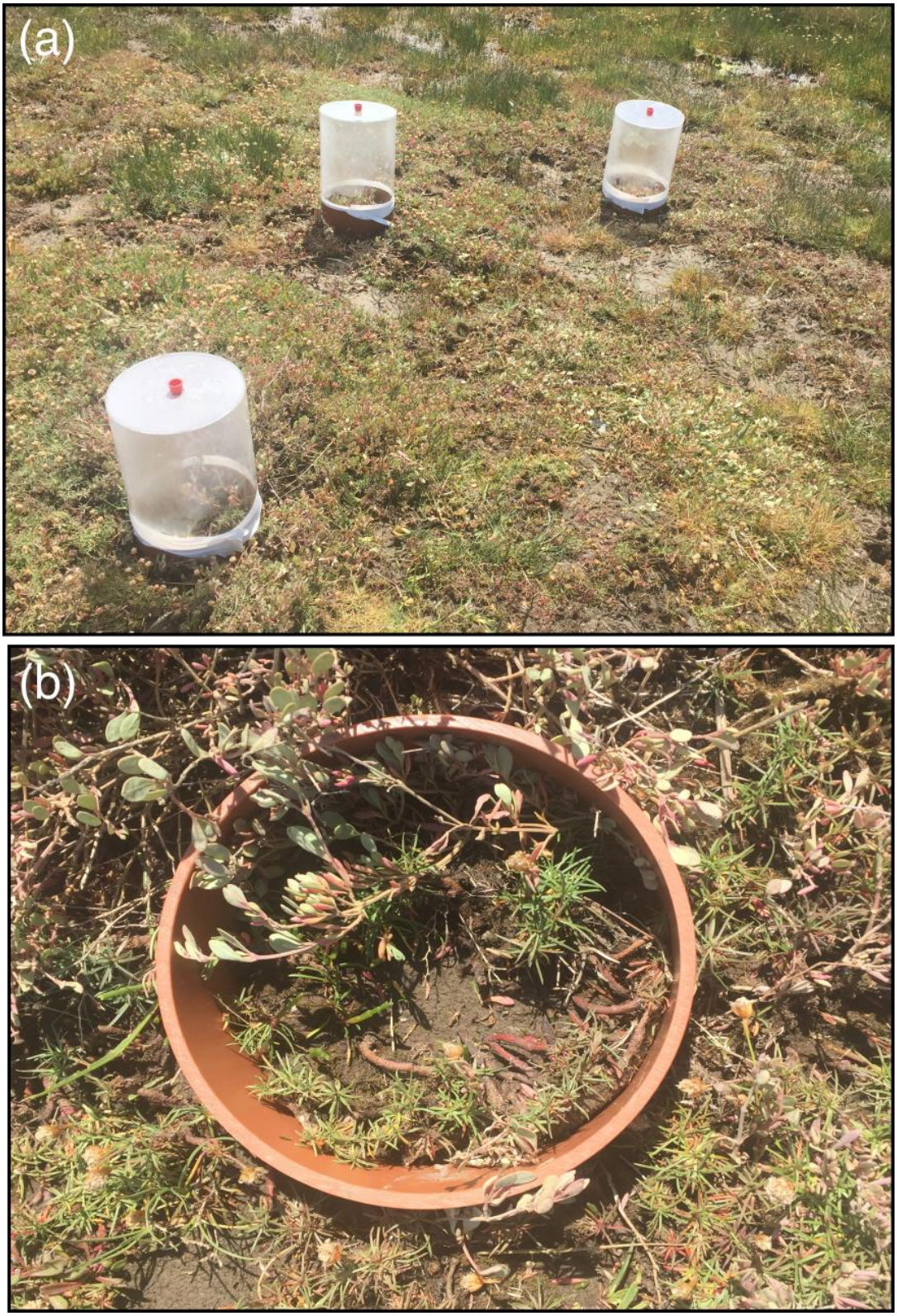

Figure 5. Photographs of site set up on the middle marsh station. The top panel shows three gas flux chambers placed on top of the collars and secured with electrical tape, while the bottom panel shows a single collar sunk into the marsh surface before the chamber was attached and the plant community within. Photographs were taken on the 20/06/2022.

When greenhouse gas fluxes were first measured, in March, a Los Gatos Research fast greenhouse gas analyser (LGR; Los Gatos Research, Mountain View, CA, USA) was also used as a form of calibration to assess the rapidity of CH_4 and CO_2 fluxes that could be expected and to determine whether the CH_4 emission was sufficiently large to cause problems with chamber over-saturation when using the previously described technique. The LGR was not used to take all the measurements as this would not have allowed N_2O fluxes to be assessed, which was determined to be essential given its status as one of the major greenhouse gases, meaning its inclusion was necessary to justify the claim that a comprehensive assessment of the net radiative balance of the ecosystem in question was being carried out. Using the LGR indicated that taking measurements for the first ten minutes after the chamber was first deployed was sufficient to accurately capture the rates of flux of these gases from the marsh. Therefore, the method was adjusted after the March visit so that samples were only taken up to ten minutes after chamber placement and an extra replicate was taken at each station across the marsh, meaning there were three replications at each station. The CH_4 flux measurements provided by the LGR were not found to be sufficiently large to invalidate the preferred method; however, the relatively small CH_4 and N_2O fluxes were found to be highly variable. This meant that taken measurements for only ten minutes often made determining the overall trend of the flux over the shorter time course difficult; therefore, from the June visit onwards, the sampling time was increased once again to forty minutes.

Varying the method used to measure the salt-marsh gas flux, can be justified by the fact that one goal of the study was to establish the best practice for using the static chamber techniques to this end. Given this aim, it was accepted from the beginning of the study that adjustments to the method would be required, and these changes have been made accordingly. What aspects of the method have been changed are not significant enough to invalidate comparisons between the fluxes measured one month with those from another; it is, however, important to note that CH_4 and N_2O fluxes were very rarely linear and that values deleted were where necessary from almost every measurement to ascertain a clear overall trend (see Materials and Methods 4.3.4 for more details).

4.3.3 Environmental Data

In addition to measuring gas flux via the static chambers, environmental data was also recorded at each station where chambers were placed. These data were temperature, pH, salinity, soil moisture and plant species and percentage cover within the collars. Temperature and pH were measured using a temperature and pH probe (Fisherbrand accumet Waterproof AP72 pH/mV/Temperature Meter) which provided instantaneous measurements. To measure soil moisture, a soil moisture meter (Theta Probe type ML2x, Delta-T Devices, Cambridge, UK) was employed, which also enabled instantaneous measurements to be collected. Conductivity was measured as a proxy for salinity; to this end, soil samples were taken in the field so that conductivity could be measured in the laboratory using a conductivity meter (HI 9033 Multi Range Conductivity Meter, HANNA Instruments). This was necessary as it was discovered that soil in the field was often too dry to produce a reading with the meter; therefore, a known quantity of each soil sample was mixed with a known volume of deionised water to produce a sample liquid enough to obtain a

measurement. Given the known conductivity value of deionised water, it was possible to calculate the conductivity of the soil before its addition.

In addition to the environmental data collected alongside the gas flux measurements, it was also possible to draw on data collected by the C-SIDE project from each of the stations in Figure 4a in April 2021. These data included bulk density, elevation and vegetation surveys.

Environmental data were collected with a view to future potential projects aiming to investigate their likely effects on salt-marsh gas flux, given that detailed analysis of these variables falls outside the scope of this project due to constraints on time and resources. However, preliminary analyses were performed; the normality of the data were tested with Shapiro-Wilks tests and linear regression was used to determine changes in these variables over the months and between marsh zones, and to assess whether the variability in flux rates that could be explained by these environmental variables.

4.3.4 Gas Chromatography

Analysis of all three gases contained within the Exetainers® was performed within a month of collection using a PerkinElmer-Arnel gas chromatograph (GC, AutoSystem XL, PerkinElmer Instruments, Shelton, CT, USA) equipped with a flame ionisation detector and a 3.7 m Porapak Q 60/80 mesh column. The carrier gas, N_2, had a flow rate of 30 mL min^{-1} and injector, column and detector temperatures were 120, 40 and 350°C respectively. Before detection, CO_2 was converted to CH_4 by a Ni reduction catalyst. CH_4 and CO_2 concentrations were detected in the fraction of the sample travelling through one channel while N_2O was detected in the fraction travelling through a separate channel.

Rates of flux were calculated from the slope of regressions of CH_4, CO_2 and N_2O concentrations. Where measurements were found to be non-linear with regressions with r^2 values less than 0.9, it was often necessary to remove outlying data. This involved first removing values that were substantially above or below ambient levels of each gas and/or the rest of the flux values in a particular measurement; next, a scatterplot of the remaining values was visually inspected and any value differing from the overall flux trend, thereby skewing the data, was also removed. These removals meant that CH_4 and N_2O measurements used for the final flux calculations were made more linear, but they rarely possessed an R^2 value greater than 0.9. Where it was not possible to identify a trend within the data due to too much variability between measurements, these measurements were not used to calculate fluxes.

Differences in emission rates between marsh zones and over the months were tested using linear regression, after Shapiro Wilks tests confirmed the normality of the data. Mean annual fluxes and standard deviations were calculated from flux rates calculated for all replicate measurements.

Following this, the net radiative balance of the high, mid and low zones of the Snook salt marsh were assessed. Again, to ensure accurate comparisons between rates of gas flux and carbon burial, these data were converted into gCO_2 equivalents (Ceq).

CH_4 and N_2O were multiplied by GWP100 conversion factors; for CH_4 a conversion factor of 28 was used, while for N_2O the conversion factor was 265; these values were obtained from the 2013 IPCC report (Myhre *et al.,* 2013). In the following results, negative values represent an uptake of the gas in question while positive values show an emission.

Chapter 5: Results

5.1 Relative Sea-Level Reconstruction

5.1.1 Modern Foraminifera in Local Training Set

The modern surface samples taken from Lindisfarne NNR were collected from two salt marshes at Fenham and the Snook (Figs. 1 and 4). Due to their close proximity (approximately 1.7 km), we assume they are undergoing the same tidal regime. In total 59 surface samples were collected – 18 from the Snook salt marsh and 41 from Fenham (Fig. 4). One sample from the upper marsh at Fenham contained no foraminifera and two more samples contain fewer than 30 dead individuals, meaning these were not included in the statistical analysis (Fig. 6a). The average count of the samples carried forward to the analysis stage was 89 individuals and the maximum count was 266 (Table S1).

Foraminifera assemblage distribution in both sites are in relatively good agreement across the samples, with no major discrepancies standing out (Fig. 6a). Twelve different species of foraminifera were identified in the dead surface assemblages; of these, four were agglutinated species and eight were calcareous (Fig. 6a). These samples show a clear vertical zonation across the surface of the marsh with agglutinated species dominating the high marsh elevations and calcareous species becoming increasingly prevalent at lower elevations (Fig. 6a). The majority of species within the modern training set show a unimodal distribution across the elevation gradient; the exceptions are *Ammonia* spp. and *Quinqueloculina* spp., which have bimodal distributions (Fig. 6a). This is likely explained by the fact that these foraminifera were only identified to genus level because of the difficulty of distinguishing between different species without using genetic techniques (Holzmann, 2000; Hayward *et al.,* 2004). Therefore, it is highly likely that multiple species of foraminifera have been lumped together.

Ten species of foraminifera were identified in the living assemblages, and they account for 16 % of the overall number of foraminifera counted across all samples (Table S2). The distribution of live species shows a consistent overlap with their dead counterparts (Fig. 6a). The main exception to this *Quinqueloculina spp*., live assemblages of which are numerous (80-100 % abundance) at elevations both higher and lower than the peaks of the dead assemblages (Fig. 6a). Again, this may reflect the lumping together of several species from the *Quinqueloculina* genus. Additionally, live assemblages of *Cornuspira involvens* tend to show a higher abundance (up to 33 %) than the dead assemblages of the same species, which only reach a peak of 16 % in one sample (Fig. 6a).

The Partitioning Around Medoids (PAM) algorithm indicates the presence of four clusters within the dead assemblages (Fig. 6b and Fig 7a). Figure 7a displays the silhouette width of each individual sample; the average width is 0.43 and only two samples from cluster four have negative width values, suggesting these samples are incorrectly classified.

The first and largest cluster covers a wide area in the high marsh zones of both marshes at elevations ranging from 2.80 m OD to 2.03 m OD and is dominated by *Entzia macrescens*, with high abundances of *Miliammina fusca*, *Haplophragmoides* spp. and *Trochammina inflata* also present at various points within the cluster.

Cluster two overlaps somewhat with both clusters one and three and contains samples from elevations of 2.25 m OD to 1.95 m OD; this cluster is dominated by *Quinqueloculina* spp. with the percentage abundance of this species ranging from 29 % to 68 % in these samples. Cluster three contains samples dominated by *Ammonia* spp. which shows a bimodal distribution and because of this, overlaps completely with cluster four. The elevation range of the samples found in this third cluster is 2.018 m OD to 0.9 m OD. The fourth cluster contains samples from elevations of 1.85 m OD to 1.3 m OD; it is dominated by a combination of *Cribroelphidium williamsoni* and *Haynesina germanica* and is characterised by very low *Ammonia* spp. abundances. At an elevation of 1.25 m OD *Ammonia* spp. again becomes dominant in the assemblages and these lowest elevation samples are classified as belonging to cluster three. The two separate peaks in *Ammonia* spp. abundance likely indicates the presence of at least two separate species of this foraminifera within the area.

NMDS analysis helps to further investigate the importance of elevation in determining foraminiferal distribution. Agglutinated and calcareous species are shown to inhabit two clearly distinct groups within the passively projected elevation gradient (Fig. 7b). *Cornuspira involvens* is the only species that can be said to occupy its own cluster, separate from either the agglutinated or calcareous species clusters (Fig. 7b); this likely corresponds to the fact that it is only found in any numbers in the mid marsh zone while the other calcareous species are found through both the mid and low marsh zones (Fig 6a).

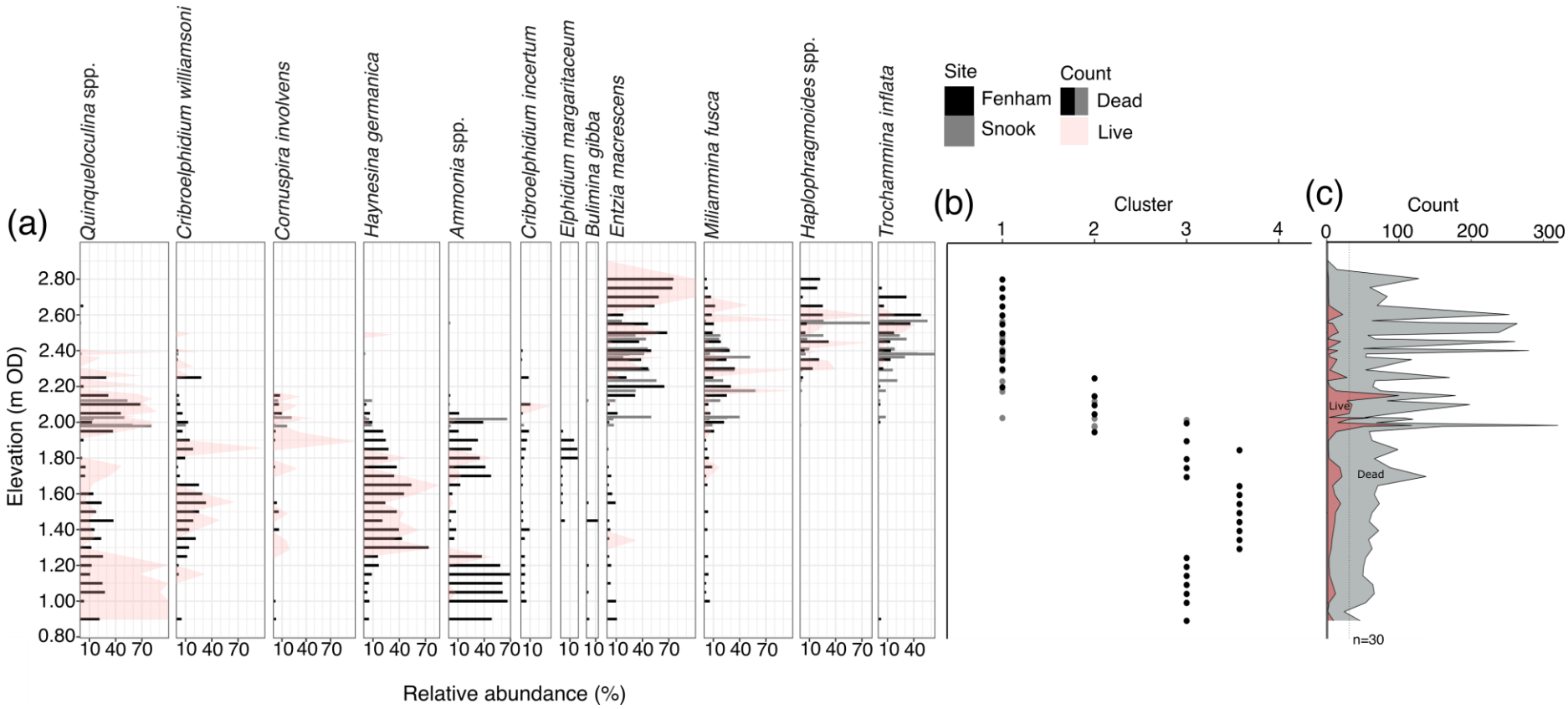

Figure 6. Distribution of dead and live modern foraminiferal populations in Lindisfarne. a) Assemblage diagram with samples from two different sites within the same tidal range indicated by different colours; filled bars indicate dead populations while the silhouette shows live populations. (b) Clustering detected by PAM analysis, with four clusters present and samples again coloured by site. (c) Total counts of live and dead foraminifera in all samples collected at elevations from the top to the bottom of the marsh; the dashed line indicates the minimum number of dead individuals required for samples to be included in further analysis.

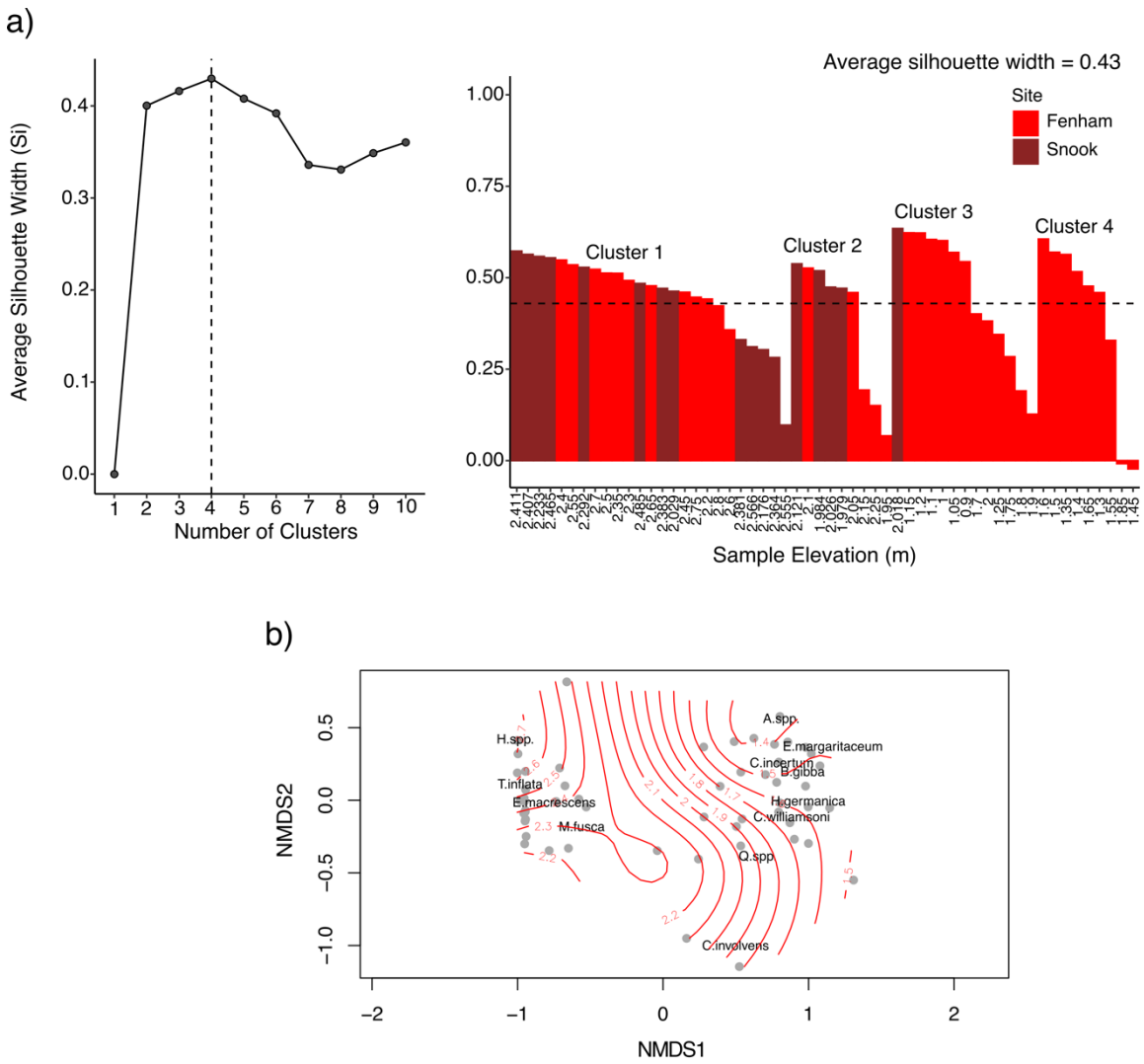

Figure 7. PAM and NMDS analysis of the Lindisfarne local training set. a) Number of clusters calculated by the PAM analysis to result in the greatest silhouette width and the average silhouette width of each individual sample with the colours corresponding to those used in Figure 1a to differentiate between clusters. b) NMDS analysis with elevation passively projected and foraminifera species labelled.

5.1.2 Comparison with a North Sea foraminiferal dataset

Combining the foraminiferal assemblages of the local Lindisfarne training set with those in the regional North Sea training set (Rush *et al.,* 2021) – normalised for tidal range differences using SWLI - showed the former is consistent with the latter both in terms of species distribution and percentage abundance of the different species generally present within the assemblages (Fig. 8). The agglutinated species especially overlap well with the peak abundances of those same species in the other North Sea sites; this is also true for the most part for calcareous species, with a few exceptions. Both *Quinqueloculina* spp. and *Ammonia* spp. have bimodal distributions in the Lindisfarne training set and continue to occur in abundance at SWLI values where these foraminifera are present less consistently and in lower numbers in the other assemblages included in the training set (Fig. 8). Additionally, *Bulimina gibba* is only found within the Lindisfarne training set and is absent from the rest of the regional assemblages. The presence of this species in the Lindisfarne samples might indicated that it has been misidentified or grouped with another species in previous studies.

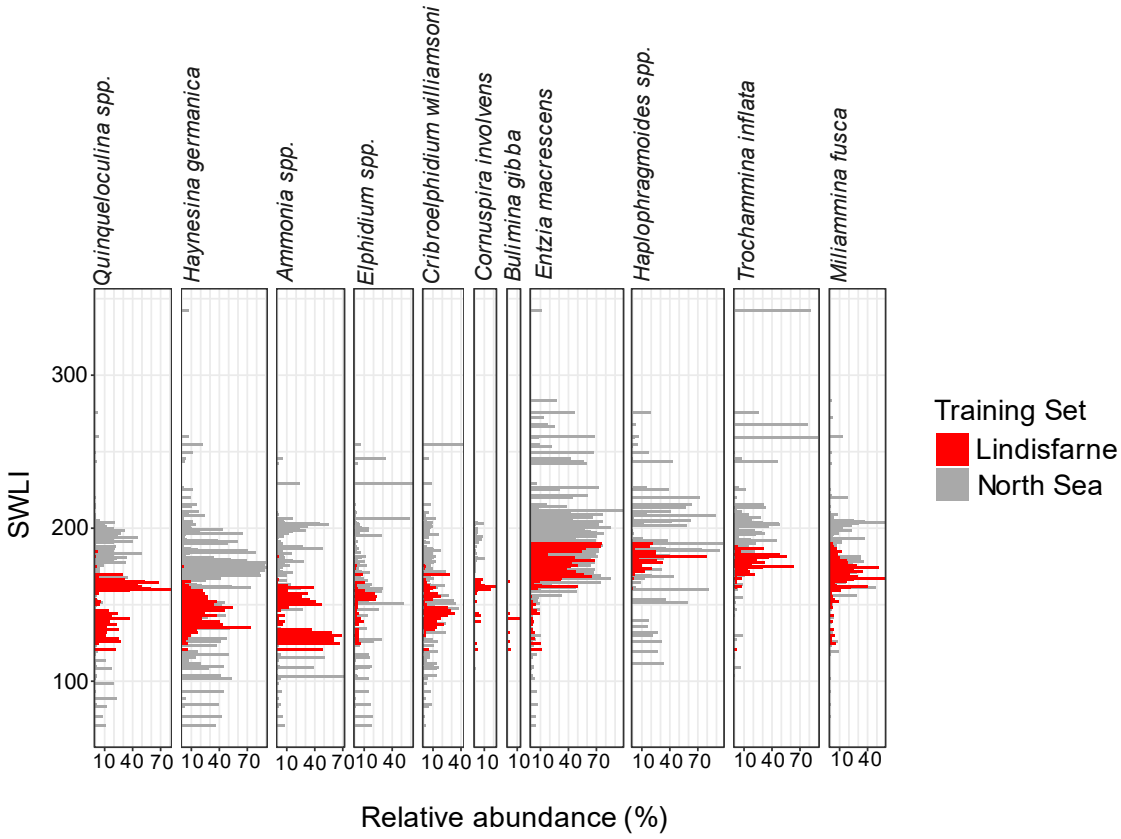

Figure 8. Distribution of modern foraminifera in the regional North Sea training set with the Lindisfarne training set included. North Sea training set data is taken from *Rush et al.* (2021).

5.1.3 Transfer Function Development

Transfer functions were first developed using the Lindisfarne local training set. The first DCCA axis gradient length was found to be 3.39 and so greater than two standard deviations, confirming that the species in the modern training set are best represented by a unimodal distribution and meaning that WA and WA-PLS transfer functions could be developed. The transfer functions developed with the local training set show a positive relationship between observed and predicted values (Fig. 9a). The observed and residual values show a weak negative correlation (Fig. 9a). These transfer functions all result in similarly large errors – likely explained by the large tidal range experienced by the area – and a similar predictive power (Table 1). Component two of the WA-PLS model was selected as the best performing transfer function trained with the local data; a decrease of more than 5% is seen in RMSEP when moving from the first to the second component which means the use of a more of a more complex model is justified (Birks, 1998).

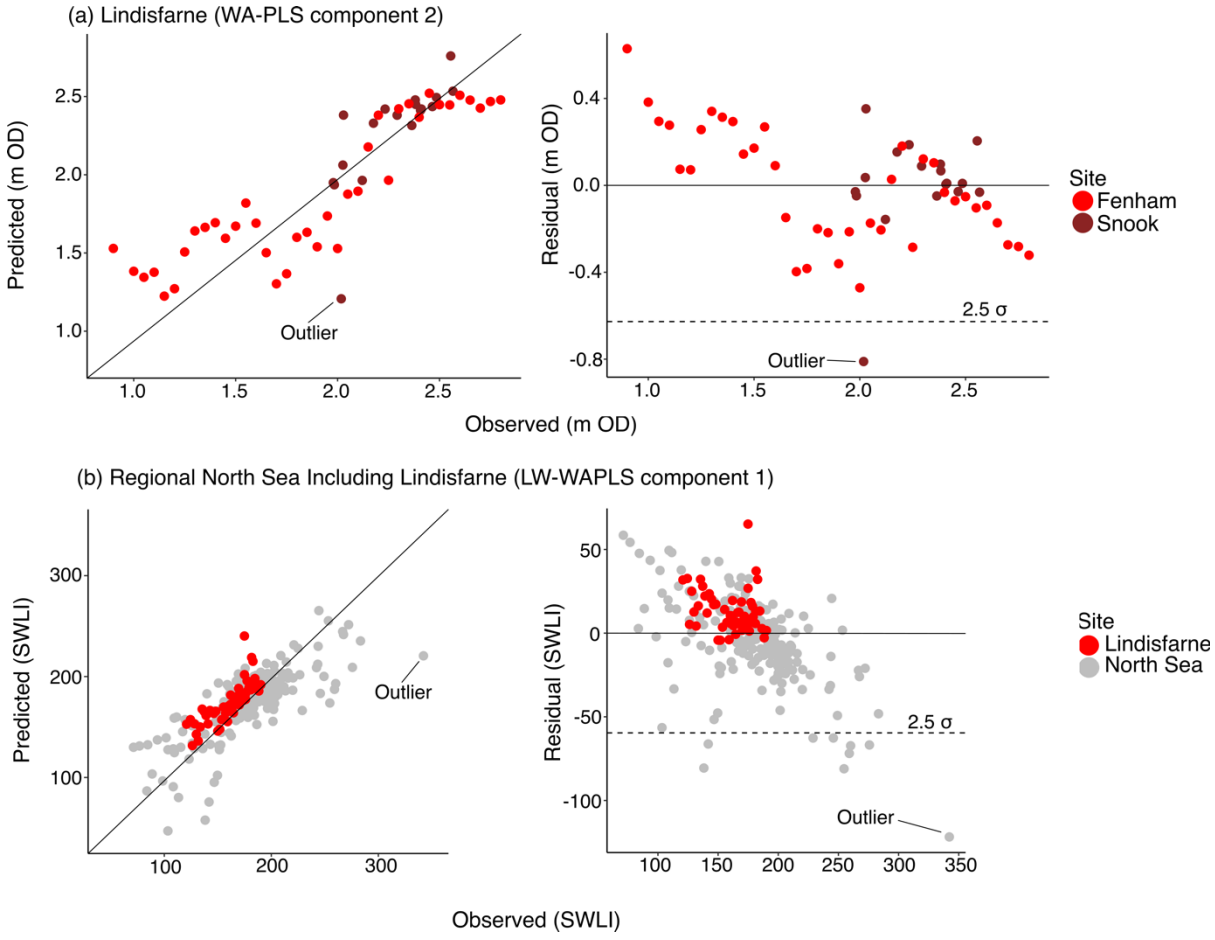

Figure 9. Performance of transfer functions highlighted in Table 1 developed using (a) the local Lindisfarne training set and (b) the regional North Sea training set. The dashed lines indicated the 2.5 σ boundary and the outlying samples that were removed from the final transfer functions are indicated.

Table 1. Transfer function performance summary statistics. The best performing transfer functions developed using the training sets that include data gathered as a part of this study are highlighted in bold. Performance statistics for the North Sea training set excluding Lindisfarne are shown for comparison and are taken from Rush *et al.* (2021). The RMSEP values in the bottom column were converted from SWLI to metres using Lindisfarne tidal data so that they are readily comparable (Rush *et al.,* 2021)

Training Set	Model	Deshrinking/ Component	Bootstrapped R^2	Bootstrapped RMSEP (m)
Lindisfarne	WA	Inverse	0.7253	0.2697
		Classical	0.7309	0.3033
	WA-PLS	1	0.7249	0.2701
		2	**0.7544**	**0.2668**
		3	0.7599	0.2748
North Sea including Lindisfarne	WA	Inverse	0.5318	0.2784
		Classical	0.5352	0.3683
	WA-PLS	1	0.5328	0.2791
		2	0.5545	0.2784
	LW	Inverse	0.6559	0.2372
		Classical	0.6081	0.2996
	LW-WAPLS	**1**	**0.6575**	**0.2365**
		2	0.6645	0.2364
North Sea excluding Lindisfarne	WA	Inverse	0.5500	0.3828
	WA-PLS	1	0.5800	0.2998
	LW-WAPLS	1	0.6000	0.2809

The agreement between observed and predicted results is strong for the majority of samples; however, one sample may be classified as an outlier with its residual value exceeding 2.5 σ (Fig. 9a). Upon further examination of this sample, it was found that it contains a high abundance of *Ammonia* spp. (66 %) at an elevation of 2.018 m OD which is considerably higher than the elevation at which similarly high abundances of this foraminifera are seen again, starting at 1.7 m OD (Fig. 6a). This high abundance could be explained by environmental variables, such as salinity or pH, deviating from their expected correlation with elevation and thus making conditions favourable for low-marsh species in the location at which this sample was taken. This suggests that the sample does not appropriately reflect the species-environment relationship. Therefore, this sample was removed from the final transfer function and Table 1 displays the performance of transfer functions generated without the inclusion of this sample.

Next, transfer functions were developed using the regional North Sea training set. Again, the first axis gradient length was confirmed by DCCA to be greater than two standard deviations at 3.19, and so a unimodal relationship is present between assemblage and environmental data. These transfer functions provided estimates of error in SWLI units which were converted to meters by calculating the value of 1 SWLI (see Materials and Methods 4.1.2)). This resulted in the development of transfer functions with lower vertical errors than those trained on the local data alone (Table 1). R^2 values were, however, slightly lower, suggesting somewhat poorer agreement between agreed and predicted results (Table 1). The best performing transfer function developed using the regional North Sea training set was the first component of the LW-WAPLS model (Fig. 9b) which had an RMSEP value of 0.2365 m; there is a decrease in RMSEP between the first and second components of this model, but it is far too minor (0.0001 m) to warrant the increased complexity. When considering the correlation between overserved and residual values for this transfer function there were several outliers which exceeded the 2.5 σ boundary (Fig. 9b). One of these, a sample from the North Sea training set, was removed from the final transfer function because it contained a very high *T. inflata* population at an elevation far higher than those at which these foraminifera is seem in other samples, even at low abundances (Fig. 8).

In addition to confirming the presence of unimodal relationships, DCCA indicated the amount of variation in assemblage data explained by the elevation gradient. For the local data, this was 26.7 % and for the regional, 6.6 %.

When the performance of transfer functions developed using the North Sea training set with Lindisfarne included is compared with those reported by Rush *et al.* (2021) a decrease in RMSEP of 0.10 m for the WA (Inverse) transfer function, 0.02 m for the first component of WAPLS and 0.04 m for the first component of LW-WAPLS is seen (Table 1). This improvement in precision arose from the inclusion of relatively few new modern samples in the training set.

Developing a locally weighted model, which selects the thirty closest analogues for each individual fossil sample, using the regional data resulted in a transfer function with a lower RMSEP value than those trained with the local data. Going forward, the transfer function developed using component one of the LW-WAPLS model trained with the regional North Sea training set was used to generate a RSL reconstruction.

5.1.4 Snook Marsh Stratigraphy and Foraminifera Assemblages

Cores of salt-marsh sediment, taken using a hand corer during the C-Side project, were used to investigate the stratigraphy of the marsh. These cores were taken from the Snook marsh and correspond to the three transects shown on the map in Figure 10.

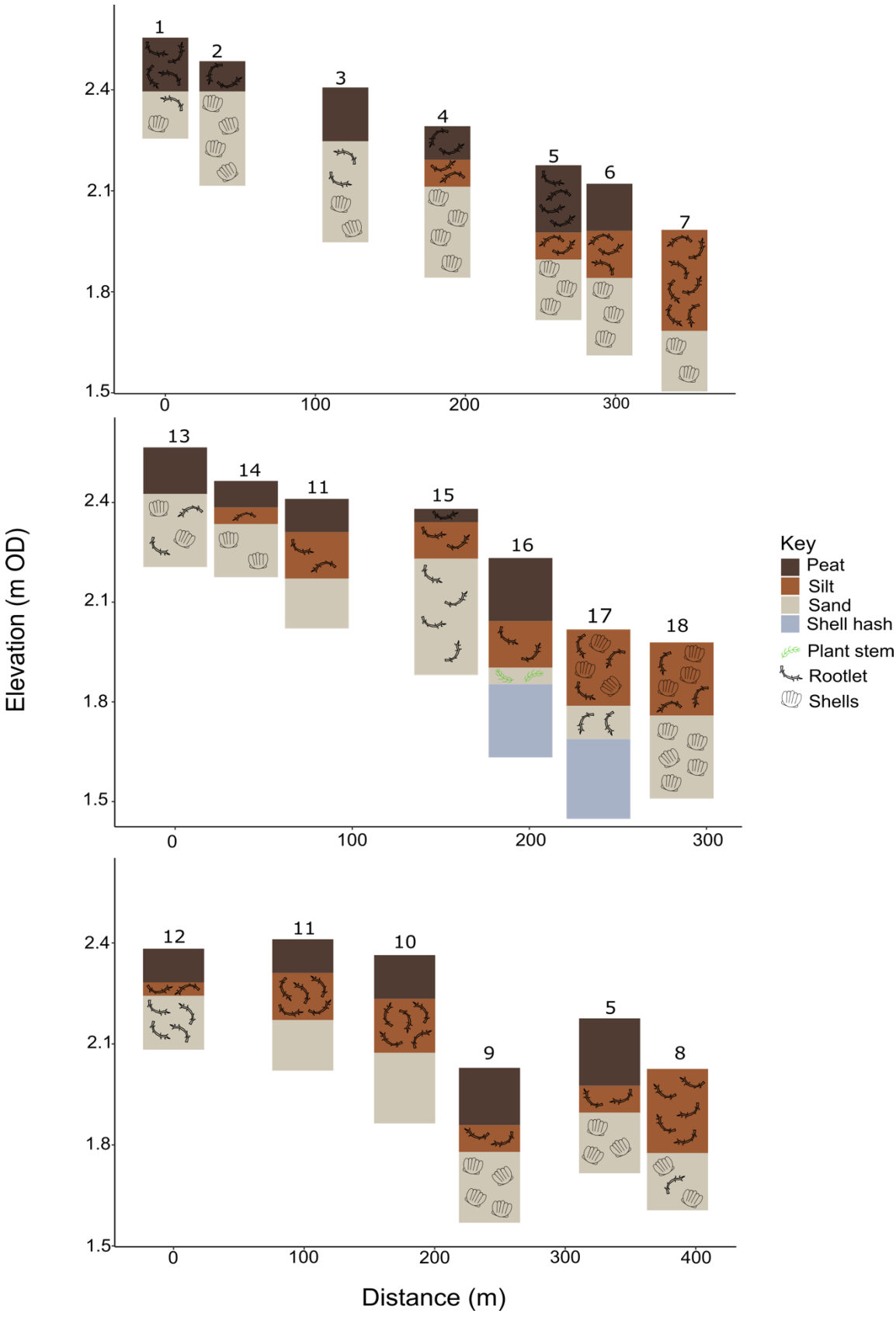

Figure 10. Stratigraphy of the Snook marsh with the numbers at the top of each bar corresponding to those in Figure 4.

Along the first transect (numbered 1-7 on Fig. 10) these cores of sediment generally consist of an underlying layer of coarse sand (14-30 cm thick), usually mid-grey in colour, which, at lower elevation, is followed by a mid-grey layer of organic silt (8-30 cm thick), often containing rootlets. Higher up the marsh, the sand layer is usually followed by a layer of mid-brown silty herbaceous peat (9-20 cm thick; Fig. 10). In the middle marsh zone, all three layers, sand, silt and peat, are usually present (Fig.10). The cores of the second transect (13-18) show a similar pattern to those of the first except for the presence of an underlying shell hash layer (16-24 cm thick) and the fact that the sand becomes fine at the lower elevations (Fig. 10). Cores from the third transect (12-8) again exhibit the pattern of coarse sand (15-21 cm thick), followed by organic silt (4-31 cm thick) and silty herbaceous peat layers (10-20 cm thick); except the lowest elevation sample, which contains coarse sand topped by a layer of organic silt alone (Fig. 10).

Core LI21/20 consists of a 19 cm thick layer of coarse sand, followed by a 17 cm thick layer of herbaceous peat. Fossil foraminiferal assemblages were counted by Eloise Bryard (University of York) and checked to ensure consistency in taxonomy (Table S3). Dead assemblages from core LI21/20 contained ten species of foraminifera: the sand layers contain calcareous species, especially *Cribroelphidium williamsoni* and *Quinqueloculina* spp, which decrease in abundance up to a depth of 18 cm (Fig. 11a and 11b). Following this, in the peat section, the agglutinated species *Entzia macrescens* and *Miliammina fusca* become predominant until a depth of 8 cm, from which point *Haplophragmoides* spp. and *Trochammina inflata* are most frequently encountered (Fig. 11b). Foraminifera were very scant low down the core; from a depth of 14 cm onwards test density jumps to and maintains a high level, with counts of above eighty individuals always being achieved (Fig. 11c). In the deeper core samples, below 15 cm, the highest count achieved was 26 individuals; these low counts sizes, coupled with the relatively high species diversity of the individual foraminifera that were found and counted, mean that it was not possible to use these samples to reconstruct RSL (Fig. 11c). To obtain a potentially usable sample from a point further down in the core than 14 cm, I considered combining the counts from 17 cm and 18 cm to obtain a sample with a count size of 39 individuals which could be used for reconstructing sea level (Fig. 11b and 11c). However, the count size would still be considerably lower than the 100 fossil tests per sample recommended by Kemp *et al*. (2020) and the species diversity high. Therefore, this course was not followed.

Applying the modern analogue technique (MAT) to determine how well the core assemblages are represented in the modern regional training data resulted in all fourteen samples being classified as having “good” analogues (Fig. 11e). This implies that the regional training set is very well suited to producing a reconstruction from these core assemblages. Given that the regional training set contains samples from a number of different sites and therefore different environmental conditions this is not unexpected. When the MAT is used similarly to test the performance of the local training set in this regard, twelve samples were classified as “good” and two as “fair”. The analogues provided by the local data alone are therefore relatively representative of the core samples; however, the regional data is even more so. This further underlines the validity of using the regional training set to reconstruct RSL.

5.1.5 Marsh surface elevation reconstruction

Applying the regional North Sea training set to the assemblages in core LI21/20 provided palaeomarsh surface elevation predictions (Fig. 11d). From the bottom of the core, these predictions show an increase in elevation from 1.91 m OD to 2.54 m OD, with a few fluctuations from this general trend. There is a steady increase from 2.11 m OD at the 13 cm sample to 2.33 m OD at 4 cm. Following this a small dip in predicted elevation is seen in samples from 3 and 2 cm and then a sharp increase to the present-day marsh elevation finishes the record. The mean prediction from the top of the core was 2.44 m OD, which shows relatively good agreement with the actual core-top elevation measured in the field, 2.56 m OD. However, the error values associated with these predictions are large, ± 0.26 m SEP on average (1σ). For example, the prediction for the uppermost sample ranges from 2.71 to 2.17 m OD, despite the close agreement of the mean value with the actual elevation of the core top. The HAT in Lindisfarne was found to be 3.07 m, meaning all PMSE predictions were lower.

The reconstruction generated by this study explained 49 % of the variation in the fossil data from core LI21/20 and so failed to outperform the 999 random transfer functions which explained 67 % (95 % percentile). This is not necessarily a cause for concern and has been observed in other studies of RSL where there is limited variation in reconstructed elevations due to the marsh successfully keeping pace with sea-level rise (Kemp *et al.,* 2013; Garrett et al., 2022).

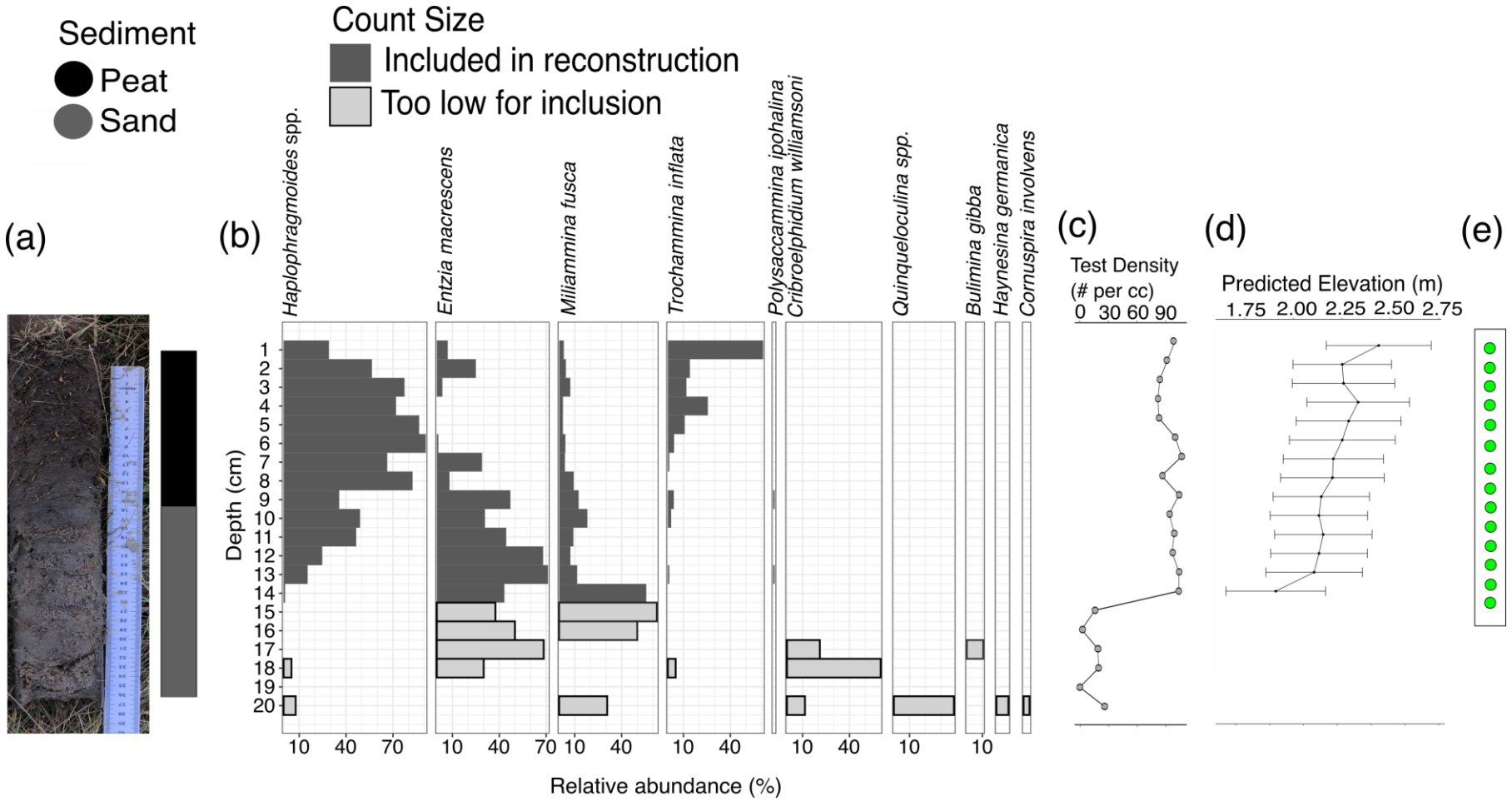

Figure 11. Core LI21/20 shown in (a) the photograph with a stratigraphic diagram indicating the transition from sand to peat. (b) Foraminiferal assemblages present in the core with samples containing count sizes large enough (>30) to be included in the analysis indicated. (c) Test density of each sample down the core and (d) palaeomarsh surface elevation generated when applying the chosen transfer function to the assemblages of core LI21/20; error bars are ± the bootstrapped standard error of prediction (SEP). Uncertainties are 1σ. (e) The results of MAT analysis with green indicating those samples with "good" modern analogues.

5.1.6 Age-Depth Model

Chronological data obtained by the C-Side project is used here to develop an age-depth model (Figure S1). The package *rplum* (Blaauw *et al.,* 2021) was employed using ^{210}Pb and ^{137}Cs data for core LI21/20 (Fig. 12). The ^{137}Cs peak is visible at a depth of around 15 cm (Fig. 12b) and so a reconstruction only employing the high-count samples encountered up to 14 cm depth in the core results in a record reaching back to approximately the 1960s. ^{210}Pb levels at the bottom of the core reach a low of 9 Bq/kg at a depth of 20 cm; the activity of this isotope increases up the core, reaching 237 Bq/kg in the upper most sample (Fig. 12c). When the age depth model itself is considered, it is clear that uncertainties are relatively consistent up to a depth of around 15 cm, after which point uncertainty increases down the core (Fig. 12a). The point at which this change occurs is approximately the same as that at which ^{210}Pb levels become very low.

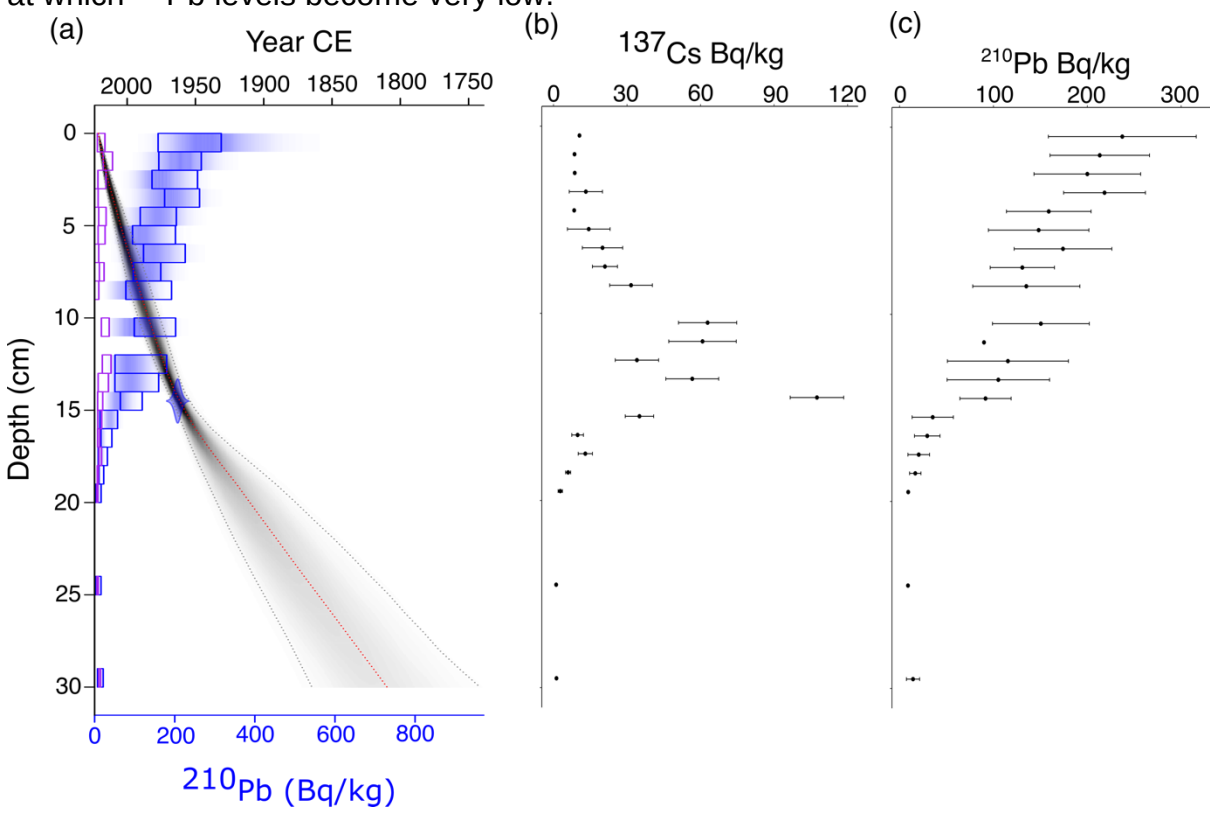

Figure 12. (a) Bayesian age-depth model for core LI21/20 generated using (b) ^{137}Cs and (c) ^{210}Pb data with the package *rplum* (Blaauw *et al.,* 2021). Error bars are ± standard error.

5.1.7 Relative Sea-Level Reconstructions

The RSL reconstruction (Fig. 13), generated by calibrating the fossil data using the first component of the regional LW-WAPLS transfer function, shows a consistent sea-level fall from 0.51 ± 0.26 SE m OD in 1965 (range: 1958-1970) to 0.18 ± 0.26 SE m OD in 2009 (range: 2004-2012) (Fig. 13). This includes a sharp decrease between 1965 and 1971 (range: 1963-1977) to 0.32 ± 0.25 SE m OD (Fig. 13). Finally, there is an increase to the present day, with an RSL of 0.28 ± 0.25 SE m OD predicted for 2016 (range: 2013-2018; Fig. 13). However, the large vertical

uncertainties associated with these data must be appreciated. For example, sea level in 1965 (range: 1958-1970) could range from 0.25 SE m OD to 0.76 m OD when only the 1σ uncertainties are considered. Therefore, the RSL reconstructed here for Lindisfarne must be viewed realistically as being of little use.

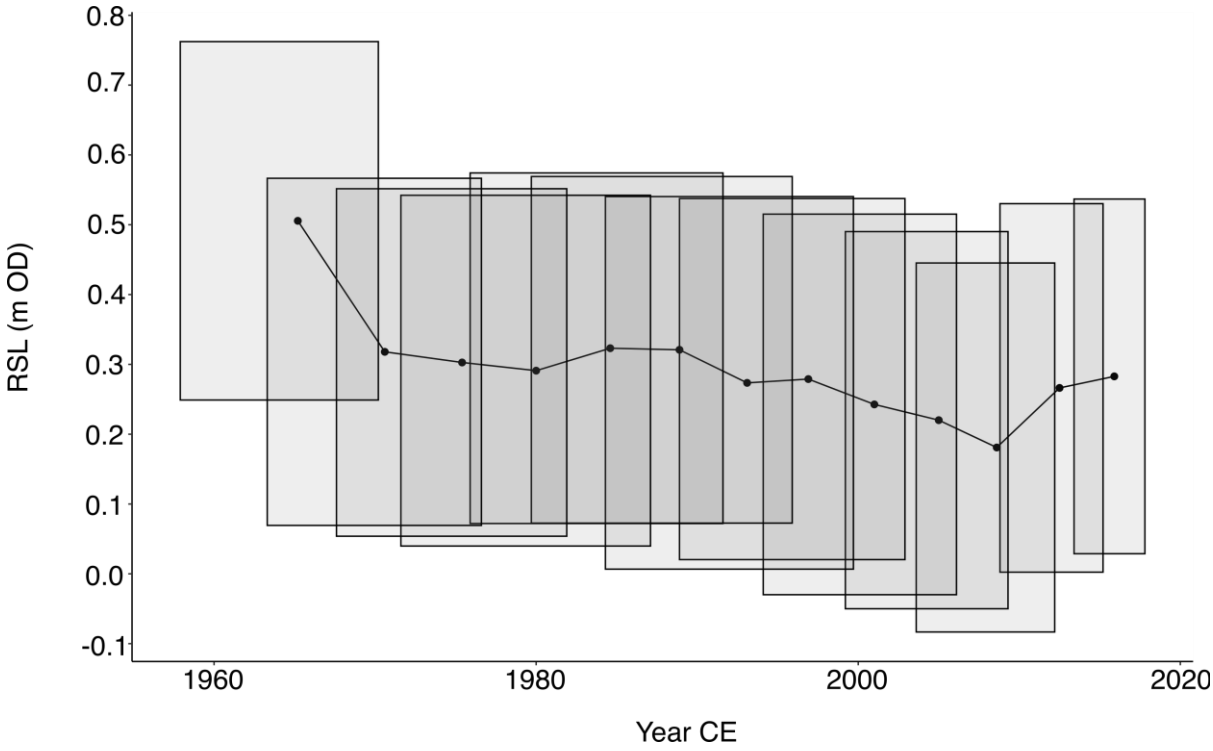

Figure 13. RSL reconstruction obtained when applying the LW-WAPLS C1 transfer function generated from the regional training set to the fossil data. Errors are 1σ and error bars are ± standard error.

5.2 Salt-Marsh Carbon Accumulation

5.2.1 Elemental, Isotope and Bulk Density Analysis

In addition to the core undergoing foraminifera analysis, a duplicate core of salt-marsh sediment was also analysed for elemental and isotope content and dry bulk density by the C-SIDE project (Craig Smeaton, personal correspondence).

From the bottom of the core until a depth of around 16 cm, OC content is very low, only ranging from 0.21-0.44 % (Fig. 14e). Following this, a large jump in OC is seen and this increase then continues steadily up the core, starting at 12 % and ending at 28 % in the uppermost sample. (Fig. 14e). Nitrogen levels follow a similar pattern; values are consistently low until a substantial increase is seen at around the same depth (Fig. 14a). The point at which these dramatic increases occur marks the transition from sand to peat in the core (Fig. 11a). The C/N ratio remains at levels of around 15 from the bottom of the core to a depth of 10 cm, from this point an increase from 17 to 40 at the top of the core is seen (Fig. 14d).

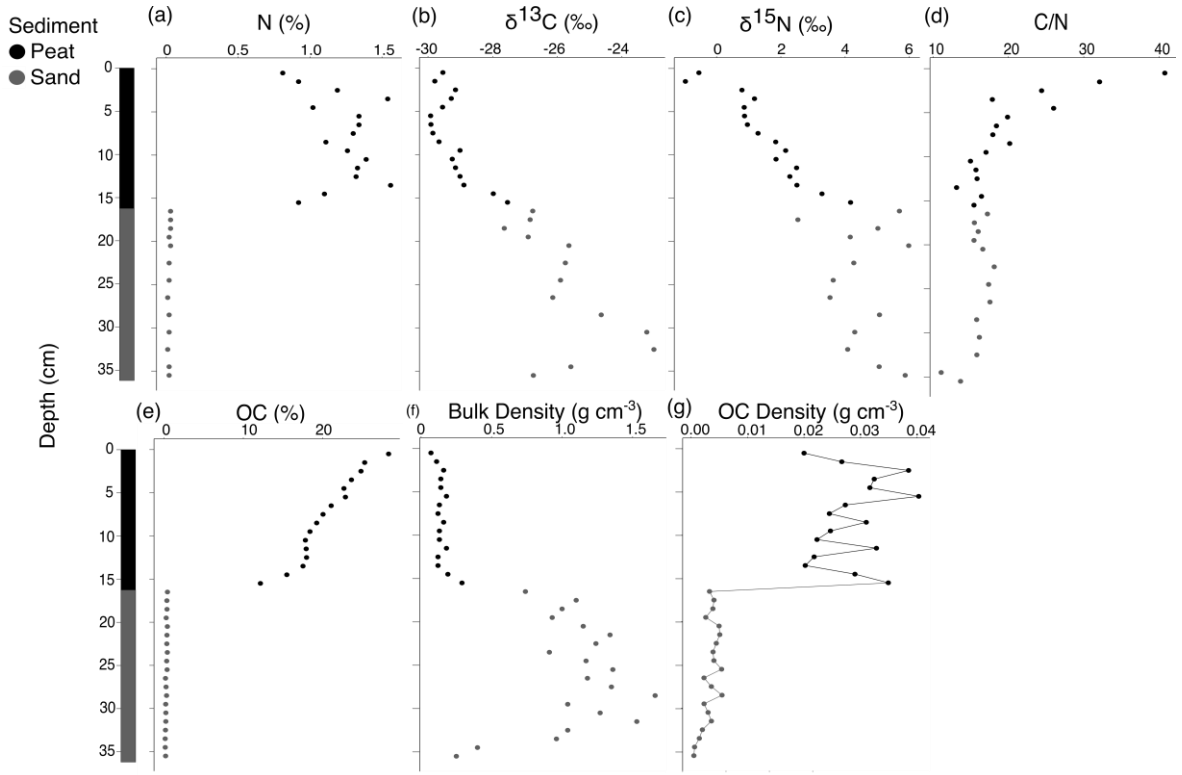

Figure 14. Elemental, isotope and bulk density analysis of core LI21/20: Elemental and isotope analysis included measurement of (a) nitrogen, (b) $\delta^{13}C$, (c) $\delta^{15}N$, (d) C/N ratio, and (e) organic carbon content. (f) Bulk density was measured and multiplied with OC content to determine (g) OC density down the core. Stratigraphy diagrams to the left and the different colours used in the scatter plots indicate the transition from sand to peat in the core.

Isotope data, $\delta^{13}C$ and $\delta^{15}N$, both have values that become increasingly negative up the core (Fig 14b and 14c). $\delta^{13}C$ levels are relatively similar and reach a high of -23 ‰ at the bottom; values decrease towards the top of the core, the uppermost sample having a value of -30 ‰ (Fig. 14b). $\delta^{13}N$ values show a more consistent decrease beginning at almost 6 ‰ at the bottom of the core and decreasing to -0.55 ‰ at the top of the core (Fig. 14c).

Bulk density in the lower half of the core, comprising sandy sediment, has highly variable values, with a peak of 1.53 g cm^{-3} at 31 - 32 cm and a low of 0.25 g cm^{-3} in the lowest sample (Fig. 14f). This latter value is similar to the bulk density of the peat segment of the core, where values remain very similar throughout with a mean of 0.15 g cm^{-3} (Figure 14f).

5.2.2 Organic Carbon Density

The OC density - the product of bulk density and OC content - of the sand section of the core ranges from 0.0055 to 0.0005 g cm^{-3} (Fig. 14g). When the peat section of core is considered, the lowermost sample has a relatively high OC density of 0.035 g cm^{-3} (Fig. 14g). Subsequently, there is a sharp drop in OC density and a low of 0.020 g cm^{-3} is reach at 13 cm depth. Density values then vary widely but reach a high of 0.040 g cm^{-3} at a depth of 5 cm (Fig. 14g). From this point, values tend to decrease, and OC density is low (0.020 g cm^{-3}) at the very top of the core (Fig. 14g).

5.2.3 Sediment Accretion and Carbon Accumulation Rates

Sediment accretion rates (SAR), obtained from *rplum*, were used in conjunction with the carbon density values discussed above to calculate the carbon accumulation rate (CAR) for each centimetre of sediment in the core (Table 2). Up the core, SAR increases with a rate of 0.99 mm y^{-1} seen for the bottommost centimetre of sediment and values staying at a similar level until around the 16 cm mark (Table 2). Following this, SAR gradually increases from 1.26 mm y^{-1} to a rate of 4.23 mm yr^{-1} in the top centimetre of the core (Table 2). The point at which SAR starts to increase coincides with the location in the core at which the foraminifera assemblages changed from predominantly calcareous to agglutinated species and with the transition from sand to peat (Fig. 11a). The product of SAR and OC density, CAR, increases up the core and shows a dramatic increase consistent with the location at which the transition from sandy sediment to peat occurs. In the sand section, CAR never exceeds 6 g m^{-2} yr^{-1}; after the transition to peat, CAR values fluctuate from 36.53 to 110.23 g m^{-2} yr^{-1}. The mean CAR of the Snook salt marsh, taken as the mean CAR of the peat section of core LI20/21, is 0.73 tonnes per hectare per year (i.e., 38.96 g m^{-2} yr^{-1}).

SAR values were compared with rates of sea-level change to determine the ability of the Snook salt marsh to adapt to these changes. As discussed above, only RSL data from the North Shields tide gauge is used for comparison and included in Table 2. The tide gauge data are not only likely to be more accurate and precise but also provide a record of RSL further back through time. Furthermore, the Leith I and II records are quite consistent with North Shields for the period they overlap, so distance from the site and GIA issues are unlikely to be problematic.

The point in the core where transition from sand to peat occurs also marks the point at which SAR rates become greater than rates of RSL change, suggesting the marsh is successfully keeping pace with sea-level rise (Table 2). Prior to this, RSL rise always exceeds SAR (Table 2). The greatest disparity between the two occurs at 16 cm depth (age range: 1942 – 1951), with sea-level rise for that period being recorded as 2.89 mm y^{-1} and SAR estimated as 1.08 mm y^{-1} (Table 2). From the 13th centimetre (age range: 1965 – 1971) onwards, SAR always exceeds the rate of sea-level rise (Table 2).

Table 2. Comparison of sediment accretion and carbon accumulation rates (SAR and CAR) and RSL change in Lindisfarne for each centimetre of core LI21/20. RSL changes are calculated by smoothing the RSL data from the tide gauge (TG) record and averaging the change over the age range given by the age model for each cm. Empty boxes indicate the end of the RSL record. Data from 2019 to the present day were not available for the North Shields tide gauge and so it was not possible to calculate a rate for the uppermost centimetre.

Depth (cm)	Year CE Deposited	SAR (mm yr^{-1})	CAR (g m^{-2} yr^{-1})	TG RSL Change (mm yr^{-1})
30 - 29	1814 - 1824	0.99	2.31	-
29 - 28	1824 - 1834	1.00	5.48	-
28 - 27	1834 - 1844	0.99	3.59	-
27 - 26	1844 - 1854	1.00	2.31	-
26 - 25	1854 - 1863	0.99	5.36	-
25 - 24	1863 - 1874	0.99	4.02	-
24 - 23	1874 - 1884	1.00	3.92	-
23 - 22	1884 - 1893	1.00	4.50	-
22 - 21	1893 - 1903	1.01	5.15	-
21 - 20	1903 - 1913	1.02	5.08	1.31
20 - 19	1913 - 1922	1.03	2.72	1.71
19 - 18	1922 - 1932	0.97	3.78	2.07
18 - 17	1932 - 1942	1.01	4.10	2.44
17 - 16	1942 - 1951	1.08	3.54	2.89
16 - 15	1951 - 1958	1.26	44.13	1.94
15 - 14	1958 - 1965	1.43	41.51	1.58
14 - 13	1965 - 1971	1.81	36.53	1.49
13 - 12	1971 - 1975	2.04	44.40	1.38
12 - 11	1975 - 1980	2.20	72.02	1.38
11 - 10	1980 - 1985	2.19	48.72	1.38
10 - 9	1985 - 1989	2.35	58.00	1.76
9 - 8	1989 - 1993	2.37	73.38	1.84
8 - 7	1993 - 1997	2.62	64.05	1.84
7 - 6	1997 - 2001	2.49	68.06	1.97
6 - 5	2001 - 2005	2.52	101.32	2.10
5 - 4	2005 - 2009	2.73	86.52	2.23
4 - 3	2009 - 2013	2.57	83.41	2.34
3 - 2	2013 - 2016	2.86	110.23	2.42
2 - 1	2016 - 2019	3.60	96.09	2.46
1 - 0	2019 - Present	4.23	84.71	-

5.3 Salt-Marsh Gas Flux

5.3.1 Greenhouse Gas Fluxes

Flux rates were calculated from the raw data made available on the data repository figshare (10.6084/m9.figshare.20940067; Table 7). This first involved removing values deemed to be inconsistent with the overall flux pattern identified for each measurement. The excluded values are highlighted (Table 7) and the remaining data points are shown in scatterplots with the R^2 value calculated to demonstrate the linearity of the data (10.6084/m9.figshare.20940067). Occasionally, as in the case of the first N_2O measurements taken in March, measurements had to be completely removed as it was impossible to accurately determine the flux seen. Generally, CH_4 and N_2O data very rarely showed a high level of linearity, suggesting very low fluxes with respect to measurement uncertainties.

Flux rates of the three greenhouse gases considered here, CO_2, CH_4 and N_2O, show a relatively consistent pattern across the months and marsh zones in which measurements were taken (Fig. 15). There is a larger degree of uncertainty associated with the CH_4 and N_2O fluxes than with those of CO_2.

There was a net uptake of CO_2 in the majority of sampling locations with the exceptions of all measurements taken in March and the two mid-marsh zone measurements of June and July (Fig. 15a). During March, there is an emission of 141.02 $\pm$ 107.29 SD mg CO_2 m^{-2} hr^{-1} and the mid marsh zone emissions were 232.89 mg CO_2 m^{-2} h^{-1} in June and 93.19 mg CO_2 m^{-2} hr^{-1} in July. The magnitude of the fluxes recorded are relatively similar across marsh zones and the months with an average flux of -67.28 $\pm$ 184.73 SD mg CO_2 m^{-2} hr^{-1} across all measurements. Excluding the March measurements, fluxes from the low marsh are generally show the largest uptake, ranging from -178.50 to -289.58 mg CO_2 m^{-2} hr^{-1}.

CH_4 fluxes are very low with a minor uptake of the gas in most measurements. The average was -0.44 $\pm$1.00 SD mg CH_4 m^{-2} hr^{-1}. The exception is a peak in uptake recorded during May in the high (-3.47 mg CH_4 m^{-2} hr^{-1}) and mid (-2.12 mg CH_4 m^{-2} hr^{-1}) marsh zones (Fig. 15b); however, the uncertainty associated with both of these measurements is an order of magnitude greater, ± 4-6 SD mg CH_4 m^{-2} hr^{-1}, than those associated with the other CH_4 measurements: a mean of ± 0.30 SD mg CH_4 m^{-2} hr^{-1}.

Similarly to CH_4 fluxes, those of N_2O are also consistently low, although most measurements show a minor emission and the average flux is 0.04 $\pm$ 0.16 SD mg N_2O m^{-2} hr^{-1} (Fig. 15c). Again, two measurements are the exceptions, one from the mid marsh in April and one from the high marsh in May, the former was a larger emission (0.51 ± 0.47 SD mg N_2O m^{-2} hr^{-1}) and the latter a larger uptake (-0.19 ± 0.40 SD mg N_2O m^{-2} hr^{-1}) than seen among the rest of the measurements (Fig. 15c). The uncertainty associated with these measurements is also considerably greater than that of the others, which ranges from ± 0.04 SD mg N_2O m^{-2} hr^{-1} to ± 0.22 SD mg N_2O m^{-2} hr^{-1}.

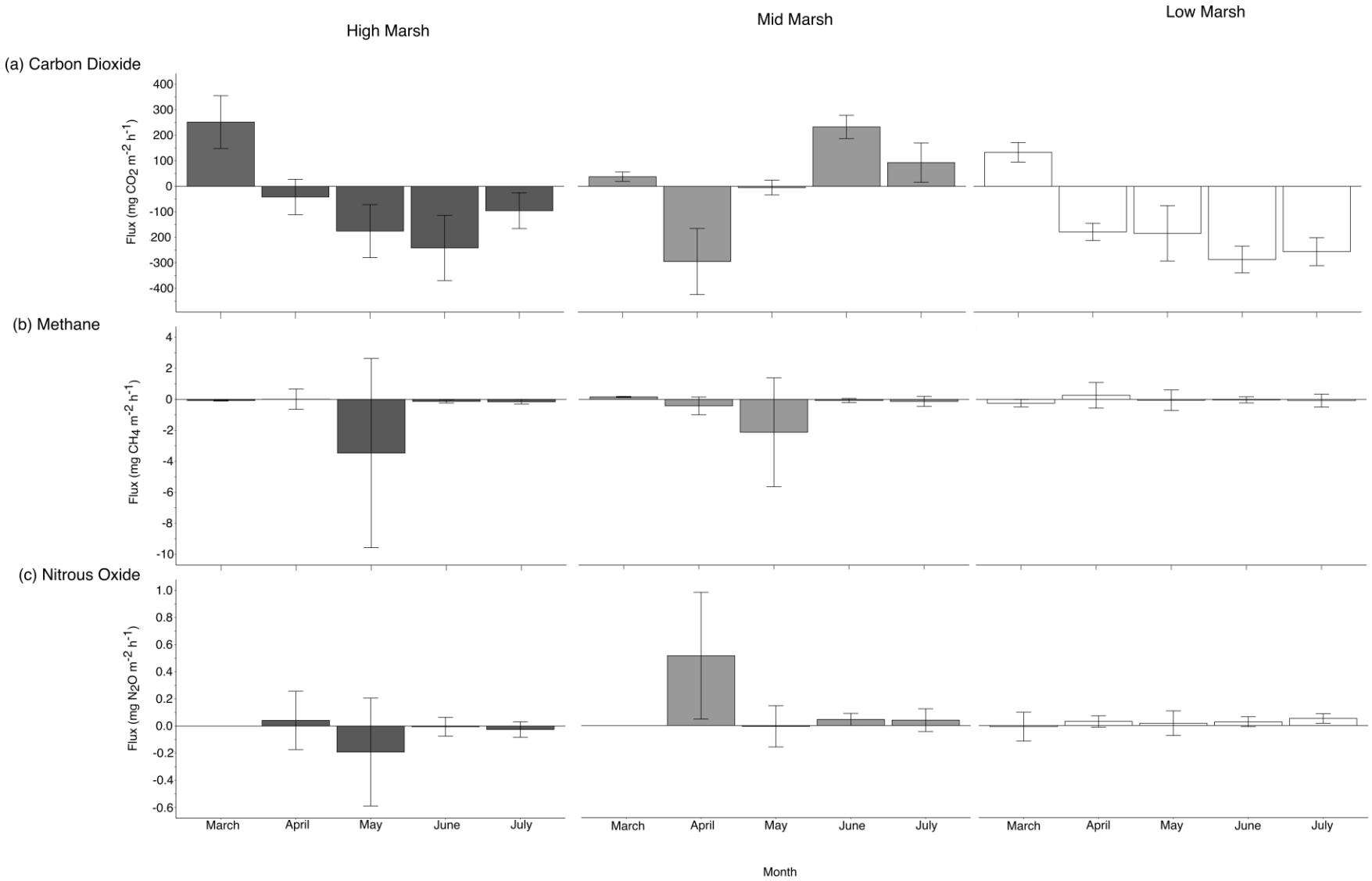

Figure 15. Fluxes of (a) carbon dioxide, (b) methane and (c) nitrous oxide from the Snook salt marsh through time and from different marsh zones. Error bars indicate mean ± SD and positive values indicate emission while negative are uptakes.

5.3.2 Environmental Variables

The environmental data collected as a part of this study included temperature, soil moisture, pH and salinity (Fig. 16; Table S6). Temperature showed a steady increase from March through to July; in March the temperature measurements had a mean value of 12 °C while the summer months during which measurements were taken had an overall mean of 21 °C (Fig. 16a). Soil moisture also shows consistent changes between months with a sharp drop in April (923 mU) compared with much higher values in March (964 mU), May (977 mU) and June (999 mU; Fig. 16b). Conversely, there are no obvious patterns of change in pH or salinity neither between months of measurements nor marsh zone.

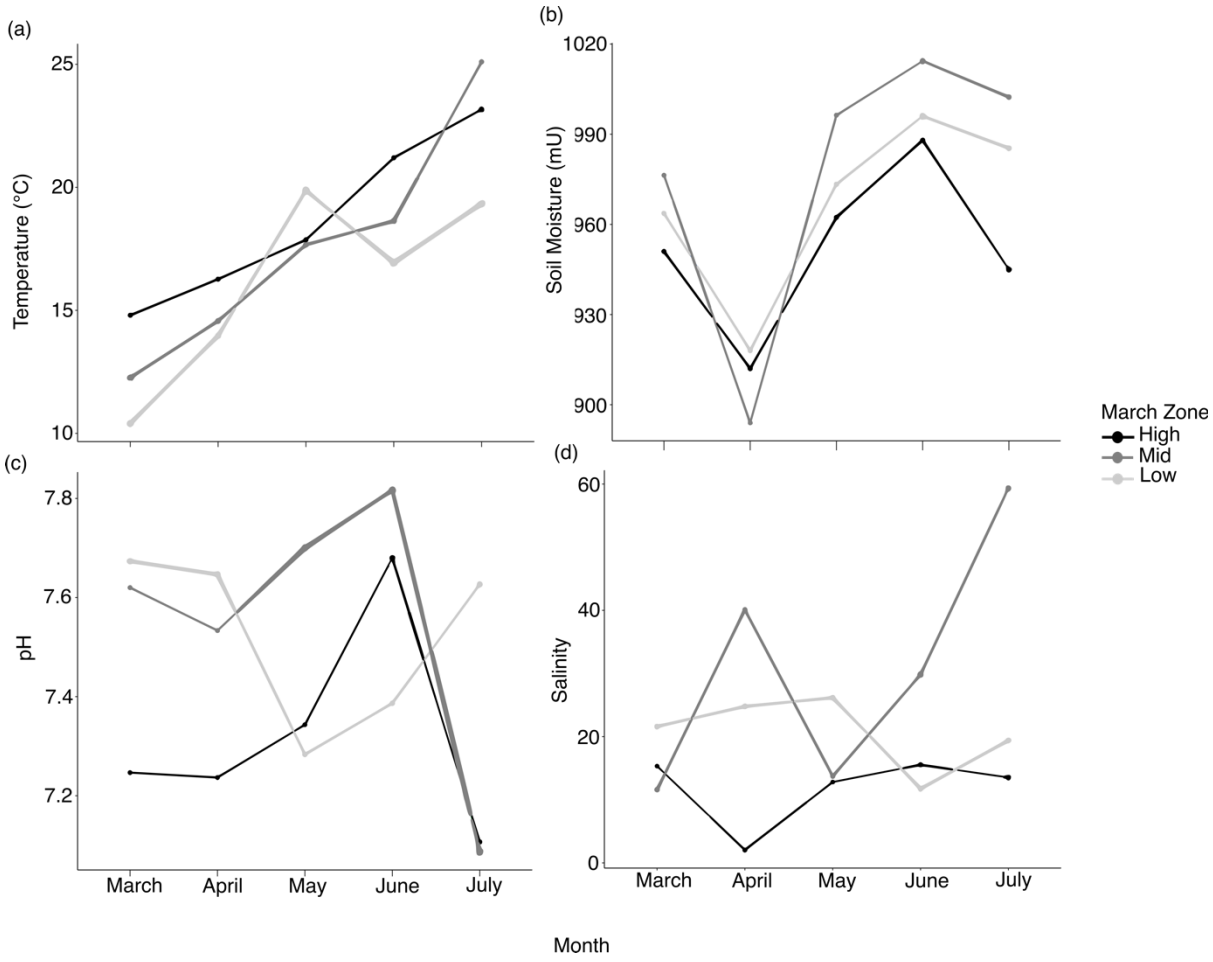

Figure 16. Environmental variables measured in different marsh zones and across each month of this study. Measured variables are (a) temperature, (b) soil moisture, (c) pH and (d) salinity.

Chapter 6: Discussion

Each component of this project links with the subsequent component discussed and so exemplifies the possibility of using various techniques and elements to build a comprehensive picture of the impact a particular ecosystem has on climate change and vice versa. Using micropaleontological techniques, it was possible to both develop a modern foraminifera training set – useful for developing records of RSL for Lindisfarne but also other areas – and to examine core LI21/20 to understand the relatively short amount of time for which the Snook salt marsh has existed. The resulting RSL reconstruction was compared with nearby tide gauge records which suggested that the latter was likely more reliable and so this data was used for comparison with the carbon content data of core LI21/20 to investigate the effect of sea-level rise on carbon accumulation rates. In addition, isotope data helped to confirm the previous conclusions drawn about when the marsh first became established. The investigation of greenhouse gas flux used the static chamber technique and measured CO_2, CH_4 and N_2O fluxes. Combining this flux data with the carbon accumulation rate of the core top allowed a net radiative balance estimate to be developed for the high zone of the Snook salt marsh while the flux data alone was employed to this same end for the mid and low marsh zones where no cores were taken.

6.1 Relative Sea-Level Reconstruction

6.1.1 Training Sets and Transfer Function Development

The transfer functions produced using the local training set all result in relatively large vertical errors; every transfer function type had an RMSEP value greater than 0.25 m which lends substantial uncertainty to any RSL reconstruction generated, regardless of whether the transfer function resulting in the smallest error is selected for this purpose.

Other studies developing local training sets from a single location succeeded in obtaining far lower vertical errors; for example, Williams *et al*. (2021) report a RMSEP value of 0.06 m for the first component of the WAPLS transfer function trained on assemblages from an Australian salt marsh while Gehrels *et al.* (2005) also obtained a value of 0.06 m for both WA and WAPLS transfer functions developed from Canadian salt marsh assemblage data. Admittedly, both sites used in these studies had considerably smaller tidal ranges than what is encountered in Lindisfarne. The Australian marsh has a mean tidal range of 0.81 m while the Canadian marsh has a value of 2.7 m (Gehrels *et al.,* 2005; Southall *et al.,* 2006). When considering the vertical errors of transfer functions developed using UK sites, there is more similarity; a local training set developed using sediment from a Norfolk salt marsh also had a vertical error range of 0.25 m (Horton and Edwards, 2005). The site used here has an even greater mean tide range (6 m) than Lindisfarne and, following Davies (1964), is classified as macrotidal while the latter is mesotidal..

The error generated by the model used in this study expressed as a percentage of tidal range is 9.74 %; a similar analysis by Williams *et al.* (2021) found several training sets that resulted in similar values. The new training sets developed by Williams *et al.* (2021) showed values between 11.60 and 14.90 %; however, the vertical error (discussed above) of these training sets was far smaller. Studies using samples from locations with a tidal range similar to Lindisfarne, such as Leorri *et al.*

(2008), had similar error values (Williams *et al.,* 2021), reinforcing the argument that the large error arises from the tidal range of the site used in this study. Interestingly, training sets developed from similar tidal settings but using different microfossils (diatoms and testate amoeba) had smaller error terms (e.g., Woodroffe and Long, 2010; Gehrels *et al.,* 2006).

Generally, in studies of sea level, it is expected that using a regional training set will result in a loss of precision (Woodroffe and Long, 2010) which this was also the case in this study for WAPLS and WA transfer functions trained on the regional, as opposed to the local, data (Table 1). However, using the LW-WAPLS transfer function means the regional training set used for the reconstruction contains fewer samples than the local data, owing to the selection of the thirty best modern analogues for each individual fossil sample, which is the key advantage of this approach. This results in a small improvement in performance (0.03 m) and, coupled with the high coverage of the fossil data in terms of modern analogues in the regional training set (Fig. 11e), suggests that this regional data, and the first component of the LW-WAPLS transfer function specifically, is most suitable for reconstructing sea-level. When not developing LW-WAPLS transfer functions, Horton and Edwards (2005) found a 0.09 m increase between the local Norfolk training set and a regional training set developed from various UK assemblages. Furthermore, the addition of Lindisfarne to the North Sea training set led to an improved performance when RMSEP values are compared with those reported by Rush *et al.* (2020) and converted to metres using the Lindisfarne tidal regime (Table 1), which suggests that this iteration of the regional training set could be useful in future studies of North Sea sea-level change.

The RMSEP values of the regional training set, despite the improvement compared with the local training set, are still relatively large. The large vertical error terms produced by both training sets are likely explained by factors beyond the large tidal range of Lindisfarne, especially given that similar RMSEP values are reported for a site with a considerably larger tidal range (Horton and Edwards, 2005). The Lindisfarne assemblages are very homogenous in the high marsh zone with the majority of samples from this area being placed in the same cluster by PAM analysis (Fig. 6a and 6b). This is often found to be the case in foraminiferal studies as high marsh assemblages are usually dominated by a few common agglutinated species (Horton and Edwards, 2005). Lower down the marsh, the clusters detected by the PAM algorithm show a great deal of overlap and a few samples are incorrectly classified (Fig. 6b and 7a), which likely arises from the greater species diversity present at lower elevations and the inability to identify certain foraminifera to species level. The bimodal distribution of both *Ammonia* spp*.* and *Quinqueloculina* spp*.* suggests that the two or more species lumped together within each of these groups do differ significantly in terms of distribution and, because of this difference, splitting these group would likely lead to improved transfer function performance (Gehrels and van de Plassche, 1999). However, accurately identifying the species in these genera with genetic techniques was outside the scope of this study.

NMDS analysis shows a clear divide on the first axis between the samples dominated by agglutinated species and those dominated by calcareous species (Fig. 7b). The passively projected elevation gradient does not show a close alignment with the first axis which could suggest that environmental factors other than elevation are

important determiners of species distribution. Samples from lower elevations in salt marsh settings are more strongly affected by salinity and caution is required when interpreting data from this setting (Horton and Murray, 2005). It may be argued that the low elevation, calcareous-species dominated samples in this study are influenced by factors other than elevation, such as oxygen (O_2) availability, pH, temperature or salinity (Avnaim-Katav *et al.,* 2017); quantifying the impact of these variables was not possible during this study, given that they were not recorded at the time of collection. The fact that the Fenham site, where the lowest elevation surface samples were collected, has only relatively recently become a characteristic salt marsh could infer that sediment accretion has not yet resulted in a clear elevation gradient from the high marsh to the low, sufficient for this variable to show a correlation with the other factors listed above strong enough to justify its use as a proxy (Murray 2001).

Another piece of evidence in support of the assertion that environmental variables other than elevation are affecting foraminiferal distribution comes from the overlapping transects on the Snook marsh (Fig. 4). Three samples from very similar elevations (2.029, 2.026 and 2.018 m OD) but different locations across the marsh (labelled 8, 9 and 17 on Fig. 4) are classified by PAM analysis as belonging to clusters 1, 2 and 3 (Fig. 6b). The foraminiferal assemblages of these clusters therefore differ significantly despite the elevations from which they were taken having a range of only 0.011 m OD. This suggests that one or more of the environmental variables discussed above is not strictly correlated with elevation but is controlled by other factors.

The elements discussed above cast doubt on the suitability of modern salt marsh sediment from the Snook and Fenham salt marshes, especially the latter, given its relatively young age, for developing foraminiferal training sets destined for use in transfer function development. The probability that factors not correlated with elevation are impacting the distribution of foraminiferal species appears likely in the low marsh zone and the inability to identify certain genera to species level could explain the uncertainty associated with the resulting transfer functions. However, comparison with other studies shows that this level of uncertainty is not particularly unusual and is only slightly higher than what is generally explained by the large tidal range of the site (Williams *et al.,* 2021). In fact, the addition of Lindisfarne to the North Sea training set leads to improvements in performance compared with values in Rush *et al.* (2021; Table 1).

6.1.2 Core LI21/20 and Snook Salt Marsh Stratigraphy

Investigating the stratigraphy at various points across the Snook salt marsh point to the fact that this is unlikely to be a particularly old marsh (Fig. 10). The silt and peat sections of these cores are, respectively, 30 cm and 20 cm deep at the most (at sites numbered 7 and 5 on Figs. 4 and 10). This is not uncommon for UK salt marshes which have been reported to possess a mean salt marsh soil unit depth of 14.2 cm ± 20.6 cm (Smeaton *et al.,* 2022). Therefore, it is not unexpected that the salt marsh sediment of the Snook does not extend to, for example, depths similar to those found on the US Atlantic coast that allow reconstructions for the past 2100 years to be developed (Kemp *et al.,* 2011). Having said this, long records of RSL have been produced for UK sites, such as Poole Harbour in the south of England (Edwards, 2001). The fact that the salt marsh selected for this study was not suitable for developing records of this magnitude is no disadvantage given the goal of using the record to examine the impact of recent (late Holocene) sea-level changes on carbon accumulation. However, a longer record, for example, into the 19th century, would have been desirable for this goal given the calculated onset of recent, rapid rates of sea-level rise (Gehrels *et al.,* 2006).

Despite the relatively large uncertainty produced by both training sets, the modern data, especially the regional training set, do provide good analogues for the entire fossil dataset from core LI21/20 (Fig. 11e). The fact that the regional data provides analogues more representative of the fossil data than the local training set is to be expected given that the former contains samples from a wider range of environmental conditions. The large number of “good” analogues found in the local modern data alone means the performance of the local training set in this regard is better than is often the case for similar data; for example, Horton and Edwards (2005) found their local Norfolk training set contained no “close” (i.e., only “fair” or “poor”) modern analogues for thirteen out of twenty-two fossil samples in a core.

The low PMSE predicted from the sample at 14 cm can be attributed to the high level of *M. fusca* (55.8 %) present, which is not seen again in any other core sample (Figs. 11b and 11d). The steady increase in PMSE observed after this point corresponds well with the increase in *Haplophragmoides* spp*.* from 15.4 % in the 13 cm sample to 77.4 % in the 3 cm sample. The peaks in PMSE seen at 4 cm but more especially in the uppermost sample correspond to peaks in *T. inflata* abundance (25.6 and 61.0 % respectively). Therefore, it is clear that the various PMSE predictions generated from core LI21/20 are attributable to the changing abundances of foraminifera up the core.

The marked increase in test density coupled with the more gradual disappearance of calcareous species suggests a transition at this point (15 cm onwards) in core LI21/20 from a tidal flat to a salt marsh environment (Figs. 11b and 10c). Indeed, this is supported by a photograph of the duplicate core where a clear transition from sand to peat at around this point can be observed (Fig. 11a). This again leads to the assertion that the Snook salt marsh is unlikely to be long established and implies that the usefulness of this area for reconstructing sea level is limited.

The failure of the selected transfer function to outperform a suit of 999 random transfer functions may be attributed to the limited variability of the predicted PMSE

values, which are relatively stable across the core (Kemp et al., 2013). Despite the substantial margin by which the regional training set fails to explain more variance than the random transfer functions, this is not necessarily a great cause for concern and has been the case in other studies (Kemp *et al.,* 2013; Garrett et al., 2022).

6.1.3 Age-Depth Model

The Bayesian age-depth model generated in this study is tightly constrained up to a depth of around 16 cm; after the point at which the ^{137}Cs peak occurs and ^{210}Pb levels become very low, the uncertainty become much greater and so the predicted age of sediment coming from deeper in core LI21/20 must be viewed with caution. The increase in uncertainty likely marks the point at which estimates of unsupported ^{210}Pb become unavailable which generally results in a decrease in model precision (Aquino-López *et al*., 2020). Given that no samples from a depth greater than 16 cm are used for reconstructing RSL, this should not be a cause for concern.

Not only is the age-depth model used as a part of the sea-level reconstruction aspect of this project, but it is also used for determining the sediment accretion rates necessary for investigating the carbon accumulation rates of the Snook salt marsh. Other studies using ^{210}Pb and ^{137}Cs to explore the sedimentation rates of sediment cores have used the constant flux model to calculate these rates (e.g., Ruiz-Fernández *et al.,* 2014; Broce *et al.,* 2022). Using *rplum* to determine the sediment accretion rate means that multiple sources of age data (e.g., ^{210}Pb and ^{137}Cs data) can be integrated and so avoids the use of a two-stage process (Aquino-López *et al*., 2020). Furthermore, sediment accretion rate is calculated as part of the age-depth model development and so was simple to obtain.

6.1.4 Proxy and Tide Gauge Records of Relative Sea-Level

The RSL predictions derived from the foraminifera-based transfer function were compared to those recorded by the tide gauges of North Shields, approximately 77 km south of the study site and Leith I and II, approximately 92 km to the northwest (Fig. 17). These different record types were not consistent with different trends of sea-level change being recorded. Both tide gauges recorded a general increase in sea level up to the present day, while the transfer function calibration predicted a persistent decrease in sea level from 1965 (range: 1958-1970) to 2009 (range: 2004-2012). The North Shields and Leith tide gauges are highly consistent in their records (Fig. 18) which leads to the expectation that a similar sea-level trend has been experienced by Lindisfarne.

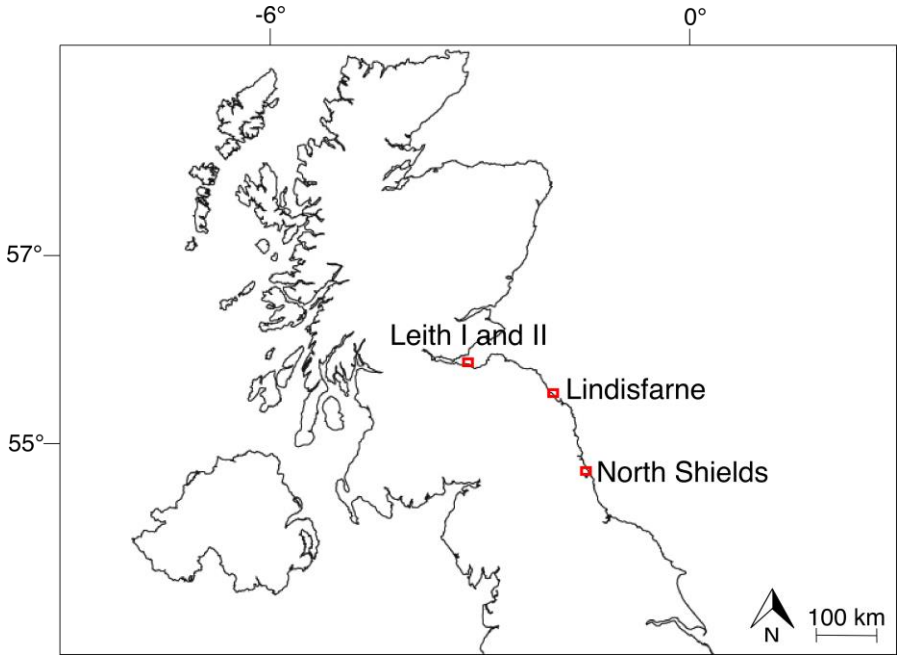

Figure 17. Locations of North Shields and Leith I and II tide gauges.

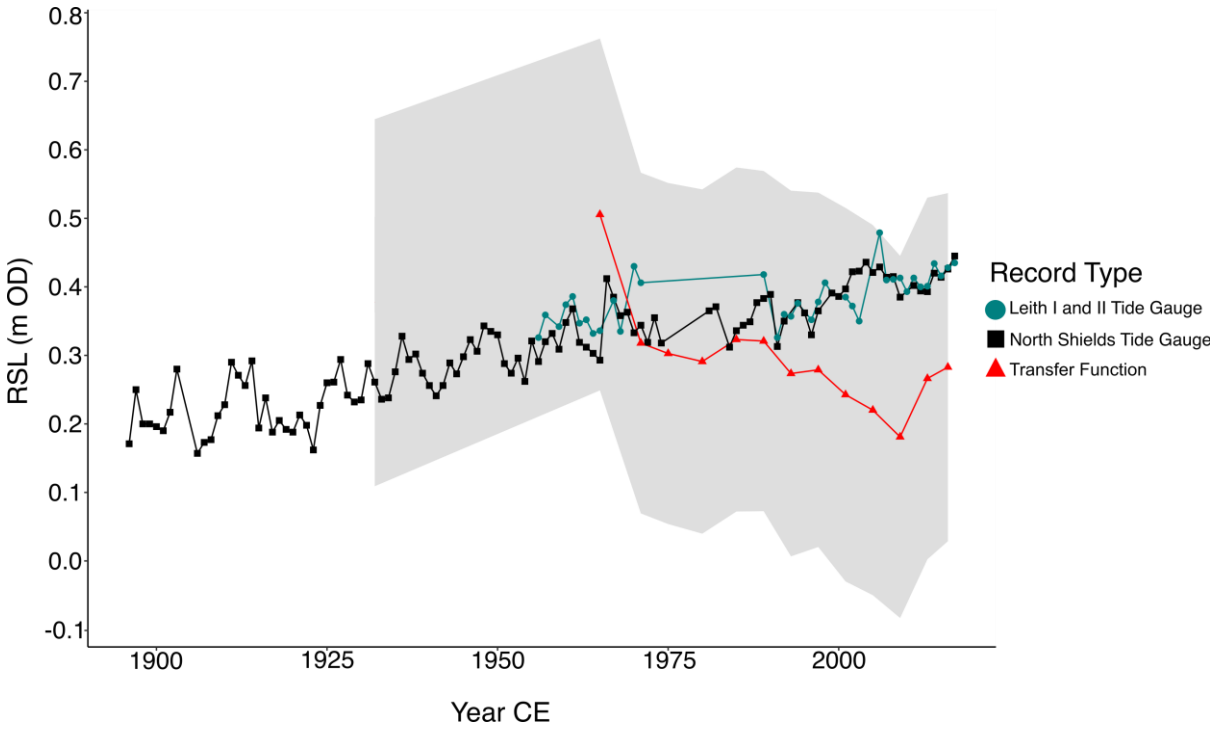

Figure 18. Comparison of RSL reconstruction generated using the regional foraminifera-based transfer function with RSL recorded by the North Shields and Leith I and II tide gauges for the same period. Shaded area represents the 1σ errors associated with the transfer function record. The records from Leith I and II were combined to achieve a longer overall record; the plateau between 1971 and 1981 represents the gap between the end of the Leith I record and the start of Leith II.

As discussed above, previous studies of RSL change along the Northumberland coast show that the area experienced low rates, generally less than 1 mm yr^{-1}, of sea-level change through the Holocene (Plater and Shennan 1992). Into the 20th century, when the transfer function record is considered, a sea-level fall of approximately 7 mm yr^{-1} is seen from 1965 (range: 1958-1970) to 2009 (range: 2004-2012; Fig. 13); for the same period in the tide gauge record, a sea-level increase of around 2 mm yr^{-1} is recorded (Fig. 18). The tide gauge record is therefore more consistent with previous changes in sea level experienced by this area.

The sea-level fall predicted in the proxy record must arise from the impact of local factors. One possible explanation is local changes in coastal morphology. For example, this could include geomorphic changes to the entrance of the bay which would result in changes to the tidal range experienced by the area (Shennan *et al.,* 2012). Models have been developed which use several variables, including tidal range, to predict coastal morphology (Masselink and Short, 1993); therefore, it is conceivable that, if changes in coastal morphology were known, these could be used to predict possible changes in tidal range over time. Having said this, morphological changes are unlikely over such a short time scale. Another possible factor could be infilling at the site which would decrease the tidal prism, meaning that any reconstruction relative to higher tide levels would differ from the records of tide gauges recording mean sea-level (Mills *et al.,* 2013),

Alternatively, the local explanation for the prediction produced could be infaunality and taphonomic processes. The former term refers to species of foraminifera found more abundantly in the subsurface than the surface sediment; meaning they would be absent from counts of modern assemblages despite having a presence in the marsh (Milker *et al.,* 2015). Taphonomic processes affect foraminifera tests after death and can change the remaining assemblage through reduced numbers of species particularly impacted by these changes (Berkeley *et al.,* 2007). Given that both live and dead assemblages were counted in the modern samples, it is possible to state that taphonomic processes are unlikely to have had a large impact. Live and dead assemblages overlap closely (Fig. 6a) which would imply that populations are not being substantially altered after death. It is more difficult to consider the impact of infaunality within the scope of this study; however, it is possible to state that no species present in the fossil samples was entirely absent from the modern surface samples or indeed to categorically determine the local factor(s) that explain the sea-level trend seen.

Given that most reconstructions of RSL extend back far further in time (into the pre-instrumental era) than the record produced by this study (e.g., Horton and Edwards, 2005; Barlow *et al.,* 2014) disparities with the tide gauge record are likely more noticeable. However, a main aim in this study is to compare the RSL record with rates of carbon accumulation, and so it is important that there is a reasonable level of confidence in the record produced. Other studies attempting to answer similar questions about the effect of sea-level rise on carbon accumulation have looked at millennial-scale variation in RSL using data from multiple sites, meaning inferring trends was easier (Rogers *et al.,* 2019), or have used stable carbon isotope data to identify changing marine influences upon a marsh (Ruiz-Fernández *et al*., 2018). The

latter data is also available in this study and can be used as another means of assessing the impact of sea-level change on carbon accumulation.

Considering the arguments discussed above, I chose to use the North Shields (being closer than Leith to the study site) tide-gauge data for comparison with the carbon data. Greater confidence can be placed in this record and sea-level change can be followed back further through time. The tide-gauge data alone, therefore, is carried into the next part of this study, namely, the investigation of salt-marsh carbon accumulation rates.

6.2 Salt-Marsh Carbon Accumulation

6.2.1 What are the sources of the carbon sequestered by the Snook salt marsh?

Core LI21/20 contains stores of OC and N, the varying levels of which can be interpreted to better understand the development of the marsh. The dramatic difference in OC and N content between the sand section of sediment at the bottom of the core and the peat section higher up is consistent with the expected characteristics of these sediment types. Sandy sediment has a low capacity for OC storage because of its unsuitability for plant growth, meaning the autochthonous carbon input is limited, and the high susceptibility of what carbon is present to breakdown by microbial activity due to its low clay content (Schapel *et al.,* 2018). Nitrogen storage is similarly dependent upon the productivity (and therefore presence) of vegetation and the decomposition of organic matter (Pastor *et al.,* 1985). The point in core LI21/20 at which OC and N content increase by several orders of magnitude (Figs. 14a and 14e) likely marks the time when plants began to colonise the marsh which led to higher inputs of organic matter and therefore sequestration of these elements (Belyea and Clymo, 2001).

Levels of $\delta^{13}C$ and the C/N ratio within sediment can be interpreted to determine the sources of the organic matter constituting each sample. Numerous studies have investigated the $\delta^{13}C$ and C/N profiles of various organic matter sources, and these findings are summarised in Khan *et al.* (2015). It is possible to use this previous work to map the sources of organic matter present in cores of sediment as is done in Figure 19.

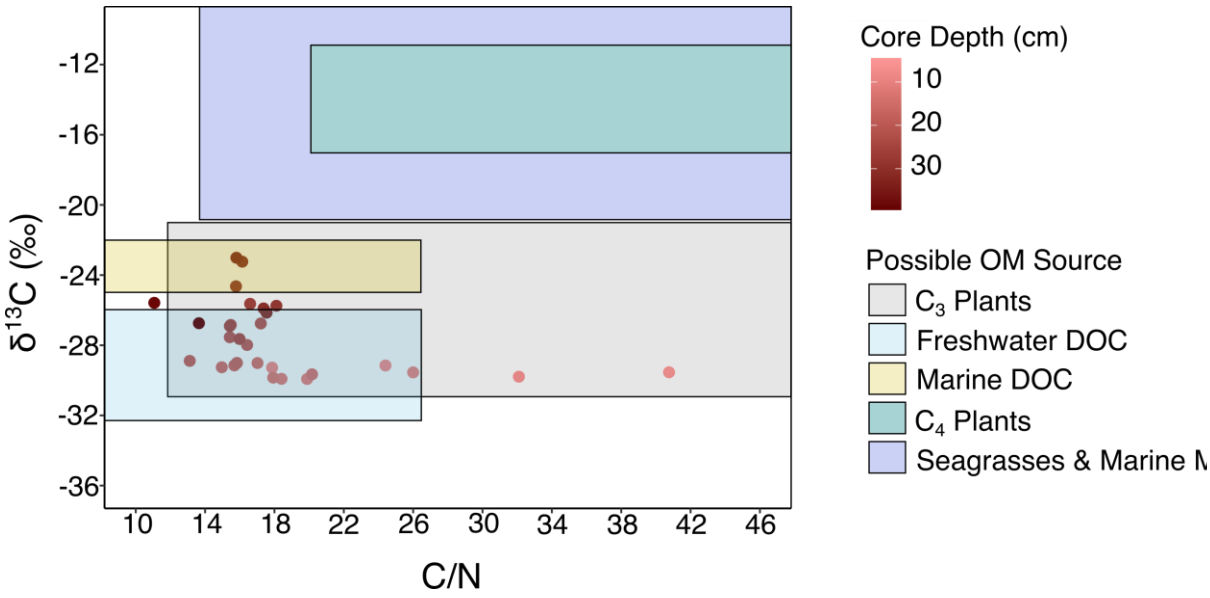

Figure 19. $\delta^{13}C$ and C/N profiles of each 1 cm segment of sediment down the core. Samples from increasing depth in the core are indicated by progressively darkening shades of red. The characteristic $\delta^{13}C$ and C/N values of different organic matter sources are overlaid and are adapted from Khan *et al. (*2015).

The main conclusion to be drawn from Figure 19 is the overwhelming contribution of C_3 plants to the carbon stored in core LI21/20. Organic matter from C_4 plants generally possesses a $\delta^{13}C$ level ranging from approximately -11 to -17.2 and a C/N ratio of around 20 to 45 and above (Ember *et al.,* 1987; Khan *et al.,* 2015). The former range of values is entirely absent from the $\delta^{13}C$ levels of the samples in this study while every sample bar one is within the C_3 plants range (Fig. 19; Table S4). This high C_3 plant contribution is consistent with observations of the plant community at the coring location (marked number 1 on Fig. 4a); *A. maritima* and *P. maritima* were seen to dominate, both of which are C_3 plants. Communities of C_4 plants would include such species as *S. anglica* and *S. europaea*. It can be concluded from this that the majority of carbon accumulated in the high marsh zone of the Snook salt marsh comes from autochthonous sources. Given that the high marsh is rarely inundated by the tide and, owing to this, there is limited opportunity for the delivery of allochthonous carbon, this is a strongly supported conclusion.

If a core from the lower marsh were to be examined in the same way as core LI21/20, it may be supposed that the contribution of C_4 plants would be far greater due to the predominance of *S. anglica* in this area, and that tidally delivered allochthonous carbon would also make a greater contribution because of the higher frequency of tidal inundation to this part of the marsh. The widely different conditions encountered in the low marsh compared with high suggests that the carbon content of this area may be considerably different and that using the carbon content of only core LI21/20 to estimate the carbon stock of the entire marsh would not lead to an accurate result. In future, following the recommendation of Howard *et al.* (2014) in the Blue Carbon Manual – namely, that the salt marsh being studied is stratified to divide large heterogeneous sites when measuring carbon stocks – could lead to a

more accurate estimate of the contribution of the Snook (and possibly the Fenham) salt marsh as a carbon sink.

As well as differentiating between the contributions of C_3 and C_4 plants, this technique can be used to determine the levels of organic matter originating from marine and freshwater sources. In this case, a relatively high number of samples possess $\delta^{13}C$ and C/N values within the range commonly attributed to freshwater organic matter sources, these generally occurring from a depth of around 20 cm to the top of the core (Fig. 19). Three 1 cm sections of sediment from lower down, at depths of between 28 and 33 cm, display profiles consistent with marine sources of organic matter (Fig. 19). This supports the conclusion that tidally delivered allochthonous organic matter was the predominant contributor to OC stores at lower depths, with the exception of the very lowest sample which has a profile consistent with freshwater DOC (Fig. 19). This is consistent with the idea of the marsh developing through time by building up sediment and the high marsh zone/coring location becoming less frequently inundated by the tide, and therefore experiencing a decreased marine influence as this process occurs.

Finally, $\delta^{15}N$ content can be used similarly to identify the contributions to N stores. Ruiz-Fernández *et al.* (2018) and references therein, interpret sources of organic matter based upon stable isotopes of nitrogen as follows: terrestrial organic matter has $\delta^{15}N$ values around 0.4 ± 0.9 ‰ while marine-derived organic matter possesses $\delta^{15}N$ values ranging from 3 ‰ to 12 ‰. Here, samples from the bottom of the core to a depth of 14 cm all have $\delta^{15}N$ values within the specified range for marine-derived organic matter (Table S4; Fig. 14c). Up the core, values remain close to the marine range; the two samples from the top of the core, however, have $\delta^{15}N$ values slightly greater than the range indicated as characteristic of terrestrial organic matter sources (Table S4; Fig. 14c; -0.55 ‰ and -0.97 ‰). These values are highly consistent with the argument that allochthonous organic matter was the main N source of the samples at lower depths, with marine-derived organic matter encountered from the bottom of the core to the depth at which sand ceases to dominate (Fig. 14c).

6.2.2 Is the salt marsh carbon “effectively stored”?

Organic carbon density, the product of bulk density and OC content, differs substantially between the sand and peat sections of the core (Fig. 14g) with low values seen for the sand section and high values for the peat. When the peat section alone is considered, OC density does not fluctuate widely, only ranging from 0.020 to 0.040 g cm^{-3} (Fig. 14g). However, it was not possible to determine the point at which the OC stocks of the marsh become effectively stored, meaning, as in Mueller *et al.* (2019), OC density in samples at three successive depths show no or a positive trend.

Differences in bulk density are related to the degree of organic matter decomposition in peat (Boelter, 1968); given the relatively consistent bulk densities recorded for the peat section of core LI21/20 (Fig. 14f), decomposition rate is unlikely to vary widely down the core. Changes to the plant community as the salt marsh develops have been shown to affect OC input to the soil and therefore OC density (Elschot *et al.,* 2015). Given the relatively recent development of the Snook salt marsh, changes to

the plant community over time as the marsh becomes established would be unsurprising. Furthermore, changes in sedimentation rate can affect OC density in a similar way through varying the input of allochthonous carbon (Mueller *et al.,* 2019); as can be seen from Table 2, sediment accretion rates in the Snook salt marsh are variable but show a consistent decline and high values do not match the OC density peaks in Figure 14g. Therefore, the inability to identify the point at which carbon becomes effectively stored may be attributed to changes in the plant community as the marsh developed which varied carbon inputs.

6.2.3 How did the Snook salt marsh develop?

This increasing SAR up the core - from the start of the peat section onwards - suggests the emergence of the marsh from the tidal frame (Table 2). If the sand section of the core is assumed to originate from a time when the Snook resembled an unvegetated mudflat, it may be suggested that the area was failing to keep pace with sea-level rise until salt marsh plants began to colonise. The presence of these plants would have assisted with sediment trapping and led to increased inputs of organic matter (Kirwan and Guntenspergen, 2012). Salt marshes are unlikely to expand over tidal flats unless sea levels are falling or rising slowly (Horton *et al.,* 2018). In this case, the rate of sea-level rise experienced by the sand section of core ranges between 0.97 and 1.26 mm yr^{-1}; a similar rate of 1 mm yr^{-1} was found by Horton *et al.* (2018) to result in a negative tendency (i.e., decreasing marine influence and the replacement of tidal flat by salt marsh deposit) in the majority of the sites they considered. Alternatively, if there is enough sediment available, marshes can also grow seaward, even with high rates of sea-level rise; however, the SAR rates of Lindisfarne do not point to a particularly high sediment supply to the area (Table 2). Therefore, given the rates of sea-level rise experienced by the Snook marsh at the time when the lower part of the core was being deposited, this a feasible possibility.

6.2.4 Does relative sea-level change explain carbon accumulation rate?

Next, CAR values were compared with rates of sea-level changes to investigate the effect they have on the rate at which carbon is accumulated. Rates of sea-level change calculated from the North Shields tide gauge data increase rapidly from the time at which the 20th centimetre (age range: 1903 – 1913) of sediment in core LI21/20 was being deposited from 1.31 mm yr^{-1} to 2.89 mm yr^{-1} during the period represented by the 16th centimetre (age range: 1942 – 1951; Fig. 20). The rate then fall to 1.38 mm yr^{-1} which was maintained from 12 cm (age range: 1971 – 1975) to 10 cm (age range: 1980-1985) depth (Fig. 20). Following this, the rate shows a consistent increase with the most recent value reaching a high of 2.46 mm yr^{-1} (Fig. 20).

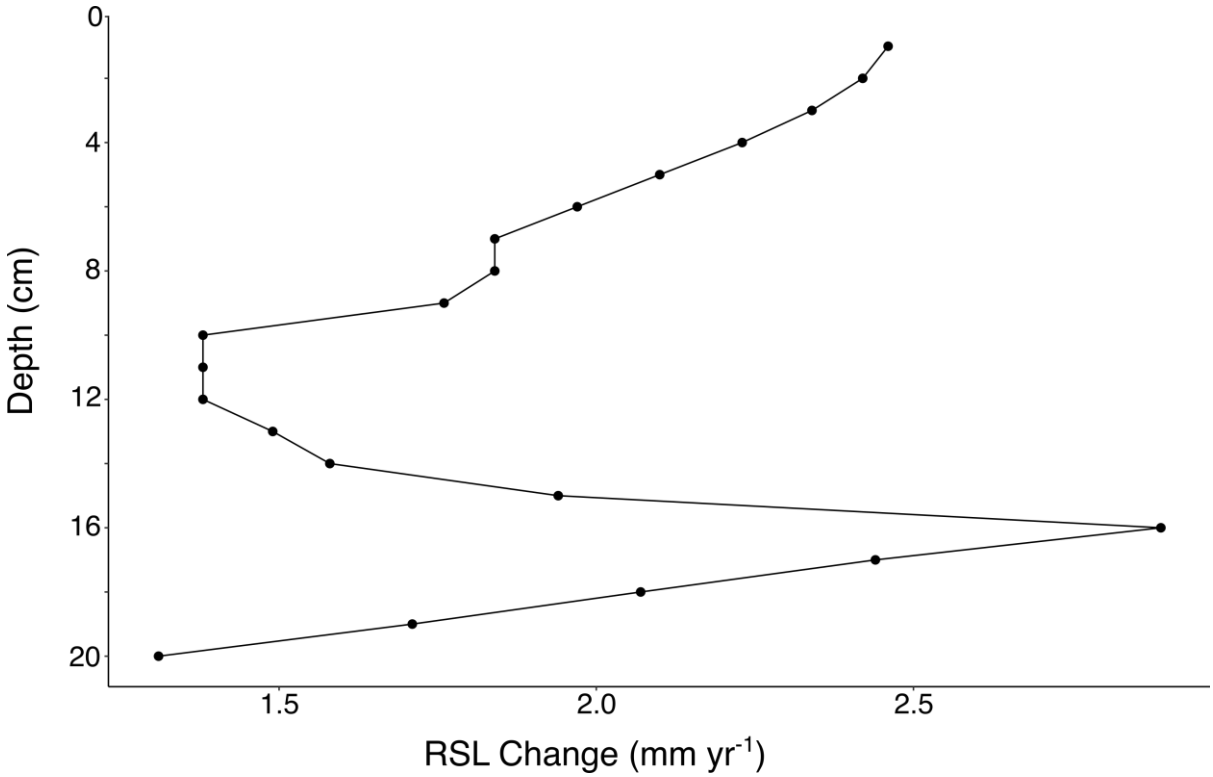

Figure 20. RSL change rate (calculated from the North Shields tide gauge record) represented by each centimetre of the core.

Regression analysis was performed to investigate whether rates of RSL change explained a significant portion of the variation in CAR. When RSL changes based on the entire tide gauge record were considered, a significant amount of the variation in CAR was not explained (ANOVA: $F = 0.49$; $d.f. = 1,18$; $p = 0.49$; Fig. 21a). However, when RSL and CAR changes that occurred for only the peat section of the core (i.e., the salt marsh section) were tested in the same manner, a significant amount of variation was explained (ANOVA: $F = 23$; $d.f. = 1,13$; $p = 0.0003$; Fig. 21b).

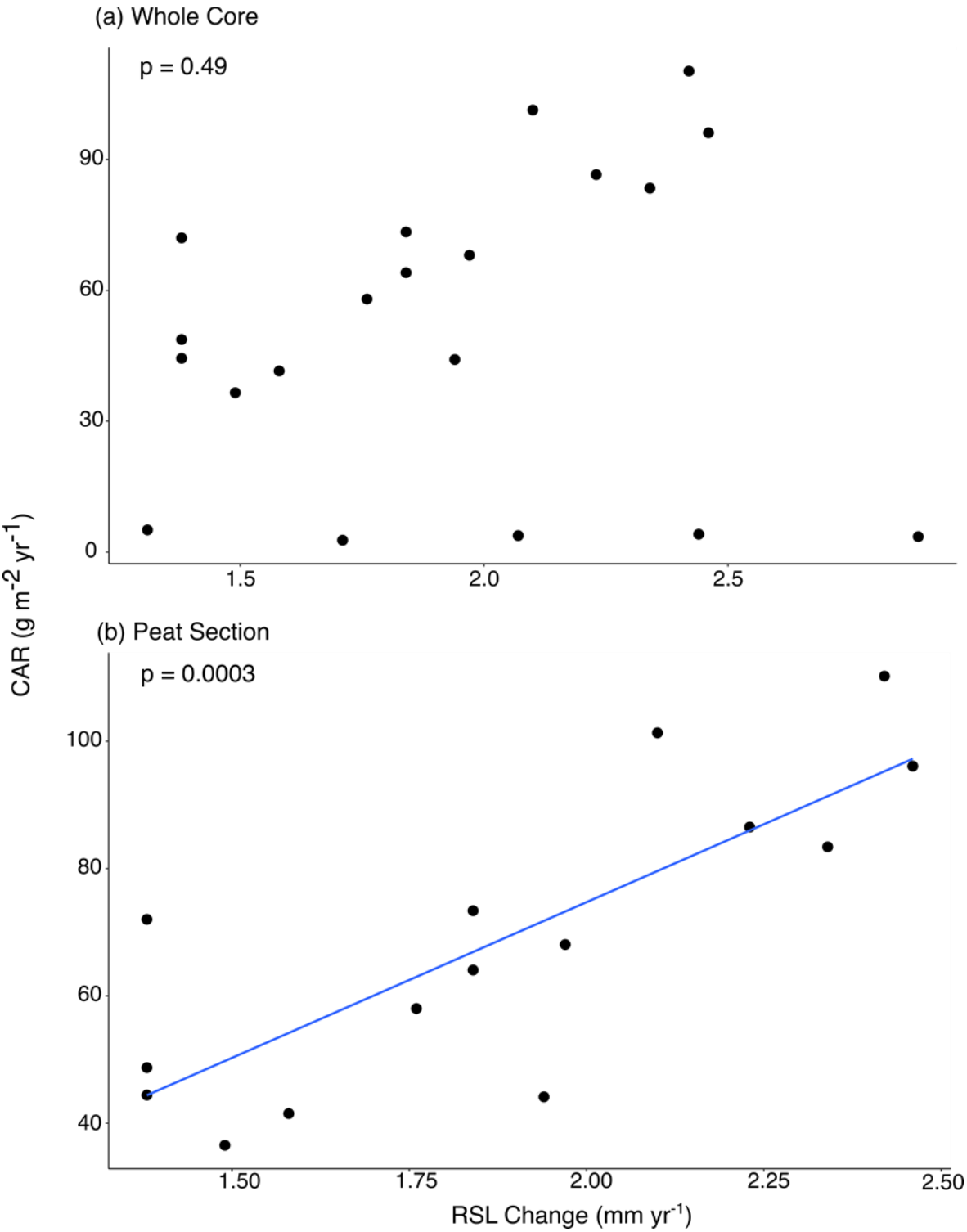

Figure 21. Regression analysis of the contribution of sea-level rise to increased CAR in (a) the entire core and (b) the peat section of the core alone.

The result of the second regression analysis, performed on only the peat section of the core (Fig. 21b), supports the hypothesis that increased rates of sea-level rise results in more rapid CAR. This has been demonstrated previously on a larger scale when Rogers *et al.* (2020) found that salt marshes from coastlines experiencing rapid rates of sea-level rise over the past few millennia have a higher soil carbon concentration. Additionally, Gonneea *et al.* (2019) found that increased carbon

storage in marshes experiencing rapid sea-level rise comes from enhanced vertical accretion of sediment as the site keeps pace with this rise. The sea-level rise experience by Lindisfarne cannot be called rapid – rates of ≥ 7.1 mm yr^{-1} are required to make marsh submergence overwhelmingly likely (Horton *et al.,* 2018) – and as opposed to considering the development of the marsh over the course of thousands of years, only the past fifty years are considered. Having said this, this result does demonstrate the relationship between carbon accumulation and sea level at a far high resolution than has otherwise, to my knowledge, been considered. This study was able to use a multi-annual scale and there was a clear relationship between rates of RSL change and rates of CAR (Fig. 21b). The fact that a significant result was achieved at this smaller scale and over a relatively short time scale is strong evidence in support of the supposed influence of sea-level change on salt marsh carbon accumulation. Further down the marsh, where tidal inundation is more frequent, this relationship may be even stronger, and a future examination of different marsh zones could also help to uncover the response of CAR in these zones to sea-level rise.

This regression analysis is, however, confounded somewhat by the fact that labile carbon is removed from the sediment over time which means that CAR values calculated for samples deeper in the core are necessarily lower. Labile carbon is the fraction of soil carbon susceptible to short-term turnover via microbial decomposition (Zhang *et al.,* 2020); therefore, lower down the core (and thus further back through time) the labile fraction of the carbon stock is more likely to have been broken down and returned to the atmosphere. Owing to this, the periods of time represented by sediment towards the bottom of the core when sea-level rise was less rapid also necessarily have lower CAR. It is difficult to quantify the magnitude of this variable, but it should be remembered as a caveat to the significant relationship detected between rate of sea-level rise and CAR. One way in which this could be overcome is using the two-pool modelling technique which would separate the accumulated carbon into a “long pool” and a “short pool” (i.e., recalcitrant and labile carbon fractions; Belshe *et al.,* 2019). The recalcitrant fraction down the core could then be compared with rates of sea-level rise so that more confidence can be placed in any significant result.

6.2.5 How do Snook sediment accretion and carbon accumulation rates compare with other sites?

If the sand section of the core LI21/20 is assumed to represent a period when the Snook area was covered by a mudflat, comparisons can be made with the literature. Mudflats investigated as a part of other studies have been shown to accrete sediment at far higher rates than those seen lower down core LI21/20 (Table 2); for example, Sanders *et al.* (2010) recorded a SAR value of 7.30 mm yr^{-1} in a Brazilian mudflat. This same site also had a high organic carbon burial rate of 1129 g m^{-2} yr^{-1} which is likely explained by the proximity of this mudflat to a mangrove forest and its ability to sequester the organic matter originating from the mangroves (Sanders *et al.*, 2010). In fact, the CAR of the mudflat is considerably larger than that of the mangrove forest, which was reported to have a rate of 353 g m^{-2} yr^{-1}. Therefore, it is not necessarily the case that a mudflat is inferior to a blue carbon ecosystem and the presence of these ecosystems neighbouring one another is potentially beneficial as the carbon not stored in the vegetated ecosystem may be tidally delivered to and

sequestered by the mudflat. This conclusion has relevance for Lindisfarne NNR and UK salt marshes more generally as other blue carbon ecosystems are often found within the same vicinity and interactions between these areas have been shown to influence carbon storage (Huxham *et al.,* 2018). Higher up the core, in the peat section, the mean SAR is 2.45 mm yr^{-1}. Similar, if slightly higher values, have been recorded for other UK salt marshes; Stiffkey marsh, Norfolk, had a mean of 3.30 mm yr^{-1} (Callaway *et al.,* 1996) and Hut marsh, Norfolk, one of 4.45 mm yr^{-1} (French and Spencer, 1993).

The CAR values of the peat section of the core are considerably higher than that of the sand section, as would be expected given the higher organic matter content of the former. The highest CAR recorded for core LI21/20 was at 2-3 cm depth (age range: 2013-2016) and had a value of 110 g m^{-2} yr^{-1}. The peat section of core LI21/20 had a mean CAR of 70 g m^{-2} yr^{-1}. This is considerably lower than the global average CAR value calculated by Ouyang and Lee (2013); the 158 sites in the Northern Hemisphere they studied had an average CAR of 242 g m^{-2} yr^{-1}. Within the 158 sites included in this review, a great many were dominated by *Spartina* plant species. Studies conducted on specific UK salt marshes also tend to record higher CAR values. Stiffkey marsh, Norfolk, which has a similar halophyte community to the Snook – *A. maritima* and *S. anglica* dominating – had a mean CAR of 172 g m^{-2} yr^{-1}. The CAR of Stiffkey marsh in the *A. maritima* zone was lower than in the *S. anglica* zone, 167 g m^{-2} yr^{-1} compared with 176 g m^{-2} yr^{-1}. The Snook core was taken from a section of the marsh with a plant community overwhelmingly dominated by *P. maritima* and *A. maritima*. Furthermore, the SAR rate of Stiffkey marsh, quoted above, is greater than that of the Snook, which would suggest a slower delivery of allochthonous carbon to the latter.

Considering these differences between the sites discussed, it may be argued that the comparatively low CAR calculated for Lindisfarne is fairly typical of the marsh zone investigated which is characterised by plant species of comparatively low productivity and by infrequent tidal inundation. In their review, Ouyang and Lee (2013) found a declining trend in CAR values from the low to the high marsh zone, which would reinforce the explanation offered here of the low CAR calculated for Lindisfarne compared with the global average and other UK sites. *Spartina alterniflora* invasion in a Chinese estuary was shown to enhance both the carbon and nitrogen stocks of the area because of its higher rates of production and low rates of decomposition compared with native species (Liao *et al.,* 2007). *Spartina anglica*, which arose from a hybridisation between *S. alterniflora* and *Spartina maritima*, has similar properties (Ayres and Strong, 2001). This again reinforces the need to conduct a more thorough investigation of the different zones of the Snook salt marsh through stratification of sampling. The low marsh, dominated by *S. anglica* and experiencing more frequent tidal inundation, may well have a considerably higher CAR than the high marsh which would alter the perceived value of this area as a carbon sink. The average CAR of the sand section of the core is 4 g m^{-2} yr^{-1}, but, as discussed above, if inorganic carbon accumulation rates were to be considered, this value could be greatly increased.

Following the emerging convention of expressing average annual CAR estimates of whole ecosystems in tonnes per hectares (Mossman *et al.,* 2021; Mason *et al.,* 2022), I have converted the Snook estimate to allow for consistent comparisons but

also report the value in g m^{-2} yr^{-1}. The estimated CAR of the entire Snook salt marsh must be viewed with caution because, as discussed above, it is based on the carbon content of just one core, contrary to the recommendations of the Blue Carbon Manual (Howard *et al.,* 2014). However, comparisons can be made with other sites. Recent studies investigating the overall CAR of newly realigned sites found values far higher than the 0.71 t ha^{-1} yr^{-1} (38.96 g m^{-2} yr^{-1}) extrapolated here for Lindisfarne. Managed realignment of a Bay of Fundy marsh resulted in an average CAR of 13.29 t ha^{-1} yr^{-1} (1329 g m^{-2} yr^{-1}; Wollenberg *et al.,* 2018) while the Steart marshes realignment site in the UK had an average organic CAR of 19.40 t ha^{-1} yr^{-1} (1940 g m^{-2} yr^{-1}; Mossman *et al.,* 2021). This disparity is to be expected given that both of these sites are newly realigned and so are likely to have large accommodation spaces which allows sediment accretion, and therefore the sequestration of allochthonous carbon, to be very rapid (Peck *et al.,* 2020). Indeed, the SAR of Steart marshes had a mean of 75 mm yr^{-1} (Mossman *et al.,* 2021), an order of magnitude greater than what is recorded for Lindisfarne. Therefore, the salt marsh investigated as a part of this study cannot be said to function as an appropriate analogue for early realigned sites. Perhaps of greater interest is the functioning of these sites a few decades post-realignment. Given that the Snook salt marsh is likely to be around 60 years old (Figs. 12a and 15), it may be useful for investigating the functioning of realigned marsh in later stages of maturity. Converting the global average CAR calculated by Ouyang and Lang (2013) into the units used here results in a value of 2.42 t ha^{-1} yr^{-1} and so the Lindisfarne estimate is 71 % lower than the global mean. Again, this should not necessarily be taken to mean that the Snook salt marsh has a low value in terms of carbon accumulation; a more thorough examination of all parts of the marsh would be necessary before reaching a reliable determination of its worth in this regard.

6.3 Salt-Marsh Gas Flux

6.3.1 Do greenhouse gas fluxes differ significantly between marsh zones and months?

Despite some differences in CO_2 fluxes (Fig. 15a), applying a linear regression model to the data showed that they do not differ significantly from one another and that neither month nor marsh zone (Table 3) explained a significant amount of the variation seen. However, if an entire year of data were available, this conclusion may well differ.

Table 3. Results of linear regressions testing the amount of variability in flux rates explained by the month and marsh zone in which measurements were taken. $p \leq 0.05$ would have represented a significant result.

Greenhouse Gas	Variable	*F*-value	*d.f.*	p-value
CO_2	Month	1.45	4, 10	0.29
	Zone	1.03	2, 12	0.38
CH_4	Month	3.14	4, 10	0.06
	Zone	0.06	2,12	0.54
N_2O	Month	1.17	4, 8	0.39
	Zone	1.81	2, 10	0.21

Again, in the case of CH_4 fluxes, none of the values differ significantly from one another but a significant relationship was found between the predictor and response variable for the May fluxes ($p = 0.02$). The month in which the measurements were taken also comes close to explaining a significant amount of the variation in flux rates (Table 3). Conversely, marsh zone was not found to be important (Table 3).

The N_2O fluxes also showed a large degree of variability, but the measurements did not differ significantly from one another and, once again, neither month of measurement nor marsh zone explained a significant proportion of the variation (Table 3). Several N_2O measurements taken during March were discounted because the overall flux could not be clearly determined and so only data from the low-marsh zone are available for this month (Fig. 15c).

6.3.2 How do the Snook fluxes compare with those of other sites, and can they be explained?

The CO_2 emission recorded in March, followed by the uptake of this gas in each subsequent month of measurements, can be explained by increased plant activity, and so higher rates of photosynthesis, into the spring and summer months. During the summer months, temperatures are closer to the optimum required for photosynthesis and so the rate of this process increases (Hikosaka *et al.,* 2006) and, in this case, exceeds the rate of respiration to result in net CO_2 uptake. Due to rates of flux not differing significantly between marsh zone or months (even the March measurements do not quite differ from the rest with $p = 0.052$), it is possible to state

that the mean CO_2 flux of the Snook salt marsh is -82.15 ± 187.76 SD mg CO_2 m^{-2} h^{-1}. It must be acknowledged that the uncertainty associated with this estimate is large and that the potential range crosses zero (as is the case for CH_4 and N_2O also). Other studies measuring CO_2 flux from salt marshes have also tended to record an uptake of this gas; in a Gulf of Mexico salt marsh, Wilson *et al.* (2015) recorded a rate of -172 ± 42 SD mg CO_2 m^{-2} h^{-1}. However, a study conducted in the Bay of Fundy, USA, taking weekly measurements from mid-July through to early September, and so covering a period that was missed by this study, recorded a mean CO_2 emission of 104 mg CO_2 m^{-2} h^{-1} (range: 13 – 154 mg CO_2 m^{-2} h^{-1}; Magenheimer *et al.,* 1996). This highlights a deficiency in this study; measurements of gas flux were not taken year-round and so a full picture of the net radiative balance of this salt marsh was not possible. Having said this, the growing season is a valuable period to capture due to higher temperatures and increased plant and microbe activity. Additionally, one of the main goals of this study was to a conduct a preliminary investigation of salt-marsh gas flux and make recommendations for future projects. Therefore, a valuable course of further investigation should involve measuring fluxes at a higher frequency and during all months of the year.

Fluxes of CH_4 were all relatively minor (-0.48 ± 1.90 SD mg CH_4 m^{-2} hr^{-1}; Fig. 15b) which could result from the salinity conditions of the marsh due to regular tidal inundation. The mean salinity of the Snook marsh is 21 ± 14 SD g/kg (Fig. 16d; Table S6), meaning it can be classified as polyhaline (which requires a salinity greater than 18). Salinity is a proxy for sulphate, the presence of which allows sulphate reducing bacteria to out-compete methanogens and thus prevent CH_4 production (Al-Haj and Fulweiler, 2020). This result is consistent with the findings of Poffenbarger *et al*. (2011) who recorded significantly lower methane emissions (0.11 ± 0.23 SD mg CH_4 m^{-2} hr^{-1}) from polyhaline marshes than from fresh, mesohaline and oligohaline marshes. Additionally, an earlier study of CH_4 emissions and salt marsh salinity recorded a mean flux of 0.64 mg CH_4 m^{-2} hr^{-1} from the highest salinity site involved (Bartlett *et al.,* 1987). The main difference between the results of this study and these others discussed is that a mean uptake of CH_4 was recorded on the Snook salt marsh while both previous studies recorded a small emission. The emissions are, admittedly, very minor and would be unlikely to detract significantly from the radiative forcing reduction resulting from the existence/creation of a polyhaline salt marsh (Poffenbarger *et al.,* 2011). In a recent review, Al-Haj and Fulweiler (2020) compiled 97 studies investigating CH_4 flux in blue carbon ecosystems and calculated a mean value of 0.16 mg CH_4 m^{-2} h^{-1} (range: -0.04 – 63.00 mg CH_4 m^{-2} h^{-1}) and so a minor emission is the general expectation.

The possible drivers of CH_4 flux are many and linked (e.g., organic matter, plant species, salinity and temperature (Al-Haj and Fulweiler, 2020); Fig. 3) and so it is difficult, within the scope of this study, to unpick the drivers behind the general uptake of CH_4 recorded here. This could be attempted by future projects through the use of more manipulative techniques in the form of mesocosm experiments; these could still be implemented in the field but would also allow environmental variables to be controlled. For example, Mueller *et al.* (2020) used this technique to test the effects of climate change on CH_4 emission from salt marshes and was able to manipulate sea level, atmospheric CO_2 and nitrogen levels.

N_2O fluxes did not differ significantly between measurements, and so the mean N_2O emission can be stated as 0.04 ± 0.22 SD mg N_2O m^{-2} h^{-1}. Since N_2O can be produced by both nitrification and denitrification it is exceedingly difficult to attribute these fluxes to particular processes and to determine the drivers. The fluxes recorded on the Snook salt marsh are comparable to those produced by similar sites studied by other projects. Blackwell *et al.* (2010) measured N_2O flux from both natural and realigned sites in the estuary of the River Torridge, Devon, and found that the former produced lower emissions of 0.27 ± 0.16 SD mg N_2O m^{-2} h^{-1} (compared to 0.65 ± 0.15 SD mg N_2O m^{-2} h^{-1} from the realigned marsh). Another site in Massachusetts, USA, recorded a mean uptake of -0.42 mg N_2O m^{-2} h^{-1} in July (Moseman-Valtierra *et al.,* 2011). This same study also investigated the impact of nitrate addition on N_2O flux and found a significant increase in emission (0.83 mg N_2O m^{-2} h^{-1}) when this treatment was applied (Moseman-Valtierra *et al.,* 2011). Therefore, there is evidence in the literature to suggest that the addition of nitrates to salt marsh sediment can have a large impact on the rate of N_2O emission. The Snook salt marsh does not receive an input of nitrate in the form of fertiliser run-off from agricultural land; however, there may be mainland sites within the NNR that are affected in this way. If so, Lindisfarne NNR would be a suitable site for future studies aiming to investigate the effect of nitrate run-off on salt marsh N_2O flux. Two nearby sites could be compared, with the Snook being used as a control. Other possible avenues for future work investigating the drivers of salt marsh N_2O flux could include an investigation of the soil microbiome; higher emissions from wetlands are correlated with the functional diversity of microbes (Bahram *et al.,* 2022) and so the presence of certain groups would be indicative of different processes. For example, certain methanotrophic bacteria have been shown to consume nitric oxide (NO) and produce small amounts of N_2O (Ren *et al.,* 2000) which suggests links between the fluxes of the different greenhouse gases and the microbiome of the soil.

6.3.3 What are the potential environmental drivers behind the fluxes?

Environmental data were primarily collected with a view to further analysis by future projects; however, some preliminary analysis of this data has been performed here in an attempt to highlight possible areas of particular interest (Fig. 16; Table S6).

When linear regression was employed to determine whether the environmental variables measured in this study could explain the variation in greenhouse gas fluxes, the resulting models did not have significant p-values for CO_2, CH_4 nor N_2O (Table 4). However, this cannot be taken to mean that none of the environmental variables discussed have any influence on flux rates. The next step when analysing these data further should be to apply a more complex model capable of more thoroughly testing the impact of each variable. This could include, for example, a generalised linear model (GLM; Zheng *et al.,* 2000) or multiple linear regression (MLR; Eberly, 2007).

Table 4. Results of linear regression to determine explanatory power of environmental variables on rates of greenhouse gas flux. Results for the significance of the whole model are displayed. $p \leq 0.05$ would have represented a significant result/useful model.

Greenhouse Gas	*F*-value	*d.f.*	p-value
CO_2	0.97	4, 10	0.46
CH_4	0.13	4, 10	0.97
N_2O	0.97	4, 8	0.47

The lack of significant relationships between the environmental variables measured as part of this study and greenhouse gas fluxes mean it is difficult to make specific recommendations of useful future work in this area. However, one of the main priorities should be designing experiments that make it possible to control these variables so that their individual effects can be gauged. Decreasing elevation across the marsh surface, and the correlation of many environmental variables with elevation, makes untangling the impact of individual variables difficult. One way in which this can be tackled is using the mesocosm experiments discussed above. Further to this, marsh organs - platforms containing mesocosms - allow elevation to be altered while holding many other factors constant; this technique may be particularly useful for examining the fluxes associated with different plant species at various elevations (Peng *et al.,* 2018). Given that Mason *et al.* (2022) identified the discovery of the environmental drivers behind carbon and greenhouse gas fluxes as one of the major areas requiring additional data within the field of blue carbon science, this should certainly be a priority.

The fact that temperature and soil moisture vary between months again emphasises the importance of conducting a year-round investigation of salt marsh gas flux. Despite the fluxes themselves not differing between months in the case of this study, more data (especially a higher number of replicates at each station) may allow for more robust statistical analysis.

6.3.4 What are the lessons learnt from this preliminary greenhouse gas flux study?

One particular issue associated with the static chamber and gas chromatography technique used in this study is the expectation that the concentration of gas within the chamber should increase or decrease linearly through time (Al-Haj and Fulweiler, 2020). Where this is not the case, data points that skew the overall trend can be removed or the nonlinear flux is designated as having a value of zero (Heiss *et al.,* 2012). In the case of this study, the former technique was employed with values that appeared to skew the trends of the fluxes discounted. This was generally only necessary with CH_4 and N_2O data as CO_2 measurements were almost always linear (10.6084/m9.figshare.20940067; Table S7). CH_4 and N_2O were essentially never linear and so it was always necessary to attempt to "uncover" the direction of the flux before making further calculations. The difficulty with this was that removing one value as opposed to another could entirely change whether that measurement is counted as an emission or an uptake of the gas. Discounting non-linear fluxes as

having zero values was avoided because it was desirable to record even very minor fluxes so that a full picture of ecosystem functioning could be developed. Therefore, in future projects attempting to take similar measurements using the static chamber technique it would be advisable to increase the number of replicates taken at each station manifold; this would enable greater certainty to be placed in the trends measured. Alternatively, it may be advantageous to disregard the static chamber and gas chromatography technique and measure fluxes via other means. Using the Los Gatos Research fast greenhouse gas analyser would allow measurements of greenhouse gas concentration to be taken every second the chamber is deployed on the marsh and so lead to a better picture of the fluxes produced. This technique was not employed in this project because the equipment available would not have allowed N_2O to be measured. Yet more different is the eddy flux tower method which allows measurements to be taken over large areas (Aubinet *et al.,* 2012). This technique has been used to measure CH_4 and CO_2 flux from a realigned site (Negandhi *et al.,* 2019) and may allow a more accurate estimate of the fluxes associated with the site as a whole to be generated.

In addition to the inability of this study to conduct year-round monitoring of greenhouse gas flux previously discussed (see Discussion 6.3.2), measurements taken under all possible conditions experienced by the marsh were also omitted. For example, taking measurements during the night when a lack of light prevents photosynthesis could result in a negation of the CO_2 uptake seen during the daytime. Additionally, the marsh is regularly inundated by the tide and so submerged in water; this is likely to drastically change the environmental conditions (temperature, salinity, O_2 availability) of the area (Blackwell *et al.,* 2010) and lead to the input of sediment and nutrients, especially phosphorus and nitrogen (Nixon *et al.,* 1996). Measuring greenhouse gas fluxes during tidal inundation of the marsh presents more logistical challenges than when the tide is out. However, one way in which it could be achieved is through the deployment of autonomous vehicles (Smyth *et al.,* 2010); this equipment has previously been used to study pH amelioration by seagrass meadows (Ricart *et al.,* 2021) and investigate seawater CO_2 (Sims *et al.,* 2022).

6.3.5 What is the net radiative balance of the Snook salt marsh?

Net radiative balance estimates were calculated for the high, mid and low zones of the Snook salt marsh using the gas flux data discussed in this section (Fig. 15) as well as, in the case of the high marsh, the CAR data dealt with previously (see Results 5.2.3). Means were taken of the five months of data collected to generate estimates of yearly fluxes. The accuracy of these estimates of net radiative balance are therefore another aspect of the study which would be improved by year-round monthly measurements of gas flux from the Snook salt marsh. CAR data is only available for the high marsh because this is the location from which core LI21/20 was taken (Table 2). When the net radiative balance was calculated for this marsh zone, therefore, CAR, N_2O and CH_4 were summed, and CO_2 flux measured using the static chamber technique was left out of the calculation (Fig. 22a). This was decided because including both CAR and CO_2 would result in double counting and the CAR of the core top is more likely to represent carbon that is sequestered and stored in the marsh, with the exception of the labile carbon mentioned above which is likely broken down over time by microbial decomposition but this is less of an issue in the uppermost sample. Furthermore, CAR also includes allochthonous carbon while the

static chamber CO_2 represents only autochthonous contributions. Net radiative balance estimates for the mid and low marsh zones differ in that CAR had to be substituted for CO_2 flux measured with the static chambers and so are not readily comparable with the high marsh estimate. Again, this emphasises the desirability of taking cores from different marsh zones to obtain CAR estimates for each location so that better estimates of salt marsh net radiative balance can be developed. This is particularly important for the mid and low marsh zones because the contribution of tidally delivered allochthonous carbon is likely greater in these areas where tidal inundation is a more frequent occurrence.

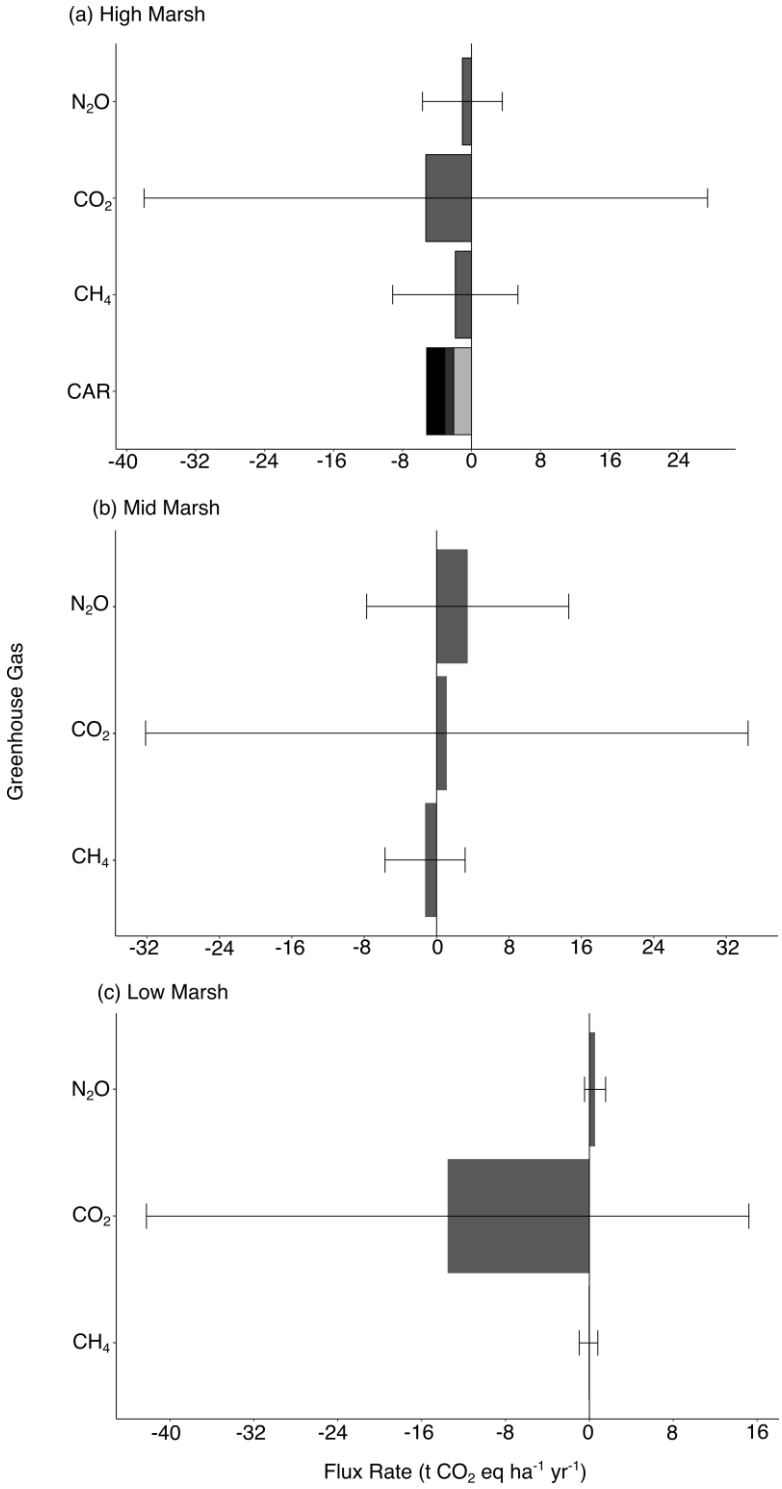

Figure 22. Net radiative balance of the (a) high, (b) mid and (c) low marsh zones. Core LI21/20 was taken from the high marsh and so carbon accumulation rate (CAR) data is available for this zone only. Carbon content of cores from the other marsh zones was not investigated and so only greenhouse gas fluxes measured with the static chamber technique are shown here. The CAR bar has the 95% confidence intervals shown in dark and light grey with the mean show in mid grey as it was not possible to obtain standard deviation values from *rplum*. Error bars for the other fluxes are mean $\pm$ SD and are 2 σ.

When the high marsh zone is considered, the net radiative balance of the salt marsh is a beneficial one, that is, higher quantities of CO_2 equivalents are taken up by the marsh than are emitted (Fig. 22a). There is a mean uptake of all three gases and calculating the net radiative balance (including CAR but not CO_2) shows an uptake of -6.03 $\pm$ 2.20 SD t CO_2 eq ha^{-1} yr^{-1}. The 2 σ uncertainty associated with CO_2 flux is very high (-5.29 $\pm$ 32.70 SD t CO_2 eq ha^{-1} yr^{-1}) which likely arises from the fact that an emission of this gas was recorded in March followed by an uptake in most measurements from subsequent months (Fig. 15a).

The mid marsh zone is the only one with a mean emission of greenhouse gas (3.30 $\pm$ 3.35 SD t CO_2 eq ha^{-1} yr^{-1}), but the uncertainty here is greater, which arises from the CO_2 flux (1.13 $\pm$ 33.29 SD t CO_2 eq ha^{-1} yr^{-1}). The N_2O emission (3.44 $\pm$ 11.17 SD t CO_2 eq ha^{-1} yr^{-1}) is the largest contributor to the overall net emission while there is a mean CH_4 uptake of -1.28 $\pm$ 4.42 SD t CO_2 eq ha^{-1} yr^{-1}, which somewhat negates this detrimental net radiative balance (Fig. 22b). The N_2O emission is greater in the mid marsh than in either of the other zones which might suggest the influence of particular environmental variables present in this area but lacking in the other two.

In the low marsh zone, the greatest beneficial net radiative balance is seen with a value of -13.05 $\pm$ 2.27 SD t CO_2 eq ha^{-1} yr^{-1}, although comparison with the high marsh is not legitimate due to the different data used in the calculations (CAR vs. CO_2). In the low marsh, CO_2 uptake is the greatest contributor to the overall figure and has a value of -13.52 $\pm$ 28.73 SD t CO_2 eq ha^{-1} yr^{-1} (Fig. 22c). The emission of N_2O (0.55 $\pm$ 1.00 SD t CO_2 eq ha^{-1} yr^{-1}) and uptake of CH_4 (-0.08 $\pm$ 0.88 SD tCO2 eq ha^{-1} yr^{-1}) make very minor contributions to the overall sum (Fig. 22c).

The total area of each marsh zone has not been mapped for the Snook salt marsh and so it was not possible to weigh the contributions of each one in terms of net radiative balance. This would certainly be a useful course for future projects to take which would allow a fuller picture of salt marsh functioning to be developed.

The most complete picture of net radiative balance was developed for the high marsh by converting the greenhouse gas fluxes discussed above and the CAR of the uppermost sample in core LI21/20 into CO_2 equivalents. This resulted in the calculation of a beneficial net radiative balance for the high zone of the Snook salt marsh. Few other studies have attempted estimates of salt-marsh net radiative balance and so it is difficult to compare the results generated here with the literature. Chmura *et al*. (2011) also summed carbon sequestration and gas flux for a macrotidal marsh in Dipper Harbour, Canada, which was found to have a radiative balance of -5.67 t CO_2 eq ha^{-1} yr^{-1}, while a microtidal marsh on Kouchibouguacis Lagoon, Canada, took up an even greater quantity of greenhouse gas (-9.81 t CO_2 eq ha^{-1} yr^{-1}). The estimate for the high marsh zone of the Snook (a mesotidal area) was -6.03 $\pm$ 2.20 SD t CO_2 eq ha^{-1} yr^{-1} and so it is relatively consistent with previous findings. Different tidal regimes can result in variations in flooding frequency between sites which in turn affects the time available for soil drainage (Byers and Chmura, 2007). Therefore, it may be expected that this would lead to differences in soil O_2 availability and, through this, variable greenhouse gas fluxes (Chmura *et al.,* 2011). However, this variation in greenhouse gas flux was not the main cause of the difference in radiative impact between the micro- and

macrotidal marshes investigated by Chmura *et al.* (2011); this arose from differences in carbon sequestration. The microtidal marsh likely has less opportunity for soil drainage and is, therefore, under anoxic conditions for longer, which means slower rates of organic matter decomposition. Furthermore, tidally delivered allochthonous carbon may be more readily available in a location where the tide does not frequently retreat far from the marsh during low tides. Taking cores from the mid and low marsh zones would help to illuminate the contribution of tidally delivered organic matter in a mesotidal marsh further.

In a recent review compiling data on carbon sequestration and CO_2, CH_4 and N_2O fluxes from a range of different studies examining natural marshes, the mean results show relatively close agreement with the findings of this project (Mason *et al.,* 2022). N_2O flux was recorded as an emission (0.1 ± 0.3 SD t CO_2 eq ha^{-1} yr^{-1}; Mason *et al.,* 2022) as was the case in the mid and low marsh zones at Lindisfarne (Figs. 22b and 22c). CO_2 (16.50 $\pm$ 16.00 SD t CO_2 eq ha^{-1} yr^{-1}) and CH_4 (1.20 $\pm$ 6.30 SD t CO_2 eq ha^{-1} yr^{-1}) uptakes were recorded (Mason *et al.*, 2022) which was generally also the case in this study. Summing the same values from Mason *et al*. (2022) as those used to calculate the net radiative balance of the high marsh in this study, resulted in a net radiative balance estimate of -9.30 $\pm$ 2.34 SD t CO_2 eq ha^{-1} yr^{-1} (Mason *et al.,* 2022), somewhat higher than the Snook and perhaps explained by the relatively low CAR rates of this area compared with other sites discussed above.

In the mid and low marsh zones, using CO_2 flux as opposed to CAR for the net radiative balance calculation places more doubt on the estimates produced because it is not possible to conclusively determine the fate of the carbon taken up (i.e., whether it actually stored in the marsh or simply released back to the atmosphere). It has, however, been shown that the largest source of recalcitrant carbon to salt marshes is that which is sequestered in-situ (Saintilan *et al.,* 2013). Therefore, a large uptake of CO_2, as is seen in the low marsh zone (Fig. 22c), suggests that this area is truly sequestering large quantities of this greenhouse gas. If allochthonous carbon were also considered in the mid and low marsh zones, the uptake would likely be even greater.

To conclude, the net radiative balance of the Snook salt marsh must be interpreted with caution due to different data being available for different marsh zones. However, given the relatively good consistency between the mean estimate of this project and those of other studies for similar, natural sites, there is a strong case for accepting the hypothesis that the overall impact of the marsh is a beneficial one. Further work conducted in the mid and low marsh zones is required to accurately quantify the magnitude of this impact.

Chapter 7: Conclusion

7.1 Key Conclusions

A proxy sea-level reconstruction was developed for Lindisfarne, using salt-marsh foraminifera as sea-level indicators, spanning the past ca. 60 years, based on a combination of modern local foraminifera and a published wider North Sea data set (Rush *et al.,* 2021). However, the reconstruction was of limited use due to large uncertainty with respect to the magnitude of sea-level change over the short duration and its predictions differing widely from the closest tide-gauge records (Fig. 18).

Analysis of carbon accumulation rates derived from core LI21/20 and tide-gauge data showed that more rapid carbon accumulation rates in peat (i.e., salt marsh) may be partially driven by increased rates of sea-level rise (Fig. 21b). This is consistent with other recent analyses pointing to this connection and implies that salt marshes experiencing rapid sea-level rise – assuming they are also able to keep pace with this rise – are acting as more powerful climate change mitigators through the sequestration of increased quantities of greenhouse gas. However, it must be stressed that labile carbon was likely lost from lower down the core which could at least partially explain the significant result generated here. This complication could be overcome in future with modelling techniques.

Examining the isotope data generated for core LI21/20 revealed that most of the carbon stored within originated from autochthonous sources and from C_3 plants, which is consistent with observations of the site's location in the high marsh and the dominant plant species in that vicinity (Fig. 19). Furthermore, isotope data helps to confirm the likely age of the marsh; carbon and nitrogen content show a marked jump at the same point as the transition to peat and agglutinated foraminifera occurs in sediment deposited in approximately the 1960s (Figs. 14a and 14e).

The greenhouse gas fluxes measured at locations across the surface of the high, mid and low marsh were broadly consistent with other values recorded in the literature for salt marshes. Taking means of the recorded values showed a yearly uptake of CO_2 and CH_4 while N_2O was emitted in a small quantity; however, these means are based on only five months of measurements. Calculating the net radiative balance by combining the gas flux and carbon data resulted in a beneficial net impact in the high marsh of -6.03 ± 2.20 SD t CO_2 eq ha^{-1} yr^{-1}.

7.2 Future Work

One of the main priorities for future projects aiming to continue the study of blue carbon – either within Lindisfarne NNR or at other salt marsh sites – should be an effort to obtain a more reliable estimate of blue carbon stocks. Stratifying the large, heterogeneous salt marsh area into more homogeneous subsections based, for example, on species diversity and geomorphology, would make this a reasonably manageable task without the need for a dense sampling regime (Howard *et al.,* 2014). The Snook salt marsh, for instance, could be split into three sub-sections: the high marsh, dominated by *P. maritima* and *A. maritima*; the mid marsh, dominated by *A. portulacoides*; and finally, the low marsh, which is dominated by *S. anglica* and *S. europaea*. Following this procedure would allow for a more reliable assessment of the net radiative balance mitigation capability of the Snook salt marsh. Similarly, the same procedure could be applied to Fenham marsh; this area was observed to be

far more homogenous than the Snook and so developing an estimate may be even less time consuming. Furthermore, assessing the carbon content of Fenham marsh would allow the carbon sequestration capability of a younger marsh to be assessed. If possible, within the scope of the future project, it would be advisable to measure inorganic carbon content as well as that of organic carbon. The contribution of inorganic carbon to low marsh stocks may be particularly important, given that regular tidal inundation could input large quantities in the form of shell fragments and so forth.

Within the scope of salt marsh blue carbon stocks also, is an examination of organic matter decomposition down the core and loss of stored carbon. The highly variable organic carbon density calculated by this study for core LI21/20 meant that at no point was it possible to describe the carbon present as stable and effectively preserved, which calls into question the efficacy of converting salt-marsh carbon stocks into carbon credits. Taking cores of sediment and measuring carbon content results in only a snapshot of carbon density and does not allow for the potential decomposition of labile carbon over time to be fully appreciated. Investigating the microbial groups associated with carbon breakdown and the abiotic factors relating to their presence or absence would allow for a more in-depth understanding of carbon storage in salt marshes to be developed. Ultimately, a study of this nature could help to determine the true value of salt marshes as carbon sinks.

When the greenhouse gas flux aspect of this project is considered, there are many potential avenues that could be pursued by future projects. The first, and another of the main priorities following this study, should involve an effort to continue taking measurements of gas flux on the Snook salt marsh year-round. This would allow for more reliable estimates of the fluxes generated by the marsh in a year, as opposed to taking means of measurements taken over only five months as was the case in this study. Further to this, but slightly more challenging, is taking measurements of gas flux under all the different conditions experienced by the marsh, such as during the night and the flood tide.

Once year-round measurements of gas flux have been achieved, a productive avenue for future projects could involve investigating the environmental drivers behind gas flux. This could be achieved using more manipulative mesocosm/marsh organ experiments. In the long run, when the environmental drivers of gas flux are better understood, this could aid with monitoring the marsh. Currently, vegetation surveys are conducted within Lindisfarne NNR every five years; a similar regime could be applied to gas flux and the associated environmental variables. For example, taking measurements every five years during the growing season would allow change in greenhouse gas fluxes in response to the effects of climate change on the related environmental variables to be monitored. This method could be applicable to other blue carbon sites and would be important for quantifying any detractions made by significant emissions of greenhouse gas from the net radiative balance of the site.

Finally, the suggestions discussed above - stratifying the marsh to obtain estimates of CAR for different marsh zones and further developing the gas flux data by taking year-round measurements - would enable more accurate estimates of net radiative balance to be calculated for the entirety of the Snook salt marsh. This would further

aid efforts to understand and utilise the potential carbon sequestration benefits of the site.

Appendix

Table S1. Percentage counts of dead foraminifera assemblages in the modern Lindisfarne training set. Shown as percentage abundances relative to the total of dead individuals in each sample.

Sample	Elevation	*Quinqueloculina* spp.	*Cornuspira involvens*	*Cribroelphidium williamsoni*	*Haynesina germanica*	*Ammonia* spp.	*Elphidium margaritaceum*	*Bulimina gibba*	*Cribroelphidium incertum*	*Trochammina inflata*	*Milliammina fusca*	*Entzia macrescens*	*Haplophragmoides* spp.
LI01	2.55	0.7	0	0	0	1.4	0	0	0	17.9	0.7	0	79.3
LI02	2.49	0	0	0	0	0	0	0	0	24	18	32	26
LI03	2.41	0	0	0	0	0	0	0	0	18.3	28.1	44.4	9.2
LI04	2.29	0	0	0	0	0	0	0	0	16	34	48	2
LI05	2.18	0	0	0	0	0	0	0	0	8.1	58.1	32.3	1.6
LI06	2.12	53.6	5.4	1.8	8.9	0	0	1.8	0	1.8	17.9	8.9	0
LI07	1.98	59.3	2	10.3	8.8	0	0	0	2.9	0	8.8	7.4	0.5
LI08	2.03	50	22	0	2	0	0	0	0	0	26	0	0
LI09	2.03	0	2	0	0	0	0	0	0	8	40	50	0
LI10	2.36	0	0	0	0	0	0	0	0	30	52	18	0
LI11	2.41	0	0	0	0	0	0	0	0	18	26	46	10
LI12	2.38	1.2	0	0	1.2	0	0	0	0	44.4	6.2	42	4.9
LI13	2.57	0	0	0	0	0	0	0	0	55.7	1.6	16.4	26.2
LI14	2.47	0	0	0	0	0	0	0	0	31.8	16.7	43.9	7.6
LI15	2.38	0	0	1.9	0	0	0	0	0	63.5	3.8	25	5.8
LI16	2.23	0	0	0	0	0	0	0	0	21.2	21.2	56.1	1.5
LI17	2.02	14.6	0	0	5.6	66.3	0	0	0	1.1	5.6	6.7	0
LI18	1.98	80.9	16.4	0	0	1.8	0	0	0	0	0.9	0	0
LI27	2.8	0	0	0	0	0	0	0	0	0	2.4	75.4	22.2
LI28	2.75	0	0	0	0	0	0	0	0	3.4	3.4	74.1	19
LI29	2.7	0	0	0	0	0	0	0	0	31.7	7.3	58.5	2.4
LI30	2.65	3	0	0	0	0	0	0	0	6	11.9	53.7	25.4
LI31	2.6	0	0	0	0	0	0	0	0	48.3	8.2	18.1	25.4
LI32	2.55	0	0	0	0	0	0	0	0	36.2	10.5	46.3	7
LI33	2.5	0	0	0	0	0	0	0	0	17.5	9	68.2	5.4
LI34	2.45	0	0	0	0	0	0	0	0	13.2	18.5	36.2	32.1
LI35	2.4	0	0	1.5	0	0	0	0	1.5	13.9	28.6	50	4.5
LI36	2.35	0	0	1	0	0	0	0	1	13.5	25	38.5	21.2
LI37	2.3	0	0	0	0	0	0	0	0	5.2	34.5	46.6	13.8
LI38	2.25	29.4	0	28	0	0	0	0	8.4	0	9.8	21.7	2.8
LI39	2.2	3.3	0	0	0	0	0	0	0	1.7	30	65	0
LI40	2.15	31.6	7.6	2.5	0	1.3	0	0	0	0	25.3	31.6	0
LI41	2.1	68.3	6.1	3.7	2.4	0.6	0		10.4	1.8	4.3	2.4	0

LI42	2.05	45.9	9.8	6.6	6.6	11.5	0	0	1.6	0	6.6	11.5	0
LI43	2	13	0	13	9.2	38.9	0	0	0	1.9	22.2	1.9	0
LI44	1.95	37	2.2	6.5	21.7	10.9	2.2	0	8.7	0	10.9	0	0
LI45	1.9	3.3	1.6	14.8	24.6	32.8	14.8	0	6.6	0	1.6	0	0
LI46	1.85	0	0	18.6	27.8	25.8	18.6	0	5.1	0	3.1	1	0
LI47	1.8	1.6	0	9.5	27	34.9	19	0	3.2	0	4.8	0	0
LI48	1.75	5.7	1.4	1.4	37.1	41.4	1.4	0	1.4	0	8.6	1.4	0
LI49	1.7	5.1	0	3.4	34.2	47.9	1.7	0	1.7	0	1.7	4.2	0
LI50	1.65	0	0	25.4	54	12.7	1.6	0	1.6	0	3.2	1.6	0
LI51	1.6	14.5	0	29.1	45.5	3.6	1.8	0	0	0	0	5.5	0
LI52	1.55	24.1	3.7	33.3	24.1	0	1.9	1.9	1.9	0	0	9.3	0
LI53	1.5	17.6	5.9	25.5	37.3	7.8	0	0	2	0	3.9	0	0
LI54	1.45	37.5	0	18.8	20.8	2.1	4.2	12.5	2.1	0	0	2.1	0
LI55	1.4	15.9	6.3	14.3	39.7	7.9	0	0	9.5	0	3.2	3.2	0
LI56	1.35	23.5	0	21.6	43.1	5.9	0	0	3.9	0	0	2	0
LI57	1.3	12.3	0	14	73.7	0	0	0	0	0	0	0	0
LI58	1.25	25.5	0	11.7	15.7	37.3	0	0	3.9	0	3.9	2	0
LI59	1.2	12.5	0	2.1	16.7	58.3	0	2.1	4.2	0	0	4.2	0
LI60	1.15	10.9	0	2.2	8.7	69.6	0	0	4.3	0	4.3	0	0
LI61	1.1	25	0	0	5.4	60.7	0	0	3.6	0	1.8	3.6	0
LI62	1.05	27.8	0	0	3.7	61.1	0	1.9	3.7	0	1.9	0	0
LI63	1	3.9	2	0	5.9	66.7	0	0	5.9	0	5.9	9.8	0
LI65	0.9	21.6	2.7	5.4	5.4	48.6	0	2.7	0	2.7	0	10.8	0

Table S2. Percentage counts of live foraminiferal assemblages in the modern Lindisfarne training set. Shown as percentage abundances relative to the total of live individuals in each sample.

Sample	Elevation	*Quinqueloculina* spp.	*Cornuspira involvens*	*Cribroelphidium williamsoni*	*Haynesina germanica*	*Ammonia* spp.	*Cribroelphidium incertum*	*Trochammina inflata*	*Milliammina fusca*	*Entzia macrescens*	*Haplophragmoides* spp.
LI01	2.55	0	0	0	0	0	0	0	0	0	0
LI02	2.49	0	0	16.7	33.3	0	0	0	0	50	0
LI03	2.41	0	0	0	0	0	0	0	0	0	0
LI04	2.29	0	0	0	0	0	0	0	100	0	0
LI05	2.18	0	0	0	0	0	0	0	100	0	0
LI06	2.12	81.5	7.4	0	0	0	0	0	7.4	3.7	0
LI07	1.98	81.2	3.4	2.6	0.9	0	0	0	7.7	4.3	0
LI08	2.03	61.4	33.3	0	0	0	0	0	5.3	0	0
LI09	2.03	50	50	0	0	0	0	0	0	0	0
LI10	2.36	0	0	0	0	0	0	0	33.3	66.7	0
LI11	2.41	0	0	0	0	0	0	0	0	0	0
LI12	2.38	25	0	25	0	0	0	0	0	50	0
LI13	2.57	0	0	0	0	0	0	0	100	0	0
LI14	2.47	0	0	0	0	0	0	0	0	0	0
LI15	2.38	100	0	0	0	0	0	0	0	0	0
LI16	2.23	0	0	0	0	0	0	0	0	0	0
LI17	2.02	53.3	33.3	0	0	10	0	0	3.3	0	0
LI18	1.98	82	16	0	0	0	0	0	2	0	0
LI27	2.8	0	0	0	0	0	0	0	0	100	0
LI28	2.75	0	0	0	0	0	0	0	0	100	0
LI29	2.7	0	0	0	0	0	0	0	0	100	0
LI30	2.65	0	0	0	0	0	0	19	50	50	0
LI31	2.6	0	0	0	0	0	0	42.9	0	0	81
LI32	2.55	0	0	0	0	0	0	26.7	0	28.6	28.6
LI33	2.5	0	0	0	0	0	0	11.1	0	60	13.3
LI34	2.45	0	0	0	0	0	0	7.1	5.6	5.6	77.8
LI35	2.4	0	0	0	0	0	0	7.7	28.6	42.9	21.4
LI36	2.35	23.1	0	0	0	0	0	0	15.4	23.1	30.8
LI37	2.3	0	0	20	0	0	0	0	0	40	40
LI38	2.25	70.4	0	14.8	0	0	0	0	0	14.8	0
LI39	2.2	66.7	0	0	0	0	33.3	0	0	0	0
LI40	2.15	64.6	33.3	0	0	0	0	0	2	0	0
LI41	2.1	70.6	29.4	0	0	0	0	0	0	0	0
LI42	2.05	86.7	6.7	0	0	0	0	0	6.7	0	0

LI43	2	78.6	7.1	0	7.1	7.1	0	0	0	0	0
LI44	1.95	58.3	33.3	0	0	0	0	0	8.3	0	0
LI45	1.9	0	100	0	0	0	0	0	0	0	0
LI46	1.85	0	0	100	0	0	0	0	0	0	0
LI47	1.8	0	0	0	50	50	0	0	0	0	0
LI48	1.75	47.1	29.4	0	0	5.9	0	0	17.6	0	0
LI49	1.7	35	0	0	45	15	0	0	5	0	0
LI50	1.65	14.3	0	0	85.7	0	0	0	0	0	0
LI51	1.6	10	0	30	60	0	0	0	0	0	0
LI52	1.55	5.6	0	66.7	22.2	5.6	0	0	0	0	0
LI53	1.5	18.2	18.2	18.2	45.5	0	0	0	0	0	0
LI54	1.45	10	0	50	40	0	0	0	0	0	0
LI55	1.4	12.5	0	25	62.5	0	0	0	0	0	0
LI56	1.35	16.7	16.7	0	33.3	0	0	0	0	33.3	0
LI57	1.3	0	20	0	80	0	0	0	0	0	0
LI58	1.25	50	0	0	0	50	0	0	0	0	0
LI59	1.2	100	0	0	0	0	0	0	0	0	0
LI60	1.15	66.7	0	33.3	0	0	0	0	0	0	0
LI61	1.1	100	0	0	0	0	0	0	0	0	0
LI62	1.05	90.9	0	0	0	9.1	0	0	0	0	0
LI63	1	100	0	0	0	0	0	0	0	0	0
LI65	0.9	100	0	0	0	0	0	0	0	0	0

Table S3. Percentage counts of dead foraminiferal assemblages in core LI21/20. Shown as percentage abundances relative to the total of live individuals in each sample.

Sample	*Cribroelphidium williamsoni*	*Bulimina gibba*	Polysaccammina ipohalina	*Trochammina inflata*	*Milliammina fusca*	*Entzia macrescens*	*Haplophragmoides* spp.
1	0	0	0	61	3	7	29
2	0	0	0	14.1	4.3	25	56.5
3	0	0	0	11.9	7.1	3.6	77.4
4	0	0	0	25.6	2.4	0	72
5	0	0	0	10.8	2.4	0	86.7
6	0	0	0	4	4	1	91
7	0	0	0	0.9	3.7	29	66.4
8	0	0	0	0	9.3	8.1	82.6
9	0	0	1	3.8	12.5	47.1	35.6
10	0	0	0	2.1	18.1	39.9	48.9
11	0	0	0	0	9.1	44.4	46.5
12	0	0	0	0	7.2	68	24.7
13	0	0	1	1	11.5	71.1	15.4
14	0	0	0	0	55.8	43.3	1
17.5	41	5.1	0	2.6	0	48.7	2.6

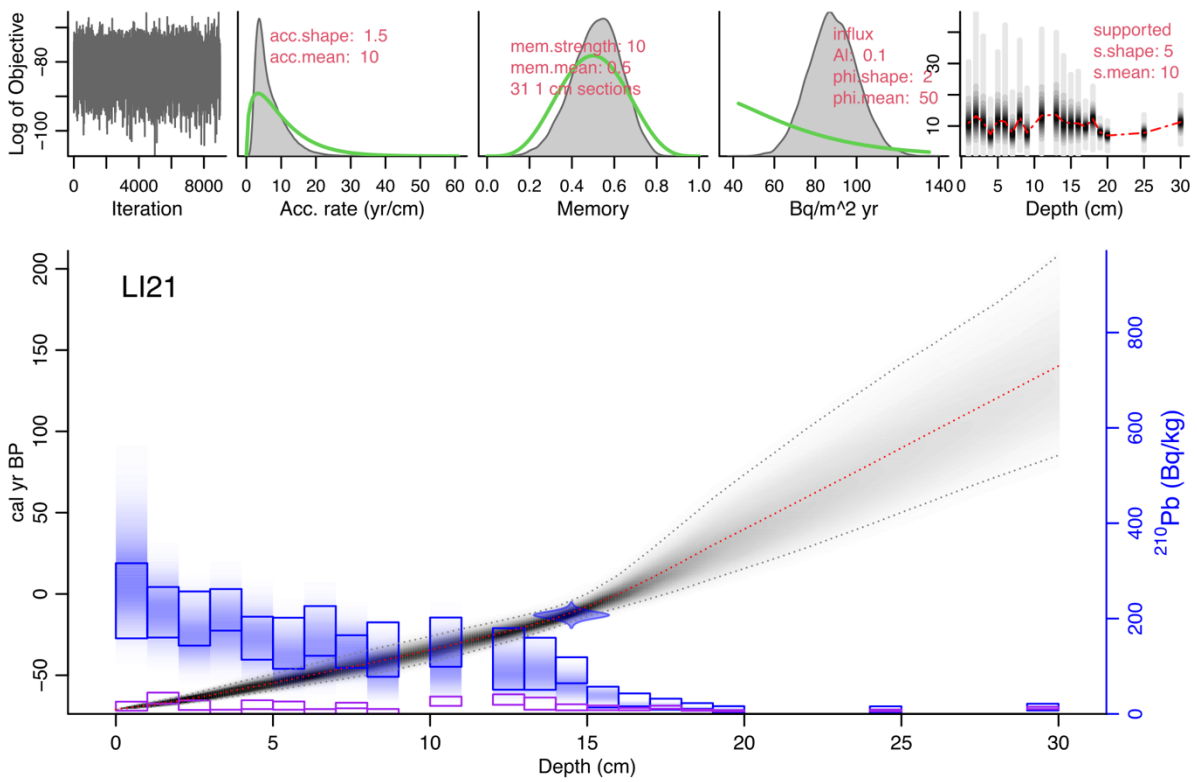

Figure S1. Age depth model generated for core LI21/20 using *rplum*.

Table S4. Bulk density, elemental and isotope data from core LI21/20 developed by the C-Side project.

Depth (cm)	Dry Bulk Density (g cm^{-3})	OC (%)	N (%)	C/N	N/C	$\delta^{13}C_{org}$ (‰)	$\delta_{15}N$ (‰)
0-1	0.07	28.30	0.81	40.76	0.02	-29.54	-0.55
1-2	0.11	25.29	0.92	32.10	0.03	-29.79	-0.97
2-3	0.16	24.82	1.19	24.40	0.04	-29.15	0.79
3-4	0.14	23.62	1.54	17.86	0.06	-29.28	1.18
4-5	0.14	22.67	1.02	26.00	0.04	-29.55	0.86
5-6	0.18	22.86	1.34	19.88	0.05	-29.92	0.87
6-7	0.13	21.07	1.34	18.41	0.05	-29.91	0.96
7-8	0.12	20.04	1.30	17.93	0.06	-29.85	1.29
8-9	0.16	19.24	1.11	20.17	0.05	-29.66	1.84
9-10	0.13	18.40	1.26	17.02	0.06	-29.01	2.15
10-11	0.13	17.82	1.39	14.96	0.07	-29.25	1.85
11-12	0.18	17.92	1.33	15.69	0.06	-29.15	2.49
12-13	0.12	17.96	1.32	25.84	0.06	-29.01	2.28
13-14	0.12	17.51	1.56	13.12	0.08	-28.89	2.50
14-15	0.19	15.48	1.10	16.42	0.06	-27.98	3.28
15-16	0.29	12.15	0.92	15.42	0.06	-27.54	4.17
16-17	0.74	0.44	0.03	17.21	0.06	-26.76	5.69
17-18	1.10	0.37	0.03	15.48	0.06	-26.84	2.53
18-19	1.00	0.39	0.03	15.99	0.06	-27.64	5.02
19-20	0.93	0.28	0.02	15.43	0.06	-26.90	4.16
20-21	1.15	0.43	0.03	16.60	0.06	-25.64	5.98
21-22	1.34	0.38	-	-	-	-	-
22-23	1.24	0.36	0.02	18.11	0.06	-25.75	4.27
23-24	0.91	0.43	-	-	-	-	-
24-25	1.17	0.35	0.02	17.37	0.06	-25.90	3.63
25-26	1.36	0.40	-	-	-	-	-
26-27	1.18	0.20	0.01	17.55	0.06	-26.14	3.53
27-28	1.35	0.27	-	-	-	-	-
28-29	1.66	0.33	0.02	15.78	0.06	-24.64	5.07
29-30	1.04	0.22	-	-	-	-	-
30-31	1.27	0.24	0.02	16.14	0.06	-23.23	4.30
31-32	1.53	0.24	-	-	-	-	-
32-33	1.04	0.20	0.01	15.81	0.06	-23.01	4.08
33-34	0.96	0.16	-	-	-	-	-
34-35	0.40	0.16	0.02	11.07	0.09	-25.58	5.06
35-36	0.25	0.21	0.02	13.64	0.07	-26.74	5.87

Table S5. Gas flux rates calculated from the raw gas flux data (10.6084/m9.figshare.20940067; Table S7) for each replicate within the different marsh zones and months of measurement.

Month	Marsh Zone	Replicate	CO_2 (mg CO_2 m^{-2} h^{-1})	CH (mg CH_4 m^{-2} h^{-1})	N_2O (mg N_2O m^{-2} h^{-1})
March	High	1	178.89	-0.05	-
March	High	2	325.00	-0.10	-
March	Mid	1	50.67	0.18	-
March	Mid	2	24.87	0.13	-
March	Low	1	106.40	-0.42	-0.08
March	Low	2	160.28	-0.08	0.07
April	High	1	-94.10	0.47	-0.20
April	High	2	-68.21	-0.45	0.21
April	High	3	37.01	-	0.12
April	Mid	1	-181.36	-1.04	1.04
April	Mid	2	-435.79	-0.32	0.16
April	Mid	3	-266.71	0.09	0.34
April	Low	1	-215.65	-0.59	0.03
April	Low	2	-149.84	1.06	0.07
April	Low	3	-170.02	0.32	-0.01
May	High	1	-262.17	-3.36	-0.38
May	High	2	-60.29	2.59	-0.46
May	High	3	-203.56	-9.62	0.27
May	Mid	1	-23.92	-1.14	-0.08
May	Mid	2	28.41	-6.02	0.17
May	Mid	3	-18.47	0.79	-0.11
May	Low	1	-296.52	-0.59	-0.88
May	Low	2	-80.14	0.68	0.07
May	Low	3	-175.57	-0.26	0.07
June	High	1	-101.59	-0.25	0.07
June	High	2	-270.46	-0.10	-0.02
June	High	3	-352.04	-0.05	-0.06
June	Mid	1	190.55	-0.13	0.09
June	Mid	2	281.45	-0.17	0.01
June	Mid	3	226.68	0.08	0.03
June	Low	1	-263.77	-0.11	0.06
June	Low	2	-249.28	-0.19	0.04
June	Low	3	-346.70	0.19	-0.01
July	High	1	-132.05	-0.03	0.04
July	High	2	-139.67	-0.11	-0.06
July	High	3	-14.82	-0.32	-0.06
July	Mid	1	91.11	0.34	-0.02
July	Mid	2	171.08	-0.31	0.13
July	Mid	3	17.38	0.25	0.01
July	Low	1	-269.46	0.021	0.04
July	Low	2	-195.57	-0.56	0.02
July	Low	3	-302.48	0.11	0.09

Table S6. Environmental data recorded at each station during gas flux measurements.

Month	Marsh Zone	Temperature (°C)	pH	Soil Moisture (mU)	Salinity
March	High	14.8	7.2	951	15.3
March	Mid	12.3	7.6	976.3	11.6
March	Low	10.4	7.7	963.7	21.6
April	High	16.3	7.2	912	2.0
April	Mid	14.6	7.5	894	40.1
April	Low	14.0	7.6	918	24.8
May	High	17.9	7.3	962	12.8
May	Mid	17.7	7.7	996	13.7
May	Low	19.9	7.3	973	26.1
June	High	21.2	7.7	988	15.5
June	Mid	18.6	7.8	1014	29.8
June	Low	16.9	7.4	996	11.7
July	High	23.2	7.1	945	13.5
July	Mid	25.1	7.1	1002.3	59.3
July	Low	19.3	7.6	985.3	19.4

Table S7. Digital object identifier (DOI) links to the raw gas flux data and age modelling R code uploaded to the data repository, figshare.

Data	File Type	DOI
Raw gas flux data	Excel Spreadsheet	10.6084/m9.figshare.20940067
Age modelling R code	R script	10.6084/m9.figshare.21151522

References

Al-Haj, A.N. and Fulweiler, R.W. (2020) ‘A synthesis of methane emissions from shallow vegetated coastal ecosystems’, *Global change biology*, 26(5), pp. 2988–3005.

Allen, J.R.L. (1990) ‘Constraints on measurement of sea-level movements from salt-marsh accretion rates’, *Journal of the Geological Society*, 147(1), pp. 5–7.

Appleby, P. G. (1997) ‘Sediment Records of Fallout Radionuclides and their Application to Studies of Sediment-Water Interactions’, *Water, air, and soil pollution*, 99(1), pp. 573–586.

Appleby, P. G. and Oldfield, F. (1978) ‘The calculation of lead-210 dates assuming a constant rate of supply of unsupported 210Pb to the sediment’, *Catena*, 5(1), pp. 1–8.

Appleby, P. G. and Oldfieldz, F. (1983) ‘The assessment of ^{210}Pb data from sites with varying sediment accumulation rates’, *Hydrobiologia*, 103(1), pp. 29–35.

Aquino-López, M.A. *et al.* (2018) ‘Bayesian analysis of ^{210}Pb dating’, *Journal of agricultural, biological, and environmental statistics*, 23(3), pp. 317–333.

Aquino-López, M.A. *et al.* (2020) ‘Comparing classical and Bayesian 210Pb dating models in human-impacted aquatic environments’, *Quaternary geochronology*, 60, p. 101106.

Aubinet, M., Vesala, T., & Papale, D. (2012). Eddy covariance: A practical guide to measurement and data analysis. Dordrecht, The Netherlands; Heidelberg, Germany; London, UK; New York, NY: Springer. https:// doi.org/10.1007/978-94-007-2351-1

Avnaim-Katav, S. *et al.* (2017) ‘Distributions of salt-marsh foraminifera along the coast of SW California, USA: Implications for sea-level reconstructions’, *Marine micropaleontology*, 131, pp. 25–43.

Ayres, D.R. and Strong, D.R. (2001) ‘Origin and genetic diversity of Spartina anglica (Poaceae) using nuclear DNA markers’, *American journal of botany*, 88(10), pp. 1863–1867.

Baggs, E.M. (2008) ‘A review of stable isotope techniques for N2O source partitioning in soils: recent progress, remaining challenges and future considerations’, Rapid communications in mass spectrometry: RCM, 22(11), pp. 1664–1672.

Bahram, M. *et al.* (2022) ‘Structure and function of the soil microbiome underlying N2O emissions from global wetlands’, *Nature communications*, 13(1), pp. 1–10.

Barbier, E.B. *et al.* (2011) ‘The value of estuarine and coastal ecosystem services’, *Ecological monographs*, 81(2), pp. 169–193.

Bartlett, K.B. *et al.* (1987) ‘Methane emissions along a salt marsh salinity gradient’, *Biogeochemistry*, 4(3), pp. 183–202.

Barkham, P. and Horton, H. (2022) ‘Five highly protected marine areas planned for English waters’, The Guardian, 20 June. Available at: https://amp.theguardian.com/environment/2022/jun/20/five-highly-protected-marine-areas-set-up-in-english-waters-fishing-ban (Accessed: 28 June 2022).

Barlow, N. L. M. *et al.* (2013) ‘Salt marshes as late Holocene tide gauges’, *Global and planetary change*, 106, p. 90.

Barlow, N.L.M. *et al.* (2014) ‘Salt-marsh reconstructions of relative sea-level change in the North Atlantic during the last 2000 years’, *Quaternary science reviews*, 99, pp. 1–16.

Belshe, E.F. *et al.* (2019) ‘Modeling organic carbon accumulation rates and residence times in coastal vegetated ecosystems’, *Journal of geophysical research. Biogeosciences*, 124(11), pp. 3652–3671.

Belyea, L.R. and Clymo, R.S. (2001) ‘Feedback control of the rate of peat formation’, *Proceedings. Biological sciences / The Royal Society*, 268(1473), pp. 1315–1321.

Berkeley, A. *et al.* (2007) ‘A review of the ecological and taphonomic controls on foraminiferal assemblage development in intertidal environments’, *Earth-Science Reviews*, 83(s 3–4), pp. 205–230.

Birks, H.J.B. 1995. Quantitative palaeoenvironmental reconstructions. In: Maddy, D. & Brew, J.S. Statistical Modelling of Quaternary Science Data. Technical guide 5, Quaternary Research Association, Cambridge, 271 pp.

Birks, H. J. B. (1998) ‘Numerical tools in palaeolimnology – Progress, potentialities, and problems’, *Journal of paleolimnology*, 20(4), pp. 307–332.

Birks, H. J. B. (2003) ‘Quantitative palaeoenvironmental reconstructions from Holocene biological data’, *Global change in the Holocene*, pp. 107–123.

Blackwell, M.S.A., Yamulki, S. and Bol, R. (2010) ‘Nitrous oxide production and denitrification rates in estuarine intertidal saltmarsh and managed realignment zones’, *Estuarine, coastal and shelf science*, 87(4), pp. 591–600.

Boelter, D.H. 1968. Important physical properties of peat materials. In: *Proceedings, third internationalpeat congress; 1968 August 18-23; Quebec, Canada. Department of Engery, Minds and Resources and National Research Council of Canada*: 150-154.

Boesch, D.F. and Turner, R.E. (1984) ‘Dependence of fishery species on salt marshes: The role of food and refuge’, *Estuaries*, 7(4), pp. 460–468.

Boorman, L.A. and Hazelden, J. (2017) ‘Managed re-alignment; a salt marsh dilemma?’, *Wetlands Ecology and Management*, 25(4), pp. 387–403.

Bradley, S. L. *et al.* (2011) 'An improved glacial isostatic adjustment model for the British Isles', *Journal of Quaternary Science*, 26(5), pp. 541–552.

Broce, K. *et al.* (2022) 'Background concentrations and accumulation rates in sediments of pristine tropical environments', *Catena*, 214(106252), p. 106252.

Burden, A., Garbutt, A. and Evans, C.D. (2019) 'Effect of restoration on saltmarsh carbon accumulation in Eastern England', Biology letters, 15(1), p. 20180773.

Byers, S. and Chmura, G. (2007) 'Salt marsh vegetation recovery on the Bay of Fundy', *Estuaries and coasts: journal of the Estuarine Research Federation*, 30(5), pp. 869–877.

Cahill, N. *et al.* (2016) 'A Bayesian hierarchical model for reconstructing relative sea level: from raw data to rates of change', *Climate of the Past*, 12(2), pp. 525–542.

Callaway, J.C., DeLaune, R.D. and Patrick, W.H., Jr (1996) 'Chernobyl137Cs used to determine sediment accretion rates at selected northern European coastal wetlands', *Limnology and oceanography*, 41(3), pp. 444–450.

Chamberlain, S.D. *et al.* (2018) 'Soil properties and sediment accretion modulate methane fluxes from restored wetlands', *Global change biology*, 24(9), pp. 4107–4121.

Chmura, G. L. *et al.* (2003) 'Global carbon sequestration in tidal, saline wetland soils', *Global biogeochemical cycles*, 17(4). doi: 10.1029/2002GB001917.

Chmura, G.L., Kellman, L. and Guntenspergen, G.R. (2011) 'The greenhouse gas flux and potential global warming feedbacks of a northern macrotidal and microtidal salt marsh', *Environmental research letters: ERL [Web site]*, 6(4), p. 044016.

Church, J. A. and White, N. J. (2011) 'Sea-Level Rise from the Late 19th to the Early 21st Century', *Surveys in Geophysics*, 32(4), pp. 585–602.

Church, J. A. , Gregory, J. M. , Huybrechts, P. , Kuhn, M. , Lambeck, K. , Nhuan, M. T. , Qin, D. and Woodworth, P. L. (2001): Changes in Sea Level , , in: J.T Houghton, Y. Ding, D.J. Griggs, M. Noguer, P.J. Van der Linden, X. Dai, K. Maskell, and C.A. Johnson (eds.): Climate Change 2001: The Scientific Basis: Contribution of Working Group I to the Third Assessment Report of the Intergovernmental Panel .

Costanza, R. *et al.* (2008) 'The value of coastal wetlands for hurricane protection', *Ambio*, 37(4), pp. 241–248.

Craft, C. *et al.* (2009) 'Forecasting the effects of accelerated sea-level rise on tidal marsh ecosystem services', *Frontiers in ecology and the environment*, 7(2), pp. 73–78.

Cundy, A. B. and Croudace, I. W. (1995) 'Physical and chemical associations of radionuclides and trace metals in estuarine sediments: an example from Poole

Harbour, Southern England', *Journal of environmental radioactivity*, 29(3), pp. 191–211.

Davies, J. L. (1964) 'A morphogenic approach to world shorelines', *Zeitschrift fur Geomorphologie*, 8, p. 127.

Duarte, C.M. *et al.* (2013) 'The role of coastal plant communities for climate change mitigation and adaptation', *Nature climate change*, 3(11), pp. 961–968.

de Rijk, S. (1995) 'Salinity control on the distribution of salt marsh foraminifera (Great Marshes, Massachusetts)', *Journal of foraminiferal research*, 25(2), pp. 156–166.

de Rijk, S. and Troelstra, S.R. (1997) 'Salt marsh foraminifera from the Great Marshes, Massachusetts: environmental controls', *Palaeogeography, palaeoclimatology, palaeoecology*, 130(1), pp. 81–112.

DeLaune, R.D., Smith, C.J. and Patrick, W.H. (1983) 'Methane release from Gulf coast wetlands', *Tellus. Series B, Chemical and physical meteorology*, 35(1), pp. 8–15.

Dollhopf, S.L. *et al.* (2005) 'Quantification of ammonia-oxidizing bacteria and factors controlling nitrification in salt marsh sediments', *Applied and environmental microbiology*, 71(1), pp. 240–246.

Eberly, L.E. (2007) 'Multiple Linear Regression', in Ambrosius, W.T. (ed.) *Topics in Biostatistics*. Totowa, NJ: Humana Press, pp. 165–187.

Edwards, R. and Wright, A. (2015) 'Foraminifera', in *Handbook of Sea-Level Research*. Chichester, UK: John Wiley & Sons, Ltd, pp. 191–217.

Edwards, R. J. and Horton, B. P. (2000) 'Reconstructing relative sea-level change using UK salt-marsh foraminifera', *Marine geology*, 169(1), pp. 41–56.

Edwards, R. J. and Horton, B. P. (2006) 'Developing detailed records of relative sea-level change using a foraminiferal transfer function: an example from North Norfolk, UK', *Philosophical transactions. Series A, Mathematical, physical, and engineering sciences*, 364(1841), pp. 973–991.

Edwards, R. J., Wright, A. J. and van de Plassche, O. (2004b) 'Surface distributions of salt-marsh foraminifera from Connecticut, USA: modern analogues for high-resolution sea level studies', *Marine micropaleontology*, 51(1-2), pp. 1–21.

Edwards, R.J. *et al.* (2004a) 'Assessing sea-level data from Connecticut, USA, using a foraminiferal transfer function for tide level', *Marine micropaleontology*, 51(3), pp. 239–255.

Edwards, R.J. (2001) 'Mid- to late Holocene relative sea-level change in Poole Harbour, southern England', *Journal of Quaternary Science*, 16(3), pp. 221–235.

Egbert, G.D., Erofeeva, S.Y. and Ray, R.D. (2010) ‘Assimilation of altimetry data for nonlinear shallow-water tides: Quarter-diurnal tides of the Northwest European Shelf’, *Continental shelf research*, 30(6), pp. 668–679.

Elschot, K. *et al.* (2015) ‘Ecosystem engineering by large grazers enhances carbon stocks in a tidal salt marsh’, *Marine ecology progress series*, 537, pp. 9–21.

Ember, L.M., Williams, D.F. and Morris, J.T. (1987) ‘Processes that influence carbon isotope variations in salt marsh sediments’, *Marine ecology progress series*, 36(1), pp. 33–42.

Emery, H.E. and Fulweiler, R.W. (2014) ‘Spartina alterniflora and invasive Phragmites australis stands have similar greenhouse gas emissions in a New England marsh’, *Aquatic botany*, 116, pp. 83–92.

Emmer, I. *et al.* (2015) ‘Methodology for Tidal Wetland and Seagrass Restoration’,

Evans, P.R. (1986) ‘Use of the Herbicide “Dalapon” for Control of Spartina Encroaching on Intertidal Mudflats: Beneficial Effects on Shorebirds’, *Colonial Waterbirds*, 9(2), pp. 171–175.

Frid, C.L.J., Chandrasekara, W.U. and Davey, P. (1999) ‘The restoration of mud flats invaded by common cord-grass (Spartina anglica, CE Hubbard) using mechanical disturbance and its effects on the macrobenthic fauna’, *Aquatic conservation: marine and freshwater ecosystems*, 9(1), pp. 47–61.

French, J.R. and Spencer, T. (1993) ‘Dynamics of sedimentation in a tide-dominated backbarrier salt marsh, Norfolk, UK’, *Marine geology*, 110(3), pp. 315–331.

Ford, H. *et al.* (2012) ‘Methane, carbon dioxide and nitrous oxide fluxes from a temperate salt marsh: Grazing management does not alter Global Warming Potential’, *Estuarine, coastal and shelf science*, 113, pp. 182–191.

Garrett, E. *et al.* (2022) *Late Holocene sea-level change in southern New Zealand*. Copernicus Meetings. doi:10.5194/egusphere-egu22-5675.

Gehrels W.R. (1994) ‘Determining Relative Sea-Level Change from Salt-Marsh Foraminifera and Plant Zones on the Coast of Maine, U.S.A’, *Journal of Coastal Research*, 10(4), pp. 990–1009.

Gehrels, W.R. (1999) ‘Middle and Late Holocene Sea-Level Changes in Eastern Maine Reconstructed from Foraminiferal Saltmarsh Stratigraphy and AMS 14C Dates on Basal Peat’, *Quaternary Research*, 52(3), pp. 350–359.

Gehrels, W.R. and Kemp, A.C. (2021) ‘Salt Marsh Sediments as Recorders of Holocene Relative Sea-Level Change’, in *Salt Marshes: Function, Dynamics, and Stresses*. Cambridge University Press, pp. 225–256.

Gehrels, W.R. and van de Plassche, O. (1999) ‘The use of Jadammina macrescens (Brady) and Balticammina pseudomacrescens Brönnimann, Lutze and Whittaker

(Protozoa: Foraminiferida) as sea-level indicators', *Palaeogeography, palaeoclimatology, palaeoecology*, 149(1), pp. 89–101.

Gehrels, W.R. and Woodworth, P.L. (2013) 'When did modern rates of sea-level rise start?', *Global and planetary change*, 100, pp. 263–277.

Gehrels, W.R. *et al.* (2005) 'Onset of recent rapid sea-level rise in the western Atlantic Ocean', *Quaternary science reviews*, 24(18), pp. 2083–2100.

Gehrels, W.R. *et al.* (2006) 'Rapid sea-level rise in the North Atlantic Ocean since the first half of the nineteenth century', *Holocene*, 16(7), pp. 949–965.

Gehrels, W.R. *et al.* (2008) 'A 20th century acceleration of sea-level rise in New Zealand', *Geophysical research letters*, 35(2), p. 2717.

Gehrels, W.R., Roe, H. M. and Charman, D. J. (2001) 'Foraminifera, testate amoebae and diatoms as sea-level indicators in UK saltmarshes: A quantitative multiproxy approach', *Journal of Quaternary Science*, 16(3), pp. 201–220.

Godwin, H. (1940) 'Studies of the post-glacial history of British vegetation - III. Fenland pollen diagrams - IV. Post-glacial changes of relative land- and sea-level in the English Fenland', *Philosophical transactions of the Royal Society of London*, 230(570), pp. 239–303.

Gonneea, M.E. *et al.* (2019) 'Salt marsh ecosystem restructuring enhances elevation resilience and carbon storage during accelerating relative sea-level rise', *Estuarine, coastal and shelf science*, 217, pp. 56–68.

Goreau, T.J. *et al.* (1980) 'Production of NO_2 and N_2O by Nitrifying Bacteria at Reduced Concentrations of Oxygen', *Applied and environmental microbiology*, 40(3), pp. 526–532.

Grace, J. *et al.* (1995) 'Carbon Dioxide Uptake by an Undisturbed Tropical Rain Forest in Southwest Amazonia, 1992 to 1993', *Science*, 270(5237), pp. 778–780.

Guilbault, J.-P., Clague, J. J. and Lapointe, M. (1995) 'Amount of subsidence during a late Holocene earthquake—evidence from fossil tidal marsh foraminifera at Vancouver Island, west coast of Canada', *Palaeogeography, palaeoclimatology, palaeoecology*, 118(1), pp. 49–71.

Hagger, V., Waltham, N.J. and Lovelock, C.E. (2022) 'Opportunities for coastal wetland restoration for blue carbon with co-benefits for biodiversity, coastal fisheries, and water quality', *Ecosystem Services*, 55, p. 101423.

Harvey, T.C. *et al.* (2021) 'Ocean mass, sterodynamic effects, and vertical land motion largely explain US coast relative sea level rise', *Communications Earth & Environment*, 2(1), pp. 1–10.

Hayward, B.W. *et al.* (2004) 'Morphological distinction of molecular types in Ammonia – towards a taxonomic revision of the world's most commonly misidentified foraminifera', *Marine micropaleontology*, 50(3), pp. 237–271.

Heiss, E.M., Fields, L. and Fulweiler, R.W. (2012) 'Directly measured net denitrification rates in offshore New England sediments', *Continental shelf research*, 45, pp. 78–86.

Hikosaka, K. *et al.* (2006) 'Temperature acclimation of photosynthesis: mechanisms involved in the changes in temperature dependence of photosynthetic rate', *Journal of experimental botany*, 57(2), pp. 291–302.

Hirota, M. *et al.* (2007) 'Fluxes of carbon dioxide, methane and nitrous oxide in two contrastive fringing zones of coastal lagoon, Lake Nakaumi, Japan', *Chemosphere*, 68(3), pp. 597–603.

Hocking, E.P., Garrett, E. and Cisternas, M. (2017) 'Modern diatom assemblages from Chilean tidal marshes and their application for quantifying deformation during past great earthquakes', *Journal of Quaternary Science*, 32(3), pp. 396–415.

Holzmann, M. (2000) 'Species Concept in Foraminifera: Ammonia as a Case Study', *Micropaleontology*, 46, pp. 21–37.

Horton, B.P. and Edwards, R.J. (2003): Seasonal distributions of foraminifera and their implications for sea-level studies. SEPM (Society for Sedimentory Geology) Special Publication 75, 21-30

Horton, B. P. and Edwards, R. J. (2005) 'The application of local and regional transfer functions to the reconstruction of Holocene sea levels, north Norfolk, England', *Holocene*, 15(2), pp. 216–228.

Horton, B.P. and Murray, J.W. (2007) 'The roles of elevation and salinity as primary controls on living foraminiferal distributions: Cowpen Marsh, Tees Estuary, UK', *Marine micropaleontology*, 63(3), pp. 169–186.

Horton, B. P., Edwards, R. J. and Lloyd, J. M. (1999a) 'UK intertidal foraminiferal distributions: implications for sea-level studies', *Marine micropaleontology*, 36(4), pp. 205–223.

Horton, B. P., Edwards, R. J. and Lloyd, J. M. (1999b) 'A foraminiferal-based transfer function: implications for sea-level studies', *Journal of foraminiferal research*, 29(2), pp. 117–129.

Horton, B.P. *et al.* (2018) 'Predicting marsh vulnerability to sea-level rise using Holocene relative sea-level data', *Nature communications*, 9(1), p. 2687.

Howard, J., Hoyt, S., Isensee, K., Pidgeon, E., Telszewski, M. (eds.) (2014). Coastal Blue Carbon: Methods for assessing carbon stocks and emissions factors in mangroves, tidal salt marshes, and seagrass meadows. Conservation International,

Intergovernmental Oceanographic Commission of UNESCO, International Union for Conservation of Nature. Arlington, Virginia, USA.

Howarth, R.W. (1984) 'The Ecological Significance of Sulfur in the Energy Dynamics of Salt Marsh and Coastal Marine Sediments', *Biogeochemistry*, 1(1), pp. 5–27.

Huxham, M. *et al.* (2018) 'Carbon in the Coastal Seascape: How Interactions Between Mangrove Forests, Seagrass Meadows and Tidal Marshes Influence Carbon Storage', *Current Forestry Reports*, 4(2), pp. 101–110.

Juggins, S., 2001. The European Diatom Database, User Guide. University of Newcastle. http://craticula.ncl.ac.uk/Eddi/docs/EddiGuide.pdf, 72 pp

Juggins, S. (2020) rioja: Analysis of Quaternary Science Data, R package version (0.9-26). (https://cran.r-project.org/package=rioja)

Juggins, S. and Birks, H.J.B. (2012) 'Quantitative Environmental Reconstructions from Biological Data', in Tracking Environmental Change Using Lake Sediments. unknown, pp. 431–494.

Kaplan, W., Valiela, I. and Teal, J.M. (1979) 'Denitrification in a salt marsh ecosystem', *Limnology and oceanography*, 24(4), pp. 726–734.

Kassambara, A. and Mundt, F. (2020). factoextra: Extract and Visualize the Results of Multivariate Data Analyses. R package version 1.0.7. https://CRAN.R-project.org/package=factoextra

Kemp, A.C. *et al.* (2011) 'Climate related sea-level variations over the past two millennia', *Proceedings of the National Academy of Sciences of the United States of America*, 108(27), pp. 11017–11022.

Kemp, A.C. *et al.* (2012) 'Quantitative vertical zonation of salt-marsh foraminifera for reconstructing former sea level; an example from New Jersey, USA', *Quaternary science reviews*, 54, pp. 26–39.

Kemp, A.C. *et al.* (2013) 'Sea-level change during the last 2500 years in New Jersey, USA', *Quaternary science reviews*, 81, pp. 90–104.

Kemp, A. C. and Telford, R. J. (2015) 'Transfer functions', in *Handbook of Sea-Level Research*. Chichester, UK: John Wiley & Sons, Ltd, pp. 470–499.

Kemp, A. C., Wright, A. J. and Cahill, N. (2020) 'Enough is Enough, or More is More? Testing the Influence of Foraminiferal Count Size on Reconstructions of Paleo-Marsh Elevation', *Journal of foraminiferal research*, 50(3), pp. 266–278.

Khan, N.S. *et al.* (2015) 'The application of δ13C, TOC and C/N geochemistry to reconstruct Holocene relative sea levels and paleoenvironments in the Thames Estuary, UK', *Journal of Quaternary Science*, 30(5). doi:10.1002/jqs.2784.

Kiesel, J. *et al.* (2020) ‘Effective design of managed realignment schemes can reduce coastal flood risks’, *Estuarine, coastal and shelf science*, 242(106844), p. 106844.

Kirschke, S. *et al.* (2013) ‘Three decades of global methane sources and sinks’, *Nature geoscience*, 6(10), pp. 813–823.

Kirwan, M.L. and Guntenspergen, G.R. (2012) ‘Feedbacks between inundation, root production, and shoot growth in a rapidly submerging brackish marsh’, *The Journal of ecology*, 100(3), pp. 764–770.

Kirwan, M.L. and Guntenspergen, G.R. (2015) ‘Response of Plant Productivity to Experimental Flooding in a Stable and a Submerging Marsh’, *Ecosystems* , 18(5), pp. 903–913.

Kirwan, M.L. and Megonigal, J.P. (2013) ‘Tidal wetland stability in the face of human impacts and sea-level rise’, *Nature*, 504(7478), pp. 53–60.

Kirwan, M.L. *et al.* (2016) ‘Overestimation of marsh vulnerability to sea level rise’, Nature climate change, 6(3), pp. 253–260.

Koch, M.S. *et al.* (1992) ‘Factors controlling denitrification rates of tidal mudflats and fringing salt marshes in south-west England’, *Estuarine, coastal and shelf science*, 34(5), pp. 471–485.

Koop-Jakobsen, K. and Giblin, A.E. (2010) ‘The effect of increased nitrate loading on nitrate reduction via denitrification and DNRA in salt marsh sediments’, *Limnology and oceanography*, 55(2), pp. 789–802.

Krammer, P., Dray, L. and Köhler, M.O. (2013) ‘Climate-neutrality versus carbon-neutrality for aviation biofuel policy’, *Transportation Research Part D: Transport and Environment*, 23, pp. 64–72.

Krause-Jensen, D. and Duarte, C.M. (2016) ‘Substantial role of macroalgae in marine carbon sequestration’, *Nature geoscience*, 9(10), pp. 737–742.

Krishnaswamy, S. *et al.* (1971) ‘Geochronology of lake sediments’, *Earth and planetary science letters*, 11(1), pp. 407–414.

Leorri, E., Horton, B.P. and Cearreta, A. (2008) ‘Development of a foraminifera-based transfer function in the Basque marshes, N. Spain: Implications for sea-level studies in the Bay of Biscay’, *Marine geology*, 251(1), pp. 60–74.

Liao, C. *et al.* (2007) ‘Invasion of Spartina alterniflora Enhanced Ecosystem Carbon and Nitrogen Stocks in the Yangtze Estuary, China’, *Ecosystems* , 10(8), pp. 1351–1361.

Long, A.J. *et al.* (2010) ‘Relative sea level change in west Greenland during the last millennium’, *Quaternary science reviews*, 29(3), pp. 367–383.

Long, A. J. *et al.* (2014) 'Contrasting records of sea-level change in the eastern and western North Atlantic during the last 300 years', *Earth and planetary science letters*, 388, pp. 110–122.

Lopes, C.L. *et al.* (2021) 'Assessing salt marsh loss and degradation by combining long-term LANDSAT imagery and numerical modelling', *Land Degradation & Development*, 32(16), pp. 4534–4545.

Maarten Blaauw, J. Andres Christen and Marco A. Aquino-Lopez (2021). rplum: Bayesian Age-Depth Modelling of Cores Dated by Pb-210. R package version 0.2.2.

MacDonald, M.A. *et al.* (2020) 'Benefits of coastal managed realignment for society: Evidence from ecosystem service assessments in two UK regions', *Estuarine, coastal and shelf science*, 244, p. 105609.

Macreadie, P. I. *et al.* (2019) 'The future of Blue Carbon science', *Nature communications*, 10(1), p. 3998.

Macreadie, P.I. *et al.* (2021) 'Blue carbon as a natural climate solution', *Nature Reviews Earth & Environment*, 2(12), pp. 826–839.

Macreadie, P. I., Randall Hughes, A. and Kimbro, D. L. (2013) 'Loss of "Blue Carbon" from Coastal Salt Marshes Following Habitat Disturbance', *PloS one*, 8(7), p. e69244.

Maechler, M., Rousseeuw, P., Struyf, A., Hubert, M., Hornik, K.(2021). cluster: Cluster Analysis Basics and Extensions. R package version 2.1.2.

Magenheimer, J.F. *et al.* (1996) 'Methane and carbon dioxide flux from a macrotidal salt marsh, bay of Fundy, New Brunswick', *Estuaries*, 19(1), p. 139.

Mariotti, G. and Carr, J. (2014) 'Dual role of salt marsh retreat: Long-term loss and short-term resilience', *Water resources research*, 50(4), pp. 2963–2974.

Mason, V.G., Wood, K.A., Jupe, L.L., Burden, A., Skov, M.W. 2022. Saltmarsh Blue Carbon in UK and NW Europe – evidence synthesis for a UK Saltmarsh Carbon Code. Report to the Natural Environment Investment Readiness Fund. UK Centre for Ecology & Hydrology, Bangor. 36pp

Masselink, G and Short, A.D. (1993) 'The Effect of Tide Range on Beach Morphodynamics and Morphology: A Conceptual Beach Model', *Journal of Coastal Research*, 9(3), pp. 785–800.

Masselink, G. *et al.* (2017) 'Evaluation of salt marsh restoration by means of self-regulating tidal gate – Avon estuary, South Devon, UK', *Ecological engineering*, 106, pp. 174–190.

MATLAB, 2018. 9.7. 0.1190202 (R2019b), Natick, Massachusetts: The MathWorks Inc.

Mcleod, E. *et al.* (2011) ‘A blueprint for blue carbon: toward an improved understanding of the role of vegetated coastal habitats in sequestering CO2’, *Frontiers in ecology and the environment*, 9(10), pp. 552–560.

Mitrovica, J. X. *et al.* (2001) ‘Recent mass balance of polar ice sheets inferred from patterns of global sea-level change’, *Nature*, 409(6823), pp. 1026–1029.

Milker, Y. *et al.* (2015) ‘Variability of intertidal foraminiferal assemblages in a salt marsh, Oregon, USA’, *Marine micropaleontology*, 118, pp. 1–16.

Mills, H. *et al.* (2013) ‘The Distribution Of Contemporary Saltmarsh Foraminifera In A Macrotidal Estuary: An Assessment Of Their Viability For Sea-Level Studies’, *Journal of Ecosystem & Ecography*, 3(3), pp. 1–16.

Moore, T.R., Heyes, A. and Roulet, N.T. (1994) ‘Methane emissions from wetlands, southern Hudson Bay lowland’, *Journal of Geophysical Research, D: Atmospheres*, 99(D1), pp. 1455–1467.

Morgan, P.A., Burdick, D.M. and Short, F.T. (2009) ‘The Functions and Values of Fringing Salt Marshes in Northern New England, USA’, *Estuaries and Coasts*, 32(3), pp. 483–495.

Moseman-Valtierra, S. *et al.* (2011) ‘Short-term nitrogen additions can shift a coastal wetland from a sink to a source of N2O’, *Atmospheric environment*, 45(26), pp. 4390–4397.

Mossman, H.L. *et al.* (2021) ‘Rapid carbon accumulation at a saltmarsh restored by managed realignment far exceeds carbon emitted in site construction’, *bioRxiv*. doi:10.1101/2021.10.12.464124.

Mueller, P. *et al.* (2019) ‘Assessing the long-term carbon-sequestration potential of the semi-natural salt marshes in the European Wadden Sea’, *Ecosphere*, 10(1), p. e02556.

Mueller, P. *et al.* (2020) ‘Plant species determine tidal wetland methane response to sea level rise’, *Nature communications*, 11(1), p. 5154.

Murray, J.W. and Bowser, S.S. (2000) ‘Mortality, Protoplasm Decay Rate, and Reliability of Staining Techniques to Recognise “Living” Foraminifera: A Review’, *Journal of foraminiferal research*, 30(1), pp. 66–70.

Murray, J. W. (2001) ‘The niche of benthic foraminifera, critical thresholds and proxies’, *Marine micropaleontology*, 41(1-2), pp. 1–7.

Murray, R.H., Erler, D.V. and Eyre, B.D. (2015) ‘Nitrous oxide fluxes in estuarine environments: response to global change’, *Global change biology*, 21(9), pp. 3219–3245.

Myhre, G., D. *et al*. 2013: Anthropogenic and Natural Radiative Forcing. In: Climate Change 2013: The Physical Science Basis. Contribution of Working Group I to the

Fifth Assessment Report of the Intergovernmental Panel on Climate Change. Cambridge University Press, Cambridge, United Kingdom and New York, NY, USA.

Natural England, (2014) *NNR Lindisfarne Leaflet.pdf*. Version 3. Natural England. Available at: https://www.lindisfarne.org.uk/general/pdf/NNRLindisfarneLeaflet.pdf.

Negandhi, K. *et al.* (2019) 'Blue carbon potential of coastal wetland restoration varies with inundation and rainfall', *Scientific reports*, 9(1), p. 4368.

Nicholls, R.J. *et al.* (2021) 'A global analysis of subsidence, relative sea-level change and coastal flood exposure', *Nature climate change*, 11(4), pp. 338–342.

Nixon, S.W. *et al.* (1996) 'The fate of nitrogen and phosphorus at the land-sea margin of the North Atlantic Ocean', *Biogeochemistry*, 35(1), pp. 141–180.

Noyce, G.L. and Megonigal, J.P. (2021) 'Biogeochemical and plant trait mechanisms drive enhanced methane emissions in response to whole-ecosystem warming', *Biogeosciences* , 18(8), pp. 2449–2463.

Nydick, K. R. *et al.* (1995) 'A sea-level rise curve from Guilford, Connecticut, USA', *Marine geology*, 124(1), pp. 137–159.

Oksanen J, Blanchet FG, Friendly M, et al. (2020) R Package 'vegan' version 2.5-6.

Ouyang, X. and Lee, S.Y. (2013) 'Carbon accumulation rates in salt marsh sediments suggest high carbon storage capacity', *Biogeosciences discussions* , 10(12), pp. 19–155.

Palmer, M.D. *et al.* (2020) 'Exploring the drivers of global and local sea-level change over the 21st century and beyond', *Earth's future*, 8(9). doi:10.1029/2019ef001413.

Parrack, J.D. (1986) 'Entomological investigation of the "Snook", Holy Island, part of the Lindisfarne NNR, during 1984-86', *The Vasculum*. Available at: http://www.the-vasculum.com/definitive_vasculum_archive/1986/1986.pdf#page=22.

Pastor, J., Zinke, P.J. and Stangenberger, A.G. (1985) 'Global patterns of soil nitrogen storage', *Nature*, 317(6038), pp. 613–616.

Peck, E.K., Wheatcroft, R.A. and Brophy, L.S. (2020) 'Controls on Sediment Accretion and Blue Carbon Burial in Tidal Saline Wetlands: Insights From the Oregon Coast, USA', *Journal of Geophysical Research: Biogeosciences*, 125(2), p. 875.

Pendleton, L. *et al.* (2012) 'Estimating global "blue carbon" emissions from conversion and degradation of vegetated coastal ecosystems', *PloS one*, 7(9), p. e43542.

Peltier, W.R., Argus, D.F. and Drummond, R. (2015) 'Space geodesy constrains ice age terminal deglaciation: The global ICE-6G_C (VM5a) model', *Journal of Geophysical Research, [Solid Earth]*, 120(1), pp. 450–487.

Peng, D. *et al.* (2018) ‘Using a marsh organ to predict future plant communities in a Chinese estuary invaded by an exotic grass and mangrove’, *Limnology and oceanography*, 63(6), pp. 2595–2605.

Percival, S.M., Sutherland, W.J. and Evans, P.R. (1998) ‘Intertidal habitat loss and wildfowl numbers: applications of a spatial depletion model’, *The Journal of applied ecology*, 35(1), pp. 57–63.

Plassche, O. van de (ed.) (1986) *Sea-Level Research: a manual for the collection and evaluation of data*. Springer, Dordrecht.

Plater, A.J. and Shennan, I. (1992) ‘Evidence of Holocene sea-level change from the Northumberland coast, eastern England’, *Proceedings of the Geologists' Association. Geologists' Association*, 103, pp. 201–216.

Poffenbarger, H.J., Needelman, B.A. and Megonigal, J.P. (2011) ‘Salinity Influence on Methane Emissions from Tidal Marshes’, *Wetlands*, 31(5), pp. 831–842.

Pullan, S., Dodds, G. and Cragg, A. (2013) ‘The use of enhanced stubbles by Light Bellied Brent geese on land that abuts Lindisfarne National Nature Reserve’, *Aspects of applied biology / Association of Applied Biologists*, 118.

Pullan, S. (2011) ‘Land use change in Northumberland from 1800’s to today–lessons from agricultural history’, *Aspects of Applied Biology Vegetation Management*, 108, *Vegetation Management*, pp. 145–151.

Ramaswamy, V. *et al.* (2019) ‘Radiative Forcing of Climate: The Historical Evolution of the Radiative Forcing Concept, the Forcing Agents and their Quantification, and Applications’, *Meteorological Monographs*, 59. doi:10.1175/AMSMONOGRAPHS-D-19-0001.1.

Ramsey, C.B. (1995) ‘Radiocarbon Calibration and Analysis of Stratigraphy: The OxCal Program’, Radiocarbon, 37(2), pp. 425–430.

R Core Team (2022). R: A language and environment for statistical computing. R Foundation for Statistical Computing, Vienna, Austria. URL https://www.R-project.org/.

Redeker, K.R., Baird, A.J. and Teh, Y.A. (2015) ‘Quantifying wind and pressure effects on trace gas fluxes across the soil–atmosphere interface’, *Biogeosciences* , 12(24), pp. 7423–7434.

Reed, D.J. (1995) ‘The response of coastal marshes to sea-level rise: Survival or submergence?’, *Earth Surface Processes and Landforms*, 20(1), pp. 39–48.

Ren, T., Roy, R. and Knowles, R. (2000) ‘Production and consumption of nitric oxide by three methanotrophic bacteria’, *Applied and environmental microbiology*, 66(9), pp. 3891–3897.

Ricart, A.M. *et al.* (2021) 'Coast-wide evidence of low pH amelioration by seagrass ecosystems', *Global change biology*, 27(11), pp. 2580–2591.

Rogers, K. *et al.* (2019) 'Wetland carbon storage controlled by millennial-scale variation in relative sea-level rise', *Nature*, 567(7746), pp. 91–95.

Roughan, B.L. *et al.* (2018) 'Nitrous oxide emissions could reduce the blue carbon value of marshes on eutrophic estuaries', *Environmental research letters: ERL [Web site]*, 13(4), p. 044034.

Rousseeuw, P.J. (1987) 'Silhouettes: A graphical aid to the interpretation and validation of cluster analysis', Journal of computational and applied mathematics, 20, pp. 53–65.

Ruiz-Fernández, A.C. *et al.* (2014) 'Chronology of recent sedimentation and geochemical characteristics of sediments in Alvarado Lagoon, Veracruz (southwestern gulf of Mexico)', *Ciencias Marinas*, 40(4), pp. 291–303.

Ruiz-Fernández, A.C. *et al.* (2018) 'Carbon burial and storage in tropical salt marshes under the influence of sea level rise', *The Science of the total environment*, 630, pp. 1628–1640.

Rush, G. *et al.* (2021) 'Development of an intertidal foraminifera training set for the North Sea and an assessment of its application for Holocene sea-level reconstructions', *Marine micropaleontology*, 169, p. 102055.

Saintilan, N. *et al.* (2013) 'Allochthonous and autochthonous contributions to carbon accumulation and carbon store in southeastern Australian coastal wetlands', *Estuarine, coastal and shelf science*, 128, pp. 84–92.

Salonen, J. S. *et al.* (2012) 'Comparing different calibration methods (WA/WA-PLS regression and Bayesian modelling) and different-sized calibration sets in pollen-based quantitative climate reconstruction', *Holocene*, 22(4), pp. 413–424.

Sanders, C.J. *et al.* (2010) 'Organic carbon burial in a mangrove forest, margin and intertidal mud flat', *Estuarine, coastal and shelf science*, 90(3), pp. 168–172.

Sasmito, S. D. *et al.* (2020) 'Organic carbon burial and sources in soils of coastal mudflat and mangrove ecosystems', *Catena*, 187, p. 104414.

Schapel, A., Marschner, P. and Churchman, J. (2018) 'Clay amount and distribution influence organic carbon content in sand with subsoil clay addition', *Soil and Tillage Research*, 184, pp. 253–260.

Scott, D. B. and Medioli, F. S. (1980) *Quantitative studies of marsh foraminiferal distributions in Nova Scotia: implications for sea level studies*. [Washington, D.C.]: Cushman Foundation for Foraminiferal Research.

Scott, D. S. and Medioli, F. S. (1978) 'Vertical zonations of marsh foraminifera as accurate indicators of former sea-levels', *Nature*, 272(5653), pp. 528–531.

Shennan, I. (1986) ‘Flandrian sea-level changes in the Fenland. II: Tendencies of sea-level movement, altitudinal changes, and local and regional factors’, *Journal of Quaternary Science*, 1(2), pp. 155–179.

Shennan, I. *et al.* (2000) ‘Late quaternary sea-level changes, crustal movements and coastal evolution in Northumberland, UK’, *Journal of Quaternary Science*, 15(3), pp. 215–237.

Shennan, I., Milne, G. and Bradley, S. (2012) ‘Late Holocene vertical land motion and relative sea-level changes: lessons from the British Isles’, *Journal of Quaternary Science*, 27(1), pp. 64–70.

Shennan, I. (2018) ‘Sea Level Studies | Overview’, in Elias, S.A. and Mock, C.J. (eds) *Encyclopedia of Quaternary Science (Second Edition)*. Amsterdam: Elsevier, pp. 369–376.

Sims, R.P. *et al.* (2022) ‘Tidal mixing of estuarine and coastal waters in the western English Channel is a control on spatial and temporal variability in seawater CO2’, *Biogeosciences* , 19(6), pp. 1657–1674.

Smeaton, C. *et al.* (2022) ‘Using citizen science to estimate surficial soil Blue Carbon stocks in Great British saltmarshes’, *Frontiers in Marine Science*, 9. doi:10.3389/fmars.2022.959459.

Smith, C.J., DeLaune, R.D. and Patrick, W.H. (1983) ‘Carbon dioxide emission and carbon accumulation in coastal wetlands’, *Estuarine, coastal and shelf science*, 17, pp. 21–29.

Smyth, T.J. *et al.* (2010) ‘Technology, Design, and Operation of an Autonomous Buoy System in the Western English Channel’, *Journal of Atmospheric and Oceanic Technology*, 27(12), pp. 2056–2064.

Southall, K. E., Roland Gehrels, W. and Hayward, B. W. (2006) ‘Foraminifera in a New Zealand salt marsh and their suitability as sea-level indicators’, *Marine micropaleontology*, 60(2), pp. 167–179.

Stuiver, M. and Quay, P. D. (1980) ‘Patterns of atmospheric 14C changes’, *Radiocarbon*, 22(2), pp. 166–176.

Telford, R.J. and Birks, H.J.B. (2009) ‘Evaluation of transfer functions in spatially structured environments’, *Quaternary science reviews*, 28(13), pp. 1309–1316.

Telford, R.J. and Birks, H.J.B. (2011) ‘A novel method for assessing the statistical significance of quantitative reconstructions inferred from biotic assemblages’, *Quaternary science reviews*, 30(9), pp. 1272–1278.

Telford, R.J. (2019) palaeoSig: Significance Tests of Quantitative Palaeoenvironmental Reconstructions, R package version (2.0-3). (http://cran.r-project.org/package=palaeoSig).

ter Braak, C.J.F. and Prentice, I.C. (1988) 'A Theory of Gradient Analysis', in Begon, M. et al. (eds) Advances in Ecological Research. Academic Press, pp. 271–317.

ter Braak, C. J. F. and Juggins, S. (1993) 'Weighted averaging partial least squares regression (WA-PLS): an improved method for reconstructing environmental variables from species assemblages', *Hydrobiologia*, 269(1), pp. 485–502.

ter Braak CJF and Šmilauer P (2002) CANOCO 4.5 Reference manual and CanoDraw for Windows User's guide: Software for canonical community ordination.

ter Braak, C.J.F. (1986) 'Canonical Correspondence Analysis: A New Eigenvector Technique for Multivariate Direct Gradient Analysis', *Ecology*, 67(5), pp. 1167–1179.

ter Braak, C.J.F. (1988) 'Unimodal Models to Relate Species to Environment', Biometrics, 44(2), p. 631.

Thompson, R.L. *et al.* (2014) 'Nitrous oxide emissions 1999 to 2009 from a global atmospheric inversion', *Atmospheric Chemistry and Physics*, 14(4), pp. 1801–1817.

Ullman, R., Bilbao-Bastida, V. and Grimsditch, G. (2013) 'Including Blue Carbon in climate market mechanisms', *Ocean & coastal management*, 83, pp. 15–18.

van der Spek, A.J.F. (1997) 'Tidal asymmetry and long-term evolution of Holocene tidal basins in The Netherlands: simulation of palaeo-tides in the Schelde estuary', *Marine geology*, 141(1), pp. 71–90. *Verified Carbon Standard.VM0033.*

Walker, M. (2005) *Quaternary Dating Methods*. John Wiley and Sons.

Walton, W.R. (1952) 'Techniques for recognition of living foraminifera', *Cushman Found. Foram. Res. Contr.*, 3(2), pp. 56–60.

Watcham, E.P., Shennan, I. and Barlow, N.L.M. (2013) 'Scale considerations in using diatoms as indicators of sea-level change: Lessons from Alaska', *Journal of Quaternary Science*, 28(2), pp. 165–179.

Whiting, G.J. and Chanton, J.P. (1993) 'Primary production control of methane emission from wetlands', *Nature*, 364(6440), pp. 794–795.

Wieser, M.E. (2006) 'Atomic weights of the elements 2005 (IUPAC Technical Report)', *Pure and applied chemistry. Chimie pure et appliquee*, 78(11), pp. 2051–2066.

Williams, S. *et al.* (2021) 'Development of a training set of contemporary salt-marsh Foraminifera for late Holocene sea- level reconstructions in southeastern Australia', *Open quaternary*, 7(1), p. 4.

Wollenberg, J.T., Ollerhead, J. and Chmura, G.L. (2018) 'Rapid carbon accumulation following managed realignment on the Bay of Fundy', *PloS one*, 13(3), p. e0193930.

Woodroffe, S. A. and Long, A. J. (2010) 'Reconstructing recent relative sea-level changes in West Greenland: Local diatom-based transfer functions are superior to regional models', *Quaternary international: the journal of the International Union for Quaternary Research*, 221(1), pp. 91–103.

Worth, D. (2005) 'Accelerating towards Climate Neutrality with the U.S. Government Stuck in Neutral: The Emerging Role of U.S. Businesses, Cities, States, and Universities in Agressively Reducing Greenhouse Gas Emissions', *Sustainable Development Law & Policy*, 5(2), pp. 4–8.

Wright, A. J., Edwards, R. J. and van de Plassche, O. (2011) 'Reassessing transfer-function performance in sea-level reconstruction based on benthic salt-marsh foraminifera from the Atlantic coast of NE North America', *Marine micropaleontology*, 81(1). doi: 10.1016/j.marmicro.2011.07.003.

Yang, S.L. *et al.* (2011) '50,000 dams later: Erosion of the Yangtze River and its delta', *Global and planetary change*, 75(1), pp. 14–20.

Yang, W.H. and Silver, W.L. (2016) 'Gross nitrous oxide production drives net nitrous oxide fluxes across a salt marsh landscape', *Global change biology*, 22(6), pp. 2228–2237.

Zhang, L. *et al.* (2020) 'Soil labile organic carbon fractions and soil enzyme activities after 10 years of continuous fertilization and wheat residue incorporation', *Scientific reports*, 10(1), p. 11318.

Zhao, Y. *et al.* (2021) 'Temperature reconstructions for the last 1.74-Ma on the eastern Tibetan Plateau based on a novel pollen-based quantitative method', *Global and planetary change*, 199, p. 103433.

Zheng, B. and Agresti, A. (2000) 'Summarizing the predictive power of a generalized linear model', *Statistics in medicine*, 19(13), pp. 1771–1781.

Ziegler, R. (2016) 'Climate Neutrality – Towards An Ethical Conception of Climate Neutrality', *Ethics, Policy & Environment*, 19(3), pp. 256–272.

Zuo, J. *et al.* (2012) 'Achieving carbon neutrality in commercial building developments – Perceptions of the construction industry', *Habitat international*, 36(2), pp. 278–286.